e-Zine for meteor observers meteornews.net

MeteorNews

ISSN 2570-4745 VOL 5 / ISSUE 2 / MARCH 2020

Fireball from 8 April 2018 in Veszprém, Hungary photographed by Mónika Landy-Gyebnár

- IAU Working List
- alpha Monocerotids
- Ursids 2019
- Radio observations
- CAMS reports
- Fireballs

Contents

Confusions in IAUMDC Meteor Shower Database (SD)

Masahiro Koseki

NMS (The Nippon Meteor Society), 4-3-5 Annaka Annaka-shi, Gunma-ken, 379-0116 Japan
geh04301@nifty.ne.jp

This study lists the erroneous combinations in the IAUMDC Meteor Shower Database (SD) based on the version of 2018 January 13 20h35m17s. The many erroneous shower maxima may confuse observers and result in more duplicated and unjustified new entries. This paper lists the problematic maxima, the spread in the position of the radiants, the questionable velocity data and the many incorrect combinations. The author suggests investigating the problems identified in this analyzes in order to avoid further confusion.

1 Introduction

SD, the IAUMDC Meteor Shower Database[1], started from a personal working list (Jenniskens, 2006) when video observations were on the dawning. There were not enough individual orbital data to detect minor showers and, therefore the dispersed data was collected into a meteor shower with errors in radiant position, velocity, and the activity period. This was widely accepted at that time.

SD has been filled up by many observers and researchers who worked by different standards and therefore arrived at different sources merged into one shower or in other cases some single meteor showers that got divided into several different showers. This paper reveals the confusions in the SD by using the SonotaCo Network[2] observations (SonotaCo, 2009).

2 The maximum of the activity

SD lists the solar longitude ($\lambda_\odot$) as the 'ecliptic longitude of the Sun at the peak the shower activity' but it often shows the averaged time derived from the mean descending node and not from the activity profile such as a ZHR curve. We know that visual observations cannot determine the real time of maximum activity in many cases, for instance when the sky conditions are too bad or when the maximum occurs during daylight. The time of the maxima, based on such data, is not representative and should not be listed. However, old radar observations are intermittent and usually did not observe the shower maxima. Photographic observations recorded only thousands of meteors and the node is averaged from a few meteor orbits only. In case of video observations, the cameras installed at a small area on the Earth may not encounter the real maximum in only one or two years of observations.

DR stands for the radiant density ratio, usually of within 3 degrees to between 3 to 6 degrees and it can reduce the influence of the different sky condition. We can use the orbit data collected during ten years by the SonotaCo Network to obtain a more plausible time of maximum than what has been listed in SD. *Table 1* lists the most problematic showers for which the difference is larger than 10 degrees in $\lambda_\odot$ (solar longitude). A more plausible maximum has been mentioned when available. No plausible maximum has been given anymore in case of uncertain showers (see *Table 5* for the comments on different *Tables*). We refer to each entry by giving the three-digit shower number with the three-character code together with an additional entry number when multiple entrees for the shower exist in the SD, e.g. 004GEM1.

3 The radiant points

In the past we used to identify radiant areas with a size of 10 degrees as one single shower. There are many such cases, even in the SD. *Table 2* lists such showers with the median values for ($\lambda - \lambda_\odot, \beta$). In the fourth column the value '*d*' gives the maximum distance in degrees for the different shower entries in the SD within the shower for the combination between the shower entry listed in the 5th and 6th column under 'Combination'.

Table 3 lists the possible related shower entries which are listed with other shower entries for which the radiant point is located within 3 degrees in ($\lambda - \lambda_\odot$, β) and the activity within 10 degrees in $\lambda_\odot$. The shower status is listed under the column S:

- –2 = shower removed from the MDC lists;
- –1 = to be removed from the MDC lists;
- 0 = single shower;
- 1 = single established shower;
- 2 = to be established shower or group;
- 4 = member of the group;
- 6 = member of the established group;
- 10 = pro-tempore status in the working group;
- 40 = group member.

There may be showers present which represent activity caused by a different source and in some cases, it concerns

[1] https://www.ta3.sk/IAUC22DB/MDC2007/

[2] http://sonotaco.jp/doc/SNM/

the same shower divided into different components (see *Table 5*).

4 The geocentric velocity

Table 4 lists showers which have a difference in geocentric velocity v_g larger than 5 km/s. For example, the difference for 195BIN is over 20 km/s! There may be several explanations for these discrepancies, observational errors, an erroneous combination of observations, insufficient statistical significance of the data for minor meteor streams and so on.

5 Notes

Some comments in *Table 5*, like 'a chance association' or 'indistinguishable from sporadic background' have the same meaning that the radiant distribution and DR curves do not show any clear activity. There are many such entries in the SD but the main concern of this paper is to show the reasons of the confusions in the SD. We can give the details of the surveys on these problems when the occasion occurs. The readers may feel that it is appropriate to mention this as simple errors and misprints in the SD but the author has given the lists of these problems few years ago (Koseki, 2016).

References

Jacchia L. G. and Whipple F. L. (1961). "Precision orbits of 413 photographic meteors". *Smithsonian Contributions to Astrophysics*, **4**, 97–129.

Jenniskens P. (2006). "Meteor Showers and their parent comets". Cambridge, Table 7, 'Working list of cometary meteor showers'. pages 691–746.

Koseki M. (2016). "Research on the IAU meteor shower database". *WGN, the Journal of the IMO*, **44**, 151–169.

SonotaCo (2009). "A meteor shower catalog based on video observations in 2007-2008". *WGN, the Journal of the IMO*, **37**, 55–62.

Table 1 – List of meteor showers with a difference in solar longitude ($\lambda_\odot$) of more than 10 degrees (SD version of 2018 January 13 20h35m17s). Plausible maximum $\lambda_\odot$ is given in case when clear DR curves were obtained (see also Table 5).

Code	$\lambda_\odot$ (°) (min)	$\lambda_\odot$ (°) (max)	$\lambda_\odot$ (°) Plausible	Code	$\lambda_\odot$ (°) (min)	$\lambda_\odot$ (°) (max)	$\lambda_\odot$ (°) Plausible	Code	$\lambda_\odot$ (°) (min)	$\lambda_\odot$ (°) (max)	$\lambda_\odot$ (°) Plausible
002STA	196	224	222	136SLE	36.7	36.7		307TPU	246.8	270.7	
009DRA	195	203.9	195	150SOP	47	70		327BEQ	89.3	106.5	
012KCG	135.8	150	140	151EAU	59	78.7		335XVI	256.7	267	
016HYD	252.9	266	252	152NOC	45.5	64.4		337NUE	163	181.4	168
017NTA	214.1	234.4	228	154DEA	48.1	63		340TPY	249.4	272	249&266
020COM	261.7	277.4	268	156SMA	47.1	62.6		372PPS	94	109.6	97
021AVB	21.7	32		161SSC	70	162.9		376ALN	135	155.9	
027KSE	15.7	25.9	25	164NZC	86	108.09	112	386OBC	200.6	214	
031ETA	45.5	58.1	45	165SZC	80	106.2	107	392NID	225.4	242	
033NIA	142	161.3	160	172ZPE	74.5	85.7		395GCM	257	270.1	
040ZCY	16	32		175JPE	107.5	120.8	108	428DSV	262	278.8	
043ZSE	0.1	12.2		176PHE	110.3	126.8		448AAL	3.1	14.4	
081SLY	167	186	168	183PAU	123.7	136	135	451CAM	39	62.9	62.9
088ODR	98.5	115.5		186EUM	87.1	106		456MPS	61.5	79.3	
093VEL	296	296		188XRI	117.7	135.5		494DEL	242.5	253.1	245
096NCC	288.2	300.2	290	194UCE	146	169.1		501FPL	296.4	317.3	
097SCC	284.1	298		195BIN	82.1	157.3		506FEV	303.9	315.3	
101PIH	271	319		202ZCA	147	160	160	507UAN	96	108.8	
103TCE	321	321		215NPI	168.3	184.1		515OLE	279.3	296	290
105OCN	323.4	323.4		216SPI	176	184		531GAQ	45	58	48
113SDL	314.7	334.7		233OCC	189.3	203.8		533JXA	107.3	119	108
115DCS	309.1	325.1		242XDR	210.8	221.4		644JLL	270.4	288	
118GNO	352.7	4		253CMI	252	255.2	259	689TAC	108.8	121	
121NHY	343.1	4.6		257ORS	243	260		706ZPI	172	188.5	
124SVI	8.7	23		288DSA	256.5	279.5					

Table 2 – List of showers which have entries with radiants at a distance larger than 10 degrees from each other. The distance d is valid for the entries listed in the column 'Combination'.

CODE	$\lambda - \lambda_\odot$ (°)	β (°)	d (°)	Combination		CODE	$\lambda - \lambda_\odot$ (°)	β (°)	d (°)	Combination	
005SDA	208.6	–7.3	35	SDA3	SDA0	151EAU	230	38.1	10.7	EAU1	EAU2
012KCG	160.4	75.1	18.8	KCG6	KCG8	152NOC	329.9	11.7	18.7	NOC1	NOC0
017NTA	192	1.9	14	NTA1	NTA0	161SSC	185.1	–2.3	18.9	SSC0	SSC1
020COM	243.3	20.6	21.9	COM2	COM6	172ZPE	348.5	5.4	10.2	ZPE2	ZPE3
021AVB	164.9	8.9	24.8	AVB0	AVB5	176PHE	252.6	–55	17.1	PHE2	PHE0
033NIA	197.7	4.3	18.5	NIA0	NIA5	186EUM	108.6	62.4	33.5	EUM0	EUM2
043ZSE	261.6	17.1	14	ZSE2	ZSE0	187PCA	305.6	53.2	10.6	PCA1	PCA0
061TAH	131.1	49.5	12.4	TAH0	TAH1	189DMC	347.3	2.4	13.3	DMC0	DMC1
063COR	111.1	–1.4	26.7	COR0	COR1	190BPE	285.1	22.7	14.4	BPE2	BPE1
069SSG	187.7	–6.1	11	SSG0	SSG1	195BIN	191	–27.8	53.5	BIN0	BIN1
076KAQ	157.8	0.9	14	KAQ0	KAQ1	215NPI	194.9	3.5	10.2	NPI3	NPI1
081SLY	294.7	32.3	16	SLY1	SLY2	216SPI	196.8	–4.1	22.3	SPI3	SPI4
088ODR	129.6	78.1	16.4	ODR0	ODR2	226ZTA	240.2	–8.7	17.6	ZTA1	ZTA0
093VEL	228.6	–65.1	23	VEL1	VEL0	232BCN	264.5	–21.5	16.2	BCN0	BCN1
094RGE	177	6.8	16.5	RGE2	RGE1	253CMI	210.1	–9.6	12	CMI0	CMI2
097SCC	188.7	–6.9	15.9	SCC1	SCC0	257ORS	183.4	–5.6	12	ORS3	ORS0
101PIH	262.6	–11.5	14.5	PIH2	PIH0	289DNA	174.2	6.2	26.7	DNA0	DNA1
103TCE	263.3	–27.3	17.7	TCE3	TCE2	337NUE	258.3	–19.2	12.1	NUE1	NUE2
105OCN	242.8	–57.8	13.3	OCN1	OCN4	343HVI	168.4	–1.2	18.4	HVI1	HVI3
106API	213.5	–80.5	12.5	API1	API2	357PHP	318.3	18.4	10.3	PHP0	PHP1
110AAN	212.5	–18.6	21.9	AAN0	AAN1	384OLP	229.3	–30.6	18	OLP0	OLP1
112NDL	179	9.5	12.4	NDL0	NDL2	424SOL	282.2	25.8	14.5	SOL1	SOL0
113SDL	169.7	1.5	18.9	SDL1	SDL2	425PSA	270.8	21.2	12.7	PSA0	PSA1
115DCS	345.7	–2	13	DCS3	DCS0	451CAM	65.8	61.5	21.8	CAM3	CAM2
118GNO	260.4	–28.7	16.4	GNO2	GNO0	456MPS	182.3	10.6	10.8	MPS3	MPS0
121NHY	171.1	–15.8	25	NHY2	NHY1	460LOP	169.8	19.1	10.6	LOP3	LOP1
133PUM	104.3	43	41.4	PUM1	PUM0	507UAN	288.4	33.8	10.3	UAN0	UAN2
136SLE	181.7	7.8	16.5	SLE2	SLE1	641DRG	212.3	7.4	10.9	DRG0	DRG1
149NOP	192.3	7.1	15.2	NOP1	NOP0	652OSP	250.3	9.4	12	OSP0	OSP1
150SOP	193	4.8	26.9	SOP5	SOP0						

Table 3 – List of possible related entries. *S* is the status listed in SD, $\lambda_\odot$ is the solar longitude for the time of activity, $\lambda - \lambda_\odot$, β is the Sun-centered ecliptic radiant, v_g the geocentric velocity. The column 'possible members' mentions the IAU code of the shower / distance in degrees between the Sun-centered ecliptic radiant positions. S - shower status : –2 shower removed from the MDC lists, –1 to be removed from the MDC lists, 0 single shower, 1 single established shower, 2 to be established shower or group, 4 member of the group, 6 member of the established group, 10 pro-tempore status in the working group, 40 group member.

Here we refer to each entry by giving the four-digit shower number with the three-character code together with the two-digit additional entry number when multiple entrees for the shower exist in the SD, e.g. 0004GEM01. This table was constructed for every entry in the original version of the SD and, therefore, it was necessary to distinguish every entry by using a different presentation from the text.

Code	*S*	$\lambda_\odot$ (°)	$\lambda - \lambda_\odot$ (°)	β (°)	v_g	Possible members
0001CAP00	1	128.9	178	10.7	22.2	692EQA1/2.50
0001CAP01	1	122.3	184.4	9.6	23.4	623XCS1/1.16, 623XCS0/1.12
0002STA00	1	224	186.5	–5	28	625LTA0/1.39, 285GTA0/2.99, 625LTA1/0.77
0002STA01	1	207.6	193.8	–5.2	27.8	028SOA2/3.09, 028SOA0/3.42, 624XAR0/1.40, 624XAR1/1.29, 626LCT1/1.66, 626LCT0/0.79
0002STA02	1	196.5	195.2	–4.3	27.92	627NPS0/2.11, 627NPS1/1.55, 028SOA1/1.60, 028SOA2/1.62, 028SOA0/1.94, 624XAR0/0.27, 624XAR1/0.33

Code	S	$\lambda_\odot$ (°)	$\lambda - \lambda_\odot$ (°)	β (°)	v_g	Possible members
0002STA03	1	219.7	191.5	–4.8	27.2	626LCT1/0.66, 626LCT0/1.74, 628STS0/0.45, 628STS1/0.63, 637FTR1/1.10, 637FTR0/1.24
0002STA04	1	196	195.6	–4.2	28.2	627NPS0/1.65, 627NPS1/1.09, 028SOA1/1.16, 028SOA2/1.20, 028SOA0/1.67, 624XAR0/0.66, 624XAR1/0.77
0002STA05	1	216	193	–4.8	26.6	624XAR1/1.92, 626LCT1/0.81, 626LCT0/0.36, 628STS0/1.03, 628STS1/0.92, 637FTR1/2.54, 637FTR0/2.70
0002STA06	10	211.3	192.3	–5.6	27	624XAR0/2.95, 624XAR1/2.82, 626LCT1/0.81, 626LCT0/1.38
0004GEM00	1	262.1	207.7	10.6	34.58	914AGE0/2.44, 641DRG0/0.15, 949SGD0/0.50
0004GEM01	1	261.6	207.9	10.4	34.6	914AGE0/2.20, 641DRG0/0.21, 949SGD0/0.32
0004GEM02	1	261.5	208	10.2	35	914AGE0/2.00, 641DRG0/0.41, 949SGD0/0.47
0004GEM03	1	261.4	208.1	10.4	33.5	914AGE0/2.20, 641DRG0/0.31, 949SGD0/0.26
0004GEM04	1	261	208.2	10.2	34.5	914AGE0/1.99, 641DRG0/0.59, 949SGD0/0.47
0004GEM05	1	262	208	10.5	33.8	914AGE0/2.29, 641DRG0/0.27, 949SGD0/0.18
0004GEM06	10	260.8	208	10.5	34.1	914AGE0/2.30, 641DRG0/0.25, 949SGD0/0.19
0005SDA01	1	127.2	208.6	–7.4	40.2	640AOA0/2.17
0005SDA05	1	128.2	208.3	–7.2	40.8	640AOA0/2.13
0005SDA07	1	129.7	207.4	–7.9	39.4	640AOA0/1.05
0005SDA08	1	128	208.8	–7.2	41.3	640AOA0/2.50
0007PER00	1	140.19	282	38.4	59.49	938PEA0/1.81, 992GPE0/0.65, 942EPE0/0.74, 981AGP0/1.39
0007PER01	1	140.19	283.1	38.3	59.38	938PEA0/1.37, 992GPE0/0.25, 942EPE0/0.24, 981AGP0/0.68
0007PER02	1	139.4	283.3	38.7	59	938PEA0/1.76, 992GPE0/0.67, 942EPE0/0.35, 981AGP0/0.98
0007PER03	1	139.5	282.4	37.6	62.1	938PEA0/1.01, 992GPE0/0.70, 942EPE0/1.05, 981AGP0/0.96
0007PER04	1	139.2	283.3	38.3	58.7	938PEA0/1.38, 992GPE0/0.39, 942EPE0/0.31, 981AGP0/0.63
0007PER05	1	140	282.7	37.7	61.4	938PEA0/0.87, 992GPE0/0.54, 942EPE0/0.89, 981AGP0/0.68
0007PER06	1	140	283.3	38.5	59.1	938PEA0/1.51, 992GPE0/0.45, 942EPE0/0.24, 981AGP0/0.75
0007PER07	10	138.1	283.4	38.2	59.1	938PEA0/1.27, 992GPE0/0.45, 942EPE0/0.44, 981AGP0/0.50
0008ORI00	1	208.6	246.6	–7.4	66.2	936STO0/0.05
0008ORI01	1	208.7	245.9	–7.5	66.53	936STO0/0.80
0008ORI02	1	209.8	246.3	–7.2	66.4	936STO0/0.45
0008ORI03	1	207.5	247.1	–7.9	66.4	936STO0/0.56
0008ORI04	1	207.9	247.4	–7.8	66.2	936STO0/0.86
0008ORI05	1	208	247.4	–8.1	65.4	936STO0/0.95
0008ORI06	1	209	246.7	–7.6	66.3	936STO0/0.15
0008ORI07	10	210.6	246.5	–7.8	66.3	936STO0/0.32
0011EVI00	1	354	186.9	3.2	29.2	123NVI0/1.29
0011EVI02	1	357	185.9	5.5	26.6	123NVI0/1.20
0011EVI03	10	356.4	187.5	5.2	27.7	123NVI0/1.39
0011EVI04	10	357.2	185.7	5.3	26.6	123NVI0/1.10
0011EVI05	10	355.1	187.1	5.3	27.4	123NVI0/1.19
0017NTA00	1	224	197	1.3	28.3	631DAT0/2.15, 631DAT1/3.11
0017NTA02	1	214.1	193.9	2.7	29.6	025NOA1/2.99, 025NOA2/0.83, 631DAT0/1.37, 631DAT1/0.38, 630TAR0/0.77, 630TAR1/0.55
0017NTA03	1	224.5	191.6	1.8	28.1	631DAT1/2.66, 630TAR0/1.76, 630TAR1/1.94, 632NET1/1.03, 632NET0/0.75, 635ATU1/0.64, 635ATU0/1.19, 629ATS0/1.48, 629ATS1/1.42
0017NTA04	1	234.4	190.2	3	29.7	632NET1/2.17, 632NET0/1.82, 635ATU1/1.56, 635ATU0/0.72, 629ATS0/0.56, 629ATS1/0.51, 634TAT1/1.41, 633PTS0/1.49, 634TAT0/2.59
0017NTA05	1	219	192.2	–0.4	28.1	631DAT0/4.09, 631DAT1/3.42, 630TAR1/3.07, 632NET1/2.90, 632NET0/2.84, 635ATU1/2.86

Code	S	$\lambda_\odot$ (°)	$\lambda - \lambda_\odot$ (°)	β (°)	v_g	Possible members
0017NTA06	1	220	192	2.5	28	631DAT1/2.13, 630TAR0/1.10, 630TAR1/1.38, 632NET1/0.27, 632NET0/0.13, 635ATU1/0.41
0017NTA07	10	218.4	192	1.5	27.7	631DAT1/2.37, 630TAR0/1.60, 630TAR1/1.70, 632NET1/1.06, 632NET0/0.93
0018AND02	1	223	166.8	17.9	18.2	018AND3/5.17
0020COM01	1	265.7	243.3	21.3	63	032DLM0/0.20, 032DLM2/0.48
0020COM03	1	275.9	242.8	20.5	67	032DLM2/0.43, 499DDL0/0.00, 499DDL1/0.65
0020COM04	1	277.4	242.2	20.2	63.06	032DLM2/1.04, 499DDL0/0.65, 499DDL1/0.00
0020COM05	1	262.2	243.4	21.1	62.3	032DLM0/0.00, 032DLM2/0.37
0020COM06	1	261.7	246.8	30	64	032DLM1/0.00
0020COM07	1	268	243	20.9	64	032DLM0/0.37, 032DLM2/0.00, 499DDL0/0.43, 499DDL1/1.04
0020COM08	1	274	242.8	20.6	63.3	032DLM2/0.38, 499DDL0/0.07, 499DDL1/0.68
0021AVB00	1	28	155	–7.1	17.6	021AVB4/23.3
0021AVB02	1	28.9	167.5	1.2	16.6	343HVI2/2.88
0025NOA00	0	201.7	197.4	6	36.3	025NOA2/4.27
0025NOA01	0	205	196.9	2.5	30.1	017NTA2/2.99
0025NOA02	10	205.4	194.7	2.7	28.9	017NTA2/0.83
0026NDA00	1	139	207.1	6.4	40.5	342BPI0/1.00, 508TPI1/0.69, 508TPI0/0.59
0026NDA01	1	140.7	206	6.3	39.78	342BPI0/2.10, 508TPI1/1.53, 508TPI0/1.48
0026NDA02	1	139.6	199.8	3.6	42.3	033NIA5/0.72, 473LAQ2/0.49
0026NDA03	1	138.5	208.5	8	37.7	342BPI0/1.38, 508TPI1/1.49, 508TPI0/1.56
0026NDA04	1	140	208	6.7	38.3	342BPI0/0.00, 508TPI1/0.84, 508TPI0/0.80
0026NDA05	1	139	208.7	7.8	37.3	342BPI0/1.30, 508TPI1/1.61, 508TPI0/1.66
0026NDA06	1	147	207.3	6.9	39	342BPI0/0.80, 508TPI1/0.11, 508TPI0/0.00
0026NDA07	1	146.5	207.3	7	38.1	342BPI0/0.84, 508TPI1/0.00, 508TPI0/0.11
0026NDA08	1	141	208.4	6.8	38.4	342BPI0/0.42, 508TPI1/1.15, 508TPI0/1.14
0026NDA09	10	146.6	207.4	7	38.2	342BPI0/0.73, 508TPI1/0.12, 508TPI0/0.09
0027KSE01	1	15.7	209.9	33.3	45.01	839PSR0/1.84
0027KSE02	1	20	213.7	36.6	46.7	839PSR0/2.79
0028SOA00	0	198.5	196	–2.6	25.6	627NPS0/1.48, 627NPS1/1.66, 002STA4/1.67, 002STA2/1.94, 624XAR0/2.20, 624XAR1/2.23, 002STA1/3.42
0028SOA01	0	196	196.8	–4.2	29	627NPS0/0.75, 627NPS1/0.13, 002STA4/1.16, 002STA2/1.60, 624XAR0/1.74, 624XAR1/1.89
0028SOA02	10	197.7	196.8	–4.4	28.9	627NPS0/0.91, 627NPS1/0.30, 002STA4/1.20, 002STA2/1.62, 624XAR0/1.73, 624XAR1/1.89, 002STA1/3.09
0032DLM00	–2	262.2	243.4	21.1	62.3	032DLM1/9.44, 020COM1/0.20, 020COM7/0.37
0032DLM01	–2	261.7	246.8	30	64	020COM6/0.00
0032DLM02	–2	268	243	20.9	64	020COM5/0.37, 020COM1/0.48, 020COM7/0.00, 020COM8/0.38, 020COM3/0.43, 499DDL0/0.43, 020COM4/1.04, 499DDL1/1.04
0033NIA00	1	147.7	180.9	6.8	31.2	033NIA5/18.4
0033NIA05	1	148	199.3	4.1	31.3	026NDA2/0.72, 473LAQ2/0.37
0040ZCY03	10	21.8	297.7	58.6	42.5	409NCY0/3.00
0043ZSE00	0	0.1	266.1	17.1	67.42	043ZSE2/13.9
0043ZSE02	0	4	251.5	18.6	63.8	759THO0/2.80
0047DLI00	0	39	187.8	8.5	28.3	047DLI1/5.25
0055ASC01	–2	55.2	187.8	–1.4	35	150SOP6/2.80
0065GDE00	0	80.4	268.2	18.2	55.7	065GDE1/9.65
0069SSG00	1	78	197.7	–4.2	19.6	069SSG1/11.01, 803LSA1/2.76
0081SLY00	0	167	294.7	32.3	61	705UYL0/1.57

Code	S	$\lambda_\odot$ (°)	$\lambda - \lambda_\odot$ (°)	β (°)	v_g	Possible members
0081SLY01	0	186	278.8	26	67.7	424SOL0/0.42
0081SLY02	10	168.7	295.2	33.4	59	705UYL0/0.40
0086OGC00	0	206.4	199.5	–24.5	3.3	407OEE0/1.47
0090JCO00	0	301	240.3	18.9	63.9	506FEV3/0.85
0090JCO01	0	304	241.6	18.8	65.7	506FEV3/0.40, 506FEV2/1.20
0093VEL02	0	296	228.6	–62.9	35	309GVE0/2.81
0105OCN01	0	323.4	242.8	–50.9	51.4	315OCA0/1.91
0105OCN02	0	323.4	242.5	–51	45.5	315OCA0/2.11
0108BTU00	0	358	301.6	–73.9	36.3	130DME0/2.37
0108BTU01	0	358.7	291.4	–72.7	32.1	130DME0/1.58
0123NVI00	0	358	186.3	4.4	23	011EVI0/1.29, 011EVI5/1.19, 011EVI3/1.39, 011EVI2/1.20, 011EVI4/1.10
0130DME00	0	356.7	293	–74.2	33	108BTU0/2.37, 108BTU1/1.58
0139GLI00	0	39	186.2	3.8	26	343HVI1/3.03
0149NOP01	0	52	184.7	11.5	28	456MPS0/1.92, 456MPS1/2.84
0149NOP02	0	58.3	196.4	6.2	28.5	150SOP3/2.51
0150SOP03	0	54	194.2	4.8	34.7	149NOP2/2.51
0150SOP06	10	53.4	188.8	–4	27.9	055ASC1/2.80
0152NOC00	1	47.8	321.6	15.4	33	357PHP1/2.68
0156SMA00	1	52.7	341.9	–4.1	28.9	355XIC0/1.77
0156SMA02	1	47.1	342	–3.7	28.3	355XIC0/2.02
0164NZC02	1	108.09	208.8	13.3	38.33	548FAQ1/1.77
0165SZC01	1	80.5	218.9	–12.8	38.6	195BIN1/2.48
0165SZC02	1	104	209.2	–11.3	39.2	370MIC0/1.13
0165SZC03	10	106.2	210	–11.8	37.6	370MIC0/0.42
0167NSS01	0	86.6	191.3	3.2	26.5	861JXS1/1.30, 861JXS0/2.24
0171ARI00	1	76.7	328.4	7.8	35.7	680JEA1/1.77, 680JEA0/2.18
0175JPE01	1	108	244.7	15.3	68.1	522SAP0/0.98
0175JPE02	1	110.9	244.1	14.5	63.9	522SAP0/0.40, 462JGP1/2.15, 462JGP0/1.01
0175JPE03	1	109	245.2	14.6	64.5	522SAP0/0.76
0175JPE04	1	120.8	243.7	13.6	62.6	522SAP0/1.06, 462JGP1/1.42, 462JGP0/0.00
0175JPE05	1	120.5	242.2	13.3	62.31	522SAP0/2.37, 462JGP1/0.00, 462JGP0/1.42
0175JPE06	1	108	244.2	14.2	64	522SAP0/0.23
0175JPE07	10	116.5	244.2	14.2	64.2	522SAP0/0.25, 462JGP1/2.12, 462JGP0/0.84
0176PHE00	0	110.3	252.6	–55	47	PHE0/176PHE1/0.00, 769PPH0/1.46
0176PHE01	0	110.3	252.6	–55	47	PHE1/176PHE0/0.00, 769PPH0/1.46
0176PHE02	10	126.8	283.5	–58.8	46.2	798ACD0/2.18
0177BCA00	0	126.6	262.1	54.1	50.4	871DCD0/2.25
0187PCA01	1	117.5	289.7	53.1	44	550KPC0/2.20
0190BPE02	10	131.1	294.2	27.5	60.5	435MPR0/1.85
0194UCE01	10	169.1	249.3	–16.8	65.4	583TTA0/0.69
0195BIN01	10	82.1	218.4	–15.3	34.8	165SZC1/2.48
0216SPI00	0	184	199.7	–4.4	26.5	627NPS0/2.76
0216SPI01	0	183	196.2	–2.5	28.6	627NPS0/1.34, 627NPS1/1.63
0216SPI02	0	182.9	196.9	–5.4	31.9	627NPS0/1.92, 627NPS1/1.37
0219SAR00	0	179	204.7	6.9	36.7	714RPI1/2.61
0219SAR02	0	180.2	209.2	8.3	31.2	714RPI0/1.79, 714RPI1/2.52
0219SAR03	0	178.3	211.3	1.2	33.7	706ZPI0/1.39

Code	S	$\lambda_\odot$ (°)	$\lambda - \lambda_\odot$ (°)	β (°)	v_g	Possible members
0226ZTA00	0	196	250.2	–8.7	67.2	718XGM0/2.00
0232BCN01	0	214	259.2	–27.9	65.1	558TSM0/1.69
0237SSA00	0	202	204.4	–2.6	40.5	946TEA0/1.35
0237SSA01	0	206	208	3.4	45.5	417ETT0/0.59
0245NHD01	10	225.7	259.4	–26.1	64.5	558TSM0/0.96, 558TSM1/1.08
0253CMI02	0	255.2	209.5	–9.6	37.7	610SGM0/1.51
0256ORN00	0	257.3	187.2	2.2	24.9	639NNT0/1.07
0256ORN01	0	266	190.6	2.6	28.2	726DEG0/2.54
0256ORN02	0	258	185.9	2.4	24.7	639NNT0/0.32, 726DEG0/2.18
0256ORN03	10	263.5	188.4	2.1	26.8	726DEG0/0.42
0257ORS02	1	257.9	183.4	–5.6	24.6	636MTA1/1.86, 638DZT1/2.88
0257ORS03	1	243	190.8	–4.7	27.9	636MTA0/2.14
0257ORS04	10	247.6	190.3	–5.2	27.6	636MTA0/1.53
0259CAR00	4	264	269.1	–70.4	38.9	312ECA0/0.10
0281OCT01	1	197.1	279.1	60.1	45.3	383LDR0/2.78
0285GTA00	0	232.8	188.7	–3	14.1	002STA0/2.99, 637FTR1/2.79, 637FTR0/2.28, /625LTA0/2.36, 625LTA1/3.64
0286FTA01	0	242	184	–6.3	23.3	625LTA1/2.40, 636MTA1/1.20
0286FTA02	10	242.3	182.8	–6.5	22.8	636MTA1/2.32
0289DNA01	10	247.2	187.2	2.7	25.9	634TAT1/1.69, 633PTS0/1.67, 634TAT0/0.46, 639NNT0/1.02
0300ZPU00	0	254.7	249.1	–60.4	39	301PUP0/1.94
0301PUP00	0	255	250.7	–62.2	38	300ZPU0/1.94, 302PVE0/3.00
0302PVE00	0	256.3	255.9	–60.5	39	746EVE0/2.95, 255PUV0/1.13, 301PUP0/3.00
0303LVL00	0	269.7	249.5	–59.5	33	304CVE0/0.91
0304CVE00	0	273	248.5	–58.8	36	303LVL0/0.91
0309GVE00	0	288	222.5	–63.3	33	093VEL2/2.81
0312ECA00	0	263.7	269.4	–70.4	39	259CAR0/0.10
0313ECR00	0	280.7	281.1	–59.6		785TCD0/0.94, 785TCD1/1.12
0315OCA00	0	322.7	245.8	–50.6	51	105OCN1/1.91, 105OCN2/2.11
0321TCB00	1	296.5	279.2	52.4	38.66	332BCB0/1.91
0330SSE00	1	275.5	325.3	20.6	42.3	320OSE0/0.61
0330SSE01	1	275	325.3	20.5	42.67	320OSE0/0.71
0332BCB00	6	296	276.1	52.7	42	321TCB0/1.91
0334DAD02	10	251.3	265	62.1	41.3	392NID1/2.22
0337NUE00	1	167.9	259.3	–20.7	65.9	030FER0/0.89
0337NUE01	1	165	268.4	–22.3	67	552PSO2/1.65, 552PSO1/2.27, 552PSO0/1.78
0340TPY00	0	249.4	262	–39.1	60.1	844DTP0/0.36
0340TPY01	0	264	259.6	–33.5	62.3	498DMH0/1.05, 498DMH1/1.14
0340TPY02	0	264	259.6	–33.5	63	498DMH0/1.05, 498DMH1/1.14
0340TPY03	10	272	260.3	–31.4	63.7	498DMH0/1.24, 498DMH1/1.47
0342BPI00	–2	140	208	6.7	38.3	026NDA3/1.38, 026NDA0/1.00, 026NDA5/1.30, 026NDA4/0.00, 026NDA1/2.10, 026NDA8/0.42, 026NDA7/0.84, 508TPI1/0.84, 026NDA9/0.73, 026NDA6/0.80, 508TPI0/0.80
0343HVI01	1	32	183.7	2.1	24.1	139GLI0/3.03
0343HVI02	1	38	169.2	–1.1	17.2	021AVB2/2.88
0355XIC00	0	54	342.9	–5.5	16.5	156SMA2/2.02, 156SMA0/1.77
0357PHP01	10	54.5	323.6	17.2	33	152NOC0/2.68
0359MZC00	0	60	272.8	43.3	29.2	665MUC0/1.66

Code	S	$\lambda_\odot$ (°)	$\lambda - \lambda_\odot$ (°)	β (°)	v_g	Possible members
0367OPG00	0	100	252.6	37.5	28.5	431JIP2/0.30, 431JIP1/0.11, 431JIP3/0.17, 431JIP0/0.23
0368JAD00	0	101	310.1	32.7	34.7	373TPR0/3.12
0370MIC00	0	104	209.9	–12.2	38	165SZC2/1.13, 165SZC3/0.42
0371APG00	0	106	255.7	18.7	35.9	867FPE0/2.56
0373TPR00	0	106	308	30.1	53	368JAD0/3.12
0383LDR00	0	196	280.6	57.4	37.5	281OCT1/2.78
0385AUM00	0	209	288.1	54.4	35.6	387OKD0/1.63
0387OKD00	0	216	286.7	55.8	37.3	385AUM0/1.63
0388CTA00	1	220	205.8	3.5	42.1	417ETT0/1.95
0388CTA01	1	221	204.9	5	41.1	417ETT0/3.00
0388CTA02	10	216.3	205.9	5.3	41.3	417ETT0/2.20
0392NID00	0	241	270.1	62.5	43	753NED0/1.01
0392NID01	0	242	260.9	63.3	41.9	334DAD2/2.22
0392NID02	10	225.4	266.7	61.7	42.4	753NED0/1.29
0394ACA00	0	247	215.8	–40.3	42	559MCB1/2.44
0394ACA01	0	245	215.6	–40	43.1	559MCB1/2.69
0394ACA02	10	247.4	215.8	–40.2	43.8	559MCB1/2.56
0395GCM01	10	270.1	209.6	–30.2	43	398DCM1/2.76
0398DCM00	0	266	211	–36	42.8	786SXP1/3.29
0398DCM01	0	272	210.2	–32.9	42.9	395GCM1/2.76
0407OEE00	0	201	199.2	–25.9	25.4	086OGC0/1.47
0409NCY00	0	30	293.7	56.5	42	040ZCY3/3.00
0411CAN01	1	107	298.1	32.9	57.5	507UAN0/1.57
0411CAN02	10	106.6	298.1	33	56.8	507UAN0/1.72
0417ETT00	0	211	207.7	3.9	47	237SSA1/0.59, 388CTA2/2.20, 388CTA0/1.95, 388CTA1/3.00
0424SOL00	0	186	278.7	25.6	68	081SLY1/0.42, 425PSA1/2.78
0424SOL01	0	178	294.8	26.8	62.4	901TLC0/0.63
0425PSA01	0	195	277.3	23.1	66	081SLY1/3.19, 424SOL0/2.78, 613TLY1/1.07, 613TLY0/0.95
0428DSV00	1	267.414	293.7	14.8	66	513EPV0/1.82
0428DSV01	1	262	295	13.5	66.2	513EPV0/0.21
0428DSV02	10	278.8	292.2	16	66.8	500JPV0/1.47, 500JPV1/1.40
0430POR00	0	178.424	256.1	–14.2	68	479SOO1/2.24
0431JIP00	1	94.456	252.9	37.4	59	367OPG0/0.23
0431JIP01	1	94	252.8	37.5	58.5	367OPG0/0.11
0431JIP02	10	93.6	252.5	37.8	58.5	367OPG0/0.30
0431JIP03	10	94	252.5	37.4	58.9	367OPG0/0.17
0435MPR00	0	139.64	296.3	27.5	54.2	190BPE2/1.85, 696OAU1/3.14, 696OAU0/3.24
0439ASX00	0	237.37	280.4	–13	68.8	483NAS0/2.22, 483NAS1/2.56
0456MPS00	0	61.5	183	10.6	25.4	149NOP1/1.92
0456MPS01	0	61.7	182	10.6	24.63	149NOP1/2.84
0456MPS03	10	79.3	173.4	16	21.2	460LOP1/2.60
0460LOP01	0	85.9	171.1	17.5	19.62	456MPS3/2.60
0462JGP00	–2	120.8	243.7	13.6	62.6	175JPE2/1.01, 522SAP0/1.06, 175JPE7/0.84, 175JPE5/1.42, 175JPE4/0.00
0462JGP01	–2	120.5	242.2	13.3	62.31	175JPE2/2.15, 522SAP0/2.37, 175JPE7/2.12, 175JPE5/0.00, 175JPE4/1.42
0473LAQ02	10	147.5	199.7	4.1	32.2	026NDA2/0.49, 033NIA5/0.37
0479SOO01	0	185.7	254.6	–12.5	66.87	430POR0/2.24

Code	S	$\lambda_\odot$ (°)	$\lambda - \lambda_\odot$ (°)	β (°)	v_g	Possible members
0483NAS00	0	231.4	281.8	–14.7	71.1	439ASX0/2.22
0483NAS01	0	232	280.3	–15.5	69	439ASX0/2.56
0488NSU00	0	241.6	244.9	42.9	55.3	527UUM0/0.66
0488NSU01	0	243	246	42.7	55.1	527UUM0/0.31
0488NSU02	10	242.3	244.8	43.3	54.9	527UUM0/0.78
0498DMH00	0	264.8	259.8	–32.5	63.8	340TPY1/1.05, 340TPY2/1.05, 340TPY3/1.24
0498DMH01	0	269	260.6	–32.8	63.7	340TPY1/1.14, 340TPY2/1.14, 340TPY3/1.47
0499DDL00	–2	275.9	242.8	20.5	67	020COM7/0.43, 032DLM2/0.43, 020COM8/0.07, 020COM3/0.00, 020COM4/0.65
0499DDL01	–2	277.4	242.2	20.2	63.06	020COM7/1.04, 032DLM2/1.04, 020COM8/0.68, 020COM3/0.65, 020COM4/0.00
0500JPV00	0	285.6	291.5	17.3	66.2	428DSV2/1.47
0500JPV01	0	288.2	290.9	16.5	65.05	428DSV2/1.40
0505AIC00	0	145.4	207.8	–7.5	37.24	640AOA0/1.57, 640AOA1/1.69
0505AIC02	10	151.8	206.9	–6.5	38.5	642PCE0/2.92
0506FEV02	1	314	240.5	18.1	62.9	090JCO1/1.20
0506FEV03	10	303.9	241.2	18.9	63.1	090JCO0/0.85, 090JCO1/0.40
0507UAN00	0	98	297.7	31.4	58.8	411CAN2/1.72, 411CAN1/1.57
0507UAN02	10	108.8	285.9	34.2	59.7	549FAN1/0.70, 549FAN0/1.09, 549FAN2/0.18
0508TPI00	–2	147	207.3	6.9	39	026NDA3/1.56, 026NDA0/0.59, 026NDA5/1.66, 026NDA4/0.80, 342BPI0/0.80, 026NDA1/1.48, 026NDA8/1.14, 026NDA7/0.11, 026NDA9/0.09, 026NDA6/0.00
0508TPI01	–2	146.5	207.3	7	38.1	026NDA3/1.49, 026NDA0/0.69, 026NDA5/1.61, 026NDA4/0.84, 342BPI0/0.84, 026NDA1/1.53, 026NDA8/1.15, 026NDA7/0.00, 026NDA9/0.12, 026NDA6/0.11
0510JRC00	1	84	262.8	54.4	50.2	521JRP0/0.18
0510JRC01	1	84	261.6	55.1	50.9	521JRP0/1.11
0510JRC02	10	84	262.5	55.4	48.5	521JRP0/1.03
0510JRC03	10	84	262.2	55.5	49.3	521JRP0/1.20
0513EPV00	0	258	294.8	13.3	66.4	428DSV1/0.21, 428DSV0/1.82
0514OMC01	10	57.7	243.5	–12.7	65	597TTS0/0.41
0515OLE00	0	296	208	–6.9	41.5	643OLS0/1.37, 793KCA1/1.29, 793KCA0/0.53
0515OLE01	10	279.3	210.2	–7.8	41.1	643OLS0/0.94, 793KCA1/1.07, 793KCA0/1.79
0521JRP00	–2	84.1	263.1	54.4	50.3	510JRC0/0.18, 510JRC1/1.11, 510JRC2/1.03, 510JRC3/1.20
0522SAP00	0	112	244.5	14.3	63.9	175JPE1/0.98, 175JPE6/0.23, 175JPE3/0.76, 175JPE2/0.40, 175JPE7/0.25, 175JPE5/2.37, 462JGP1/2.37, 175JPE4/1.06, 462JGP0/1.06
0527UUM00	0	240.4	245.8	43	55.1	488NSU0/0.66, 488NSU2/0.78, 488NSU1/0.31
0542DES00	0	263.3	257.1	–10.3	69.4	824DEX0/2.94
0548FAQ01	0	113	207	13.4	37.7	164NZC2/1.77
0549FAN00	1	114	284.7	34.8	60.1	507UAN2/1.09
0549FAN01	1	112	286.4	34.8	60.2	507UAN2/0.70
0549FAN02	10	116.8	286	34.1	59.2	507UAN2/0.18
0550KPC00	0	119	286.2	52.6	50.2	187PCA1/2.20
0552PSO00	0	166.3	268.7	–24	66.5	337NUE1/1.78
0552PSO01	0	159	269.5	–24.3	65.8	337NUE1/2.27
0552PSO02	10	158.4	267.4	–23.6	66.1	337NUE1/1.65
0558TSM00	0	221	260.3	–26.6	64.2	232BCN1/1.69, 245NHD1/0.96
0558TSM01	0	227	258.5	–25.4	64.6	245NHD1/1.08, 245NHD0/2.08
0559MCB01	10	241.1	215.6	–42.7	43.2	394ACA1/2.69, 394ACA0/2.44, 394ACA2/2.56

Code	S	$\lambda_\odot$ (°)	$\lambda - \lambda_\odot$ (°)	β (°)	v_g	Possible members
0583TTA00	0	164	249.6	–17.4	65.2	194UCE1/0.69
0597TTS00	0	53	243.2	–12.3	67	514OMC1/0.41
0610SGM00	0	263	209.1	–8.1	40.7	253CMI2/1.51
0613TLY00	0	202	277.2	24	64	425PSA1/0.95
0613TLY01	10	200.4	276.9	22.1	67.4	425PSA1/1.07
0623XCS00	0	120	183.7	8.8	24.5	001CAP1/1.12
0623XCS01	10	117.1	184	8.5	24.5	001CAP1/1.16
0624XAR00	0	205	195.1	–4.6	28.5	002STA4/0.66, 028SOA1/1.74, 002STA2/0.27, 028SOA2/1.73, 028SOA0/2.20, 002STA1/1.40, 002STA6/2.95, 626LCT1/2.86
0624XAR01	10	206	194.9	–4.5	28.4	002STA4/0.77, 028SOA1/1.89, 002STA2/0.33, 028SOA2/1.89, 028SOA0/2.23, 002STA1/1.29, 002STA6/2.82, 626LCT1/2.71, 002STA5/1.92, 626LCT0/1.63
0625LTA00	0	231	187.8	–5.2	25.7	002STA0/1.39, 637FTR1/2.61, 637FTR0/2.52, 285GTA0/2.36
0625LTA01	10	232.8	186.3	–5.8	24.1	002STA0/0.77, 285GTA0/3.64, 286FTA1/2.40
0626LCT00	0	216	193.3	–4.6	27.9	624XAR1/1.63, 002STA1/0.79, 002STA6/1.38, 002STA5/0.36, 002STA3/1.74, 628STS0/1.30, LCT0/628STS1/1.15, 637FTR1/2.84, 637FTR0/2.96
0626LCT01	10	215	192.2	–4.8	27.4	624XAR0/2.86, 624XAR1/2.71, 002STA1/1.66, 002STA6/0.81, 002STA5/0.81, 002STA3/0.66, LCT1/628STS0/0.22, 628STS1/0.20, 637FTR1/1.76, 637FTR0/1.89
0627NPS00	0	189	197.1	–3.5	29.4	216SPI2/1.92, 216SPI1/1.34, 216SPI0/2.76, 002STA4/1.65, 028SOA1/0.75, 002STA2/2.11, 028SOA2/0.91, 028SOA0/1.48
0627NPS01	10	190.6	196.7	–4.1	28.9	216SPI2/1.37, 216SPI1/1.63, 002STA4/1.09, 028SOA1/0.13, 002STA2/1.55, 028SOA2/0.30, 028SOA0/1.66
0628STS00	0	223	192	–4.7	28.2	626LCT1/0.22, 002STA5/1.03, 626LCT0/1.30, 002STA3/0.45, 637FTR1/1.55, 637FTR0/1.67
0628STS01	10	223	192.1	–4.6	28.6	626LCT1/0.20, 002STA5/0.92, 626LCT0/1.15, 002STA3/0.63, 637FTR1/1.74, 637FTR0/1.81
0629ATS00	0	233	190.2	2.4	27.5	017NTA3/1.48, 632NET1/2.04, 632NET0/1.66, 635ATU1/1.37, 635ATU0/0.30, 017NTA4/0.56, 634TAT1/1.39, 633PTS0/1.43
0629ATS01	10	233	190.4	2.5	27.6	017NTA3/1.42, 632NET1/1.93, 632NET0/1.55, 635ATU1/1.26, 635ATU0/0.23, 017NTA4/0.51, 634TAT1/1.50, 633PTS0/1.54
0630TAR00	0	220	193.1	2.6	28.1	017NTA2/0.77, 631DAT0/2.11, 631DAT1/1.05, 017NTA7/1.60, 017NTA6/1.10, 017NTA3/1.76, 632NET1/0.83, 632NET0/1.22, 635ATU1/1.51
0630TAR01	10	221.6	193.4	2.5	28.9	017NTA2/0.55, 631DAT0/1.82, 631DAT1/0.75, 017NTA7/1.70, 017NTA5/3.07, 017NTA6/1.38, 017NTA3/1.94, 632NET1/1.11, 632NET0/1.48, 635ATU1/1.78, 635ATU0/2.85
0631DAT00	0	216	195.2	2.4	29.3	017NTA2/1.37, 017NTA5/4.09, 630TAR0/2.11, 630TAR1/1.82, 017NTA0/2.15, 632NET1/2.92
0631DAT01	10	216.2	194.1	2.5	29	017NTA2/0.38, 017NTA7/2.37, 017NTA5/3.42, 017NTA6/2.13, 630TAR0/1.05, 630TAR1/0.75, 017NTA0/3.11, 017NTA3/2.66, 632NET1/1.86
0632NET00	0	227	191.9	2.4	28	017NTA7/0.93, 017NTA5/2.84, 017NTA6/0.13, 630TAR0/1.22, 630TAR1/1.48, 017NTA3/0.75, 635ATU1/0.29, 635ATU0/1.37, 629ATS0/1.66, 629ATS1/1.55, 017NTA4/1.82
0632NET01	10	225.4	192.3	2.5	28.3	631DAT0/2.92, 631DAT1/1.86, 017NTA7/1.06, 017NTA5/2.90, 017NTA6/0.27, 630TAR0/0.83, 630TAR1/1.11, 017NTA3/1.03, 635ATU1/0.68, 635ATU0/1.75, 629ATS0/2.04, 629ATS1/1.93, 017NTA4/2.17
0633PTS00	0	240	188.8	2.4	26.7	635ATU0/1.72, 629ATS0/1.43, 629ATS1/1.54, 017NTA4/1.49, 634TAT1/0.13, 634TAT0/1.22, 289DNA1/1.67, 639NNT0/2.65
0634TAT00	0	244	187.6	2.5	25.8	017NTA4/2.59, 633PTS0/1.22, 289DNA1/0.46, 639NNT0/1.44
0634TAT01	10	239.8	188.9	2.5	26.7	635ATU0/1.69, 629ATS0/1.39, 629ATS1/1.50, 017NTA4/1.41, 633PTS0/0.13, 289DNA1/1.69, 639NNT0/2.68

Code	S	$\lambda_\odot$ (°)	$\lambda - \lambda_\odot$ (°)	β (°)	v_g	Possible members
0635ATU00	0	231	190.5	2.4	27.4	630TAR1/2.85, 017NTA3/1.19, 632NET1/1.75, 632NET0/1.37, 629ATS0/0.30, 629ATS1/0.23, 017NTA4/0.72, 634TAT1/1.69, 633PTS0/1.72
0635ATU01	10	228.8	191.6	2.4	28.4	017NTA5/2.86, 017NTA6/0.41, 630TAR0/1.51, 630TAR1/1.78, 017NTA3/0.64, 632NET1/0.68, 632NET0/0.29 629ATS0/1.37, 629ATS1/1.26, 017NTA4/1.56
0636MTA00	0	252	188.7	–5.3	27.4	257ORS3/2.14, 257ORS4/1.53, 638DZT0/2.16, 638DZT1/2.45
0636MTA01	10	250.1	185.2	–6.2	24.4	286FTA1/1.20, 286FTA2/2.32, 257ORS2/1.86, 638DZT0/1.76
0637FTR00	0	225	190.3	–4.6	27.4	626LCT1/1.89, 002STA5/2.70, 626LCT0/2.96, 002STA3/1.24, 628STS0/1.67, 628STS1/1.81, 625LTA0/2.52, 285GTA0/2.28
0637FTR01	10	224.5	190.5	–5.2	26.7	626LCT1/1.76, 002STA5/2.54, 626LCT0/2.84, 002STA3/1.10, 628STS0/1.55, 628STS1/1.74, FTR1/625LTA0/2.61, 285GTA0/2.79
0638DZT00	0	260	186.6	–5.1	25.8	636MTA1/1.76, 636MTA0/2.16
0638DZT01	10	260.3	186.3	–5.3	25.9	636MTA0/2.45, 257ORS2/2.88
0639NNT00	10	249	186.2	2.5	24.9	634TAT1/2.68, 633PTS0/2.65, 634TAT0/1.44, 289DNA1/1.02, 256ORN0/1.07, 256ORN2/0.32
0640AOA00	0	137	206.8	–8.7	38.2	005SDA1/2.17, 005SDA8/2.50, 005SDA5/2.13, 005SDA7/1.05, 505AIC0/1.57
0640AOA01	10	140.5	206.6	–8.7	37.8	505AIC0/1.69
0641DRG00	0	262	207.8	10.5	39.5	004GEM6/0.25, 004GEM4/0.59, 004GEM3/0.31, 004GEM2/0.41, 004GEM1/0.21, 004GEM5/0.27, 004GEM0/0.15 949SGD0/0.39
0642PCE00	0	161	204.4	–8.1	36.5	505AIC2/2.92
0643OLS00	0	287	209.3	–7.4	44.9	515OLE1/0.94, 793KCA1/0.27, 793KCA0/0.85, 515OLE0/1.37
0644JLL00	0	288	207.3	7.5	38.6	747JKL0/2.81
0644JLL01	10	270.4	210.1	7.2	38	914AGE0/2.43
0652OSP01	10	21.5	244.4	7.7	66.7	958SXS0/1.34
0665MUC00	10	58.7	274.9	42.8	57.1	359MZC0/1.66
0680JEA00	0	85	326.8	9.2	39.1	171ARI0/2.18
0680JEA01	10	83.8	328.9	9.5	39.1	171ARI0/1.77
0692EQA01	10	134.1	175.5	10.9	20.9	001CAP0/2.50
0696OAU00	0	148	298	24.6	62.1	435MPR0/3.24
0705UYL00	0	169	295.4	33.7	59.2	081SLY0/1.57, 081SLY2/0.40
0706ZPI00	0	172	209.9	1.2	38.2	219SAR3/1.39
0710IOL00	0	317	211.8	6.2	40.4	748JTL0/1.37
0714RPI00	0	177	210.3	6.8	43.9	219SAR2/1.79
0714RPI01	10	182.2	207.3	6.6	41.2	219SAR0/2.61, 219SAR2/2.52
0718XGM00	0	206	250.8	–10.6	68.1	226ZTA0/2.00
0726DEG00	0	268	188	2.3	26.8	256ORN2/2.18, 256ORN3/0.42, 256ORN1/2.54
0746EVE00	0	252	261.2	–59.3	44.4	255PUV0/1.96, 302PVE0/2.95
0747JKL00	10	287.6	209.8	6.2	39.5	644JLL0/2.81
0748JTL00	10	311.3	210.5	5.8	40.2	710IOL0/1.37
0749NMV00	0	339	208.2	6.4	42.7	980SEV0/2.75
0753NED00	0	232.8	268	62.9	42	392NID2/1.29, 392NID0/1.01
0758VOL00	0	279.197	301.3	–78.1	28.4	787KVO0/0.57
0758VOL01	10	279.4	299.7	–77.5	29.8	787KVO0/0.87
0759THO00	0	8	248.5	18.7	57	043ZSE2/2.80
0761PPC00	40	200	287.2	–53.7	32.9	773THP0/0.00
0769PPH00	0	111	251.3	–53.7	37.6	176PHE0/1.46, 176PHE1/1.46
0770LCA00	0	195	232.9	–55.2	40.5	904OCO0/1.86
0773THP00	0	200	287.2	–53.7	32.9	761PPC0/0.00

Code	S	$\lambda_\odot$ (°)	$\lambda - \lambda_\odot$ (°)	β (°)	v_g	Possible members
0777OPU00	0	212	289.4	–53.8	31.9	779OLV0/1.43
0779OLV00	0	221	291	–52.7	33.9	777OPU0/1.43
0780NPU00	0	224	280.5	–57.5	35.4	781NLV0/2.38
0781NLV00	0	232	284.9	–57.7	36.5	780NPU0/2.38
0785TCD00	0	276	282.4	–60.3	41.7	313ECR0/0.94
0785TCD01	10	277.9	280.1	–58.6	46.3	313ECR0/1.12
0786SXP01	10	275.7	207.5	–37.8	40.5	398DCM0/3.29
0787KVO00	0	280	303.6	–77.8	29.6	758VOL0/0.57, 758VOL1/0.87
0793KCA00	0	289	208.5	–7	47.3	515OLE1/1.79, 643OLS0/0.85, 515OLE0/0.53
0793KCA01	10	288.6	209.1	–7.6	46.9	515OLE1/1.07, 643OLS0/0.27, 515OLE0/1.29
0798ACD00	10	130.5	287.5	–59.5	44.5	176PHE2/2.18
0803LSA01	10	76.3	200.3	–3.3	36.9	069SSG0/2.76
0823FCE00	10	163.9	213.6	–32.3	44.8	976SON0/2.83
0824DEX00	10	268.3	254.7	–12.1	69.3	542DES0/2.94
0827NPE00	10	28.9	303.5	14.5	61.8	985TFA0/0.44
0839PSR00	10	25.1	211.7	34.3	46.3	027KSE1/1.84, 027KSE2/2.79
0844DTP00	10	249.6	261.5	–39.1	60.6	340TPY0/0.36
0849SZE00	10	172.5	230.8	–25	56.9	948SER0/0.31
0861JXS00	0	93	190	5	30.5	167NSS1/2.24
0861JXS01	10	92.2	190.8	4.4	29.6	167NSS1/1.30
0862SSR00	10	362.2	239.8	13.6	62.7	968UOD0/2.75
0867FPE00	10	96.7	254.6	16.4	66.8	371APG0/2.56
0871DCD00	10	122.9	258.6	55.1	49.9	177BCA0/2.25
0874PXS00	10	174.8	250.7	17	66.5	208SPE3/3.38
0877OHD00	10	205.7	296.4	–6.8	67	959TLD0/0.30
0896OTA00	10	179.3	267.4	–5.5	72.4	984OST0/2.48
0901TLC00	10	183.4	294.8	27.4	61.4	424SOL1/0.63
0904OCO00	10	198.3	236	–54.7	42.1	770LCA0/1.86
0914AGE00	10	261.9	207.8	8.2	12.2	004GEM6/2.30, 004GEM4/1.99, 004GEM3/2.20, 004GEM2/2.00, 004GEM1/2.20, 004GEM5/2.29, 641DRG0/2.34, 004GEM0/2.44, 949SGD0/2.44, 644JLL1/2.43
0924SAN00	10	196.7	214.4	29.4	16.8	986SAD0/1.07
0936STO00	10	208.8	246.7	–7.5	50.79	008ORI3/0.56, 008ORI4/0.86, 008ORI5/0.95, 008ORI0/0.05, 008ORI1/0.80, 008ORI6/0.15, 008ORI2/0.45, 008ORI7/0.32
0938PEA00	10	139	283.4	37	45.08	007PER7/1.27, 007PER4/1.38, 007PER2/1.76, 007PER3/1.01, 992GPE0/1.32, 942EPE0/1.60, 007PER5/0.87, 007PER6/1.51, 007PER0/1.81, 007PER1/1.37, 981AGP0/0.81
0942EPE00	10	139.9	283	38.5	20.26	007PER7/0.44, 938PEA0/1.60, 007PER4/0.31, 007PER2/0.35, 007PER3/1.05, 992GPE0/0.35, 007PER5/0.89, 007PER6/0.24, 007PER0/0.74, 007PER1/0.24, 981AGP0/0.91
0946TEA00	10	199.3	203.2	–3.2	34.95	237SSA0/1.35
0948SER00	10	171.3	231.1	–25	55.36	849SZE0/0.31
0949SGD00	10	262.3	208.2	10.6	24.02	004GEM6/0.19, 004GEM4/0.47, 004GEM3/0.26, 004GEM2/0.47, 004GEM1/0.32, 914AGE0/2.44, 004GEM5/0.18, 641DRG0/0.39, 004GEM0/0.50
0958SXS00	10	25.6	243.1	7.6	64.9	652OSP1/1.34
0959TLD00	10	204.4	296.7	–6.8	65.41	877OHD0/0.30
0968UOD00	10	4.8	241.9	11.8	63.71	862SSR0/2.75
0976SON00	10	169	216.9	–32.6	45.42	823FCE0/2.83
0980SEV00	10	337.9	205.4	6.3	38.52	749NMV0/2.75

Code	S	$\lambda_\odot$ (°)	$\lambda - \lambda_\odot$ (°)	β (°)	v_g	Possible members
0981AGP00	10	141.1	283.6	37.8	39.97	007PER7/0.50, 938PEA0/0.81, 007PER4/0.63, 007PER2/0.98, 007PER3/0.96, 992GPE0/0.76, 942EPE0/0.91, 007PER5/0.68, 07PER6/0.75, 007PER0/1.39, 007PER1/0.68
0984OST00	10	170.6	268.6	–3.3	70.3	896OTA0/2.48
0985TFA00	10	24.3	303.6	14.9	60.61	827NPE0/0.44
0986SAD00	10	194.8	214.6	28.4	16.43	924SAN0/1.07
0992GPE00	10	139.5	282.8	38.2	32.86	007PER7/0.45, 938PEA0/1.32, 007PER4/0.39, 007PER2/0.67, 007PER3/0.70, 942EPE0/0.35, 007PER5/0.54, 007PER6/0.45, 007PER0/0.65, 007PER1/0.25, 981AGP0/0.76
1030FER00	10	167.8	258.5	–21.2	65.7	337NUE0/0.89

Table 4 – List of showers with a difference in geocentric velocity of more than 5 km/s (SD version 2018 January 13 20h35m17s).

Code	v_g min	v_g max	Code	v_g min	v_g max	Code	v_g min	v_g max	Code	v_g min	v_g max
003SIA	28.9	34.8	105OCN	38.4	51.4	188XRI	38.4	45.4	257ORS	21.5	27.9
011EVI	26.6	34.2	107DCH	34.2	42.6	189DMC	24.3	31.1	288DSA	15.2	21.4
015URS	32.6	37.6	118GNO	56	68	190BPE	60.5	67.4	289DNA	14.6	25.9
020COM	62.3	67.7	150SOP	24.3	34.7	195BIN	14.1	34.8	319JLE	51.4	60.4
025NOA	28.9	36.3	152NOC	33	40.3	215NPI	25.6	31.2	320OSE	38.9	45
026NDA	37.3	42.3	161SSC	23	28.1	216SPI	23.6	31.9	323XCB	44.25	50.1
065GDE	55.7	64.9	165SZC	33.2	39.2	219SAR	31.2	36.7	341XUM	40.2	45.6
069SSG	19.6	25.7	171ARI	35.7	41.5	226ZTA	56.5	67.2	343HVI	17.2	24.1
081SLY	59	67.7	175JPE	61.3	68.1	233OCC	10	15.3	424SOL	62.4	68
088ODR	19.6	28.6	179SCA	26.9	34.1	237SSA	40.5	45.5	641DRG	39.5	45.4
103TCE	59	64.6	182OCY	32	39.4	243ZCN	63.4	69	712FDC	32	37.7

Table 5 – Comments for Tables 1 to 4.

Code	Comments
001CAP	623XCS is near CAP1
002STA	consisted of 2 components at least / second peak around $\lambda_\odot$ = 200 / many related activities: 028SOA, 216SPI, 257ORS, 624XAR, 625LTA, 626LCT, 627NPS, 628STS, 636MTA, 637FTR, 638DZT.
003SIA	velocity difference seems to be because the influence of 005SDA; nearer and faster.
004GEM	related activities: 641DRG0, 644JLL1, 914AGE0, 944TGD0, 949SGD0.
005SDA	RP of SDA3 has an error.
007PER	related activities: 938PEA0, 942EPE0, 981AGP0, 992GPE0, 997FTP0.
008ORI	related activities: 718XGM0, 936STO0.
009DRA	difficult to catch exact maximum except for its outburst.
011EVI	123NVI0 should be included in EVI / EVI1 locates over 5 degrees west of the center.
012KCG	necessary to distinguish 7 years periodic component from annual activity / confused with 184GDR (peak around $\lambda_\odot$ = 125)/annual KCG activity does not show clear maximum.
015URS	insignificant in average years and the contamination from the sporadics affects the deviation of the velocity.
016HYD	Solar longitude ($\lambda_\odot$) of HYD3 is listed as 266.0 but its node is 256.5; the node fits the time of maximum.
017NTA	many related activities: 025NOA, 215NPI, 256ORN, 629ATS, 630TAR, 631DAT, 632NET, 633PTS, 634TAT, 635ATU, 639NNT.
020COM	member of COM complex; 020COM, 032DLM, 090JCO, 506FEV/DR shows a sharp peak at $\lambda_\odot$ =261 coincident with original DLM (December Leonis Minorids) when the upper half area is used for DR calculation.
021AVB	AVB0~3 are chance associations and AVB4 and 5 seem to form an independent shower with 343HVI1 and 136SLE2 possibly/not original α Virginids.
025NOA	on the following ascending activities of 215NPI to 017NTA.

Code	Comments
026NDA	026NDA2 is based on a few photographic data and differs from other entries a little / the peak of the activity is broad and the dispersion of RP is rather large / 508TPI should be included in NDA / not original Northern δ Aquariids / proper to name β Piscids (BPI).
027KSE	uncertain activities / not original κ Serpentids.
028SOA	a part of STA/coincident with its secondary peak $\lambda_\odot$ = 200.
031ETA	ETA5 lists parent body 1P/Halley's node as $\lambda_\odot$ and does not represent observational results.
032DLM	core of COM complex.
033NIA	NIA2, 3 and 6 seem to form a new shower / NIA1, 4 and 5 are various activities and not significant.
040ZCY	possibly composite of 2 small activities; ZCY0, 1 and 3: $\lambda_\odot$ = 16 and $\lambda_\odot$ = 33.
043ZSE	possibly chance association / ZSE0 and 1 each are based on only 1 meteor; Nos. 5688 and 3024 in Harvard Precision 413 meteors respectively (Jacchia and Whipple, 1961).
055ASC	ASC1 is close to 150SOP6 / ASC0 is not significant.
061TAH	2 entries more than 10 degrees apart, both are indistinguishable from the sporadic background.
063COR	2 entries more than 20 degrees apart, both no significant identity.
069SSG	not significant, though 803LSA1 is near SSG0 / SSG0 is over 5 km/s slower than the others.
076KAQ	2 entries more than 10 degrees apart, both indistinguishable from the sporadic background.
081SLY	705UYL0 should relate to SLY0 and 2 / 424SOL0 coincides with SLY1 (possibly with SOL2) and they might represent another activity.
088ODR	3 different activities; possibly chance associations though ODR2 is slightly suggestive.
090JCO	a part of COM complex's descending skirts followed by 506FEV.
093VEL	$\lambda_\odot$ seemed to be adjusted by the supposition / RP of VEL1 is more than 15 degrees apart from the other entries.
094RGE	entries are unrelated to each other; RPs are over 10 degrees in distance from each other / not significant activities.
096NCC	one of unclear ANT activity / might be secondary at $\lambda_\odot$= 305 and third at $\lambda_\odot$= 275 activities.
097SCC	chance groups on the descending slope of ANT activity.
101PIH	PIH0 and 1 may be better displayed by 530ECV / PIH2 is quite different and 729DCO0 is possibly concerned though diffuse.
103TCE	$\lambda_\odot$ seemed to be adjusted by the supposition / the radiants of the 4 entries are about 10 degrees apart from each other / only TCE0 is a candidate for TCE; recognizable from the northern hemisphere video observations around $\lambda_\odot$ = 315.
105OCN	$\lambda_\odot$ seemed to be adjusted by the supposition / OCN0~2 are reviews and OCN3 and 4 are intermittent radar observations; $\lambda_\odot$ of OCN3 and 4 are more than 20 degrees different from their nodes, OCN1 and 2 coincide with 315OCA0.
106API	API1 is more than 10 degrees apart from API0 and 2.
108BTU	130DME coincides with this shower.
110AAN	RP of AAN0 is about 20 degrees apart from the other entries / AAN4 represents this activity.
112NDL	possibly chance associations.
113SDL	possibly chance association / SDL1 is over 15 degrees apart from the others.
115DCS	possibly different activities; the $\lambda_\odot$ of DCS0 and DCS2 are 325.1 and 309.1 respectively / DCS3 and 4 are about 10 degrees north from DCS0, 1 and 2.
118GNO	conglomerate based on unreasonable combinations; 3 groups are more than 10 degrees apart in their positions from each other: (GNO0, GNO4, GNO5), (GNO1, GNO2), GNO3.
121NHY	possibly chance association / NHY2 is close to 11EVI1 and 124SVI1, RPs of all entries are very loose.
123NVI	NVI0 should be included in 011EVI / NVI1 is located more than 5 degrees west of the center.
130DME	coincides with 108BTU.
133PUM	very low activities/unreasonable combination: PUM0 and 1 are about 20 degrees apart at opposite position relative to PUM2 and 3.
136SLE	SLE0 and 1 are of chance / SLE2 might form an independent shower with 021AVB4 and 5 and 343HVI1.
138ABO	$\lambda_\odot$ seems to be adjusted by supposition, possibly chance associations.
149NOP	dispersed chance groups of ANT activity / NOP and SOP are overlapping each other / NOP1 is possible early 456MPS activity / not significant activities.
150SOP	dispersed chance groups of ANT activity / NOP and SOP are overlapping each other / not significant activities; SOP6 is only slightly suggestive and 055ASC1 is close to it.
151EAU	EAU2 is later than the other 2 entries and more than 10 degrees in distance from EAU1 / no significant activities.

Code	Comments
152NOC	NOC1 is more than 10 degrees in $\lambda_\odot$ later than the other 2 entries and possibly affected by ARI / NOC2 and 3 consist of a clear concentration around $\lambda_\odot$ = 50 / 357PHP1 is near NOC0.
154DEA	unreasonable combination of intermittent radar observations: difference of 15 degrees in $\lambda_\odot$.
156SMA	SMA1 is more than 10 degrees in $\lambda_\odot$ later than the other 2 entries / 355XIC0 is located between SMA0~1 and 2 in position and in $\lambda_\odot$ though XIC0 is more than 10 km/s slower than SMA.
161SSC	quite different in $\lambda_\odot$ and an erroneous combination / SSC1 locates at the border of Pisces and not in Capricornus.
164NZC	NZC0 ($\lambda_\odot$ = 86) seems to be the precursor of NZC and not representative / 548FAQ1 is close to NZC2 and FAQ1 seems to be the best representative of NZC activity.
165SZC	SZC0~1 and 2~3are different activities and the former two may be observable by radar only / SZC2 and 3 coincide with 370MIC0; SZC2 and 3 should be added to MIC because MIC was reported earlier than SZC2 and 3 / 195BIN1 is close to SZC1.
171ARI	the difference in the velocity seems to come from the difference in the observational techniques; radar velocity observations are slower than optical ones.
172ZPE	the maximum is unclear; possibly around $\lambda_\odot$ = 80 / entries seem to represent only a part of the shower.
175JPE	JPE4, 5 and 7 are missing the maximum / JPE0 is located more than 5 degrees south from the center / 462JGP and 522SAP should be included in JPE / velocity of JPE01 is higher than the others; based on single station observations.
176PHE	176PHE0 and 176PHE1 are not two sources but one. 176PHE0 and 176PHE1 are given as two 'likely extremes' by Cook and, therefore, v_g = 44km/s for 176PHE0 as lower limit and v_g = 50km/s for 176PHE1 as upper limit; The IAUMDC lists the average of both two as v_g / PHE2 is a different activity; RP of PHE2 is at 17 degrees distance from the other 2/769PPH coincides with PHE0 and 1 / 798ACD0 coincides with PHE2.
177BCA	871DCD coincides with BCA but might be a sporadic deviation.
179SCA	SCA0 is referred from Sekanina but his 'sigma Capricornids' are different; this entry is his 'Tau-Capricornids' / possibly different activities.
182OCY	source of OCY0 is unknown and its velocity is uncertain.
183PAU	PAU 2, 4 and 5 form a new shower different from the classic PAU.
186EUM	EUM1 and 2 are a quite different activity from EUM0 and former 2 entries are near 170JBO / not significant activity.
187PCA	PCA1 is closer to 550KPC0 than the other PCA members / no significant activities; possibly $\lambda_\odot$ = 105.
188XRI	the maximum may be around $\lambda_\odot$ = 137 judging from CMOR2 observation though CMOR2 data is not included in IAUMDC, XRI0 and 1 may be early activity of XRI not covering the maximum because they are intermittent observations.
189DMC	more than 10 degrees in distance from each other / CMOR does not show significant activity.
190BPE	435MPR0 is close to BPE2 / BPE1 located between 547KAP0 and 2 and is closer to them than BPE0 / only BPE2 is suggestive; all are located near to Perseids and the apex.
194UCE	UCE0 and 1 differ over 20 degrees in $\lambda_\odot$, clearly separate activity / 583TTA0 coincides with UCE1; they are suggestive and TTA displays the activity better.
195BIN	quite different activities / BIN1 is close to 165SZC1.
202ZCA	ZCA0 is an intermittent observation and may cover early ZCA activity.
215NPI	seems to concentrate around ($\lambda - \lambda_\odot$, β) = (196, 4); NPI3 seems to miss the center / Two peaks seem to occur around $\lambda_\odot$ = 160 and $\lambda_\odot$ = 180 though this may be possibly sporadic fluctuation or the ascending slope of 017NTA.
216SPI	no hillock on the ascending slope of 002STA complex activity / no grounds for including SPI3; over 15 degrees distance from the other SPI.
219SAR	SAR1~3 are independent activities according to the original author / 714RPI is surrounded by 4 radiants of SAR / 706ZPI0 is close to SAR3 / no significant activities.
226ZTA	3 different activities surrounding the Orionids; more than 10 degrees apart from each other / ZTA0 locates between Orionids and 479SOO; a part of Orionids tail and near 718XGM0/ZTA1 locates between 556PTA and 608FAR/ZTA2 is near 820TRD0.
232BCN	more than 15 degrees apart from each other / BCN0 is indistinguishable from the sporadic background / BCN1 coincides with 558TSM0 followed by 245NHD1; better displayed by NHD1 (see 245NHD).
233OCC	no significant activities in all entries.
237SSA	insignificant activities near 002STA and 017NTA.
242XDR	indistinguishable from sporadic background.
243ZCN	$\lambda_\odot$ of ZCN0 may be 235.4 calculated from its node; possibly different activities.
245NHD	558TSM0 coincides with NHD1 / suggesting one minor shower which continues to be active in the following order 232BCN1, 558TSM0, 245NHD1, 558TSM1 and 245NHD0 finally; represented better by NHD1.

Code	Comments
253CMI	250NOO is located 6 degrees west of CMI and weak activities continue over a long time; $\lambda_\odot$ of CMI is disturbed by this / CMI0 is clearly distinct from CMI1 and 2 / CMI1 and 2 are followed by 610SGM0; SGM seems to be on the ascending slope of 515OLE activity.
255PUV	other 4 showers are within 5 degrees: 302PVE0, 746EVE0, 301PUP0, 300ZPU0, possibly EVE represents this activity better.
256ORN	on the descending slope of 017NTA.
257ORS	2 different groups: ORS0~2 and ORS3~4 / 636MTA0 and 1 located between ORS0~2 and ORS3~4.
259CAR	identical with 312ECA0 though ECA is from an unknown source.
281OCT	383LDR0 is near OCT1.
285GTA	locates between STA and NTA / many showers are nearby: 637FTR0, 625LTA0, 637FTR1, 2STA0.
288DSA	DSA0 is quite different from DSA1 and 2 / possibly chance associations.
289DNA	both entries are quite different / DNA1 is in NTA associated activities: 634TAT0, 639NNT0, 633PTS0.
300ZPU	near 301PUP0.
301PUP	near 300ZPU0 and 302PVE0.
302PVE	near 255PUV0, 746EVE0 and 301PUP0 / possibly EVE represents this activity better.
303LVL	unknown source / coincides with 304CVE0.
304CVE	unknown source / coincides with 303LVL0.
307TPU	source of TPU0 ($\lambda_\odot$=246.8) is unknown and quite different from TPU1 ($\lambda_\odot$=270.7) though both RP in (α, δ) are close.
312ECA	unknown source / identical with 259CAR0.
313ECR	785TCD should be included in ECR though the source of ECR is unknown.
315OCA	unknown source / coincides with 105OCN1 and 2.
319JLE	JLE1 and 3 are based on single station observations; give higher velocity.
320OSE	330SSE is located between OSE0~1 and 2 / OSE0 coincides with 330SSE0 and 1 / OSE0 is based on radar observations; its velocity is lower.
321TCB	332BCB0 coincides with TCB.
323XCB	XCB1 and 3 are based on single station observations; give higher velocity.
327BEQ	BEQ1 and 2 are more than 15 degrees later than BEQ0/possibly chance association.
330SSE	SSE locate between 320OSE0~1 and 2 / 320OSE0 coincides with SSE0 and 1.
332BCB	coincides with 321TCB.
335XVI	radiant moves on ($\lambda - \lambda_\odot$, β) rather fast / double peaks around $\lambda_\odot$ = 255 and $\lambda_\odot$ = 265 are clear even though taking the radiant drift into account.
337NUE	a part of the Orionid tail / NUE3 may show another sub-maximum around $\lambda_\odot$ = 177 / NUE1 is at about 10 degrees distance from other NUE entries and rather close to 552PSO / 1030FER0 coincides with NUE0.
340TPY	including two different activities; TPY0 ($\lambda_\odot$ = 249) and others ($\lambda_\odot$ = 266) / TPY0 coincides with 844DTP0 and TPY1~3 coincide with 498DMH / no reason to keep TPY1; TPY1 is revised to TPY2 by the authors.
341XUM	XUM1 is based on single station observations; give higher velocity.
342BPI	not original Northern δ Aquariids; proper to name β Piscids (BPI).
343HVI	HVI1 is quite different from others and forms possibly a different shower with AVB4 and 5, 136SLE2.
345FHE	no reason to keep FHE1; FHE1 is revised to FHE2 by the authors.
347BPG	no reason to keep BPG1; BPG1 is revised to BPG2 by the authors.
355XIC	surrounded by 156SMA0~2 in position and in $\lambda_\odot$ though XIC is over 10 km/s slower.
357PHP	PHP 0 and 1 are 10 degrees apart in position and PHP1 is near 152NOC0.
359MZC	665MUC0(v_g = 57.1km/s) coincides with MZC (v_g = 29.2km/s) in position but much faster/video observations are in favor of MUC though weak.
370MIC	165SZC2 and 3 coincide with MIC; they should be added to MIC because MIC was reported earlier than SZC2 and 3.
372PPS	suggesting multiple activities; main peak at $\lambda_\odot$ = 97 and secondary at $\lambda_\odot$ = 108.
376ALN	quite different activity / insignificant.
383LDR	is located 5 degrees south of 281OCT and 10 degrees north of 333OCU though about 10 km/s slower than these sources / possibly chance association.
384OLP	OLP0 and 1 are distant from each other and 825XIE0 lies between them/insignificant diffuse activities though 825XIE is rather suggestive.

Code	Comments
386OBC	924SAN0 is rather near OBC1 and 2 than OBC0 both in $\lambda_\odot$ and RP, though SAN0 is slow (v_g = 16.8km/s).
392NID	NID2 might be different activity, though 753NED0 lies between NID0 and 2 both in position and $\lambda_\odot$ / $\lambda_\odot$ of NID1 is 242 but its node is 254.4; if $\lambda_\odot$ is correct NID1 might be early activity of 334DAD, if 254.4, might be 336DKD.
395GCM	possibly different activities / GCM1 is close to 398DCM1 and strongly affected by 331AHY.
411CAN	507UAN0 might be early activity of CAN.
424SOL	081SLY1 coincides with SOL0 and SOL2 may be part of it / SOL1 is different from SOL0 and 2; 901TLC0 may coincide with SOL1.
425PSA	PSA0 and 1 are more than 10 degrees apart in position and the latter possibly coincides with 613TLY0 and 1.
428DSV	showing a broad maximum $\lambda_\odot$ = 258~286 or multiple activities / should be named DSV complex / The radiant shift of DSV strongly suggests 500JPV0~2 and 513EPV0 might be part of DSV complex and their $\lambda_\odot$ (peak activity) coincide with the ending and starting plateau of the flat maximum respectively.
435MPR	190BPE2 is close and MPR might be late activity of BPE2.
448AAL	AAL2 is more than 10 degrees earlier in $\lambda_\odot$ than other entries, insignificant activities.
451CAM	CAM0~2 are over 15 degrees apart from CAM3 and 4 in both $\lambda_\odot$ and RP / CAM3 and 4 represent the 2014 outburst, it displayed a narrow activity period and a similar short-lived maximum was again observed in 2019 / CAM0~2 are different unclear activities.
456MPS	MPS0~2 are barely recognizable and the maximum is possibly around $\lambda_\odot$ = 60 / MPS0 and 1 are near 149NOP1 / MPS3 is more than 10 degrees in both $\lambda_\odot$ and RP different from the other 3 entries and different, weak indistinguishable from sporadic activity.
460LOP	LOP0 and 1 are suggestive and LOP2 may fail the center / LOP3 is different indistinguishable from sporadic activity.
462JGP	clearly coincides with 175JPE and should be included in JPE.
488NSU	527UUM0 coincides with NSU and should be included in NSU.
494DEL	DEL0 and 1 missed the center of RP and DEL2 is probably better.
498DMH	coincides with 340TPY1~3.
500JPV	might be a member of DSV complex (see 428DSV).
501FPL	possibly different activities / both indistinguishable from sporadic background /FPL1 locates 5 degrees east of 96NCC.
506FEV	FEV3 coincides with 90JCO, followed by FEV0~2 / on the descending slope of COM complex.
507UAN	possibly different activities / UAN0 seems to be early activity of 411CAN / UAN1 is at a distance of 8 degrees from UAN0 and more than 10 degrees apart in $\lambda_\odot$ from UAN2 / UAN1 node suggests its $\lambda_\odot$ should be 111 and UAN1 close to UAN2 / UAN2 might be early activity of 549FAN and $\lambda_\odot$ might be earlier than listed peak; affected by 444ZCS and early 007PER activities and a plausible peak may be around $\lambda_\odot$ = 103.
508TPI	should be included in 026NDA.
510JRC	521JRP0 should be included in JRC.
513EPV	might be a member of the DSV complex (see 428DSV).
514OMC	597TTS0 coincides with OMC1 and OMC0 corresponds to their late activity.
515OLE	OLE0 and 1 are over 15 degrees apart in $\lambda_\odot$ suggesting a broad maximum / prominent maximum at $\lambda_\odot$ = 290; second ($\lambda_\odot$ = 275) and third ($\lambda_\odot$ = 282) peak might be suggested / 643OLS0, 793KCA0 and 1 should be included in OLE; these are located between OLE0 and 1 in the RP position and in $\lambda_\odot$.
521JRP	should be included in 510JRC / IAUMDC remarks JRP is a duplicate entry.
522SAP	should be included in 175JPE.
527UUM	should be included in 488NSU.
530ECV	101PIH0 and 1 may be late activity of ECV.
531GAQ	GAQ2 and 3 are insignificant.
533JXA	JXA3 is over 10 degrees earlier than JXA0 and 2 but JXA3 represents the main activity ($\lambda_\odot$ = 108) / a weak activity 2 degrees east of the main activity may be active and reaches its maximum $\lambda_\odot$ = 118: possibly coincides with JXA0 and 2.
542DES	824DEX0 seems to represent this activity better.
547KAP	190BPE1 locates between KAP0 and 2 / KAP0 is on the outskirts of PER and KAP2 is near the apex / may be fluctuations in sporadic activity.
548FAQ	FAQ1 is close to 164NZC2 and FAQ1 seems to be the best representative of NZC activity.
549FAN	507UAN2 (and UAN1 possibly) might be early activity of 549FAN and $\lambda_\odot$ might be earlier than the listed peak; affected by 444ZCS and early 007PER activities and plausible peak may be around $\lambda_\odot$ = 103.
550KPC	coincides with 187PCA1 but other PCA members are distant / no significant activities.

Code	Comments
552PSO	coincides with 337NUE1 but other NUE members are distant / on the outskirts of Orionids tail.
558TSM	coincides with 232BCN1 and 245NHD1 / 245NHD1 represents better this activity (see 245NHD).
583TTA	coincides with 194UCE1; suggestive and TTA displays better.
597TTS	coincides with 514OMC1.
623XCS	1CAP1 is near.
624XAR	a related activity of 002STA.
625LTA	a related activity of 002STA.
626LCT	a related activity of 002STA.
627NPS	a related activity of 002STA.
628STS	a related activity of 002STA.
629ATS	a related activity of 017NTA.
630TAR	a related activity of 017NTA.
631DAT	a related activity of 017NTA.
632NET	a related activity of 017NTA.
633PTS	a related activity of 017NTA.
634TAT	a related activity of 017NTA.
635ATU	a related activity of 017NTA.
636MTA	636MTA0 and 1 locate between ORS0~2 and 257ORS3~4 / 638DZT0 and 1 locate between MTA0 and 1 though about 10 degrees later in $\lambda_\odot$ / related to 002STA possibly.
637FTR	a related activity of 002STA.
638DZT	locates between MTA0 and 1 though about 10 degrees later in $\lambda_\odot$ / surrounded by 257ORS / possibly related to 002STA.
639NNT	late 017NTA activity or early 256ORN.
641DRG	DRG0 is a part of GEM / DRG1 is at about a distance of 10 degrees from DRG0 and insignificant.
643OLS	OLS, 793KCA0 and 1 are located between 515OLE0 and 1, both in the RP position and in $\lambda_\odot$ / should be included in OLE / (see 515OLE).
644JLL	two different activities / 747JKL0 coincides with JLL0 / JLL1 is difficult to distinguish late GEM.
652OSP	OSP0 and 1 are more than 10 degrees apart in position / OSP0 is insignificant and 958SXS0 coincides with OSP1 though weak.
665MUC	MUC0 (v_g = 57.1) coincides with 359MZC0 (v_g = 29.2) in position but much faster in velocity, video observations are in favor of MUC though weak.
689TAC	possibly both chance associations.
705UYL	should relate to SLY0 and 2.
706ZPI	ZPI0 and 1 are more than 15 degrees apart in $\lambda_\odot$ / ZPI0 might be a chance association.
712FDC	the difference in the velocity is 5.7 km/s but identified by the same authors; this difference seems to be too large.
714RPI	locates within the area of 219SAR though RPI is about 5 km/s faster and insignificant.
718XGM	within Orionids activity area 5 degrees apart; difficult to distinguish / or the root of Orionid tail
729DCO	DCO0 may be related to 101PIH2 / DCO1 seems to be out of the center.
747JKL	JKL0 coincides with 319JLL0.
753NED	lies between 392NID0 and 2 both in position and $\lambda_\odot$.
758VOL	coincides with 787KVO0.
759THO	coincides with 43ZSE2 though THO is more than 5 km/s slower and insignificant.
761PPC	773THP0 is a duplicate entry of PPC though PPC lacks radiant shift.
769PPH	coincides with 176PHE0 and 1 in position / PHE is about 10 km/s faster though the velocity of PHE0 and 1 are adopted values.
770LCA	904OCO0 coincides with LCA.
773THP	761PPC0 is a duplicate entry of THP.
785TCD	should be included in 313ECR though the source of ECR is unknown.
787KVO	coincides with 758VOL.

Code	Comments
793KCA	643OLS0, KCA0 and 1 locate between 515OLE0 and 1 in the position and in $\lambda_\odot$ / should be included in OLE (see 515OLE).
798ACD	coincides with 176PHE2.
803LSA	LSA1 is near SSG0 though SSG0 is over 15 km/s slower and not significant.
824DEX	seems to be better data for 542DES.
827NPE	985TFA0 coincides with NPE.
844DTP	coincides with 340TPY0.
849SZE	948SER0 coincides with SZE.
862SSR	968UOD0 coincides with SSR; $\lambda_\odot$ of SSR should be read 2.2 though listed as 362.2.
871DCD	coincides with 177BCA0 but might be sporadic deviations.
877OHD	959TLD0 coincides with OHD.
904OCO	770LCA0 coincides with OCO.
914AGE	coincides with 004GEM but more than 20 km/s slower.
936STO	coincides with 008ORI but more than 15 km/s slower.
938PEA	coincides with 007PER but about 15 km/s slower.
942EPE	coincides with 007PER but about 40 km/s slower.
944TGD	located 10 degrees west of 004GEM.
948SER	coincides with 849SZE.
949SGD	coincides with 004GEM but 10km/s slower.
959TLD	coincides with 877OHD.
968UOD	coincides with 862SSR.
981AGP	coincides with 007PER but about 20 km/s slower.
985TFA	coincides with 827NPE.
992GPE	coincides with 007PER but nearly 30 km/s slower.
997FTP	locates about 7 degrees south-west of 007PER.

Using meteor interarrival times to obtain the rate of the alpha Monocerotid outburst

J. Andreas (Andy) Howell

Coordinator, CAMS-Florida, USA
camsflorida@gmail.com

Historically, observers have counted meteors to obtain an estimate of a meteor shower's rate. This paper presents an alternative method that uses measurements of meteor interarrival time to calculate a meteor shower's rate. Low-light level video meteor cameras and GPS timing are ideally suited to measurement of interarrival time with a precision of 30-40 milliseconds. Each arrival of a new meteor generates another measurement of interarrival time, from which the instantaneous meteor arrival rate can be calculated. In addition, upper and lower confidence limits of meteor arrival rate are presented. The method described in this paper is applied to analysis of the forty-four meteors observed by CAMS-Florida during the outburst of the alpha Monocerotid (AMO#246) meteor shower on 22 November 2019. The results show that the meteor arrival rate climbed steadily from 04h38m to 05h08m UT, peaking at about 100-200 per hour. There are indications of even higher, momentary surges that approached 1000 per hour. The conclusion is that the peak rate of the AMO outburst observed by CAMS-Florida is not inconsistent with the predicted zenithal hourly rate of 100-1000 per hour for the 2019 outburst.

1 Introduction

The MeteorNews article dated 6 November 2019 by Esko Lyytinen and Peter Jenniskens (2020) alerted meteor observers to the possibility of a "short-lived outburst" of the alpha Monocertid (AMO#246) meteor shower on the night of November 21–22. The prediction was for the outburst to last from 15–40 minutes, centered on 22 November 04^h50^m UT with a zenithal hourly rate (ZHR) ranging from "about a hundred to even storm level (with a ZHR of more than 1000)." The last outburst of this meteor shower occurred in 1995, and the prospect of another one generated much interest in the meteor community.

2 The CAMS-Florida Network

The CAMS-Florida network monitors an annulus about 77000 km^2 in area at 90 kilometers altitude, centered at 29.3N, 82.3W (*Figure 1*). Stations of the CAMS-Florida network are listed in *Table 1*.

Table 1 – CAMS-Florida Sites.

Location	Long.	Lat.	No. of Cameras	Operator
Gainesville	-82.3752	29.66915	10	A. Howell
New Smyrna Beach	-81.1259	28.91578	2	B. Harris
Melbourne	-80.624	28.06245	1	C. Palotai
Ocala	-82.1739	29.16576	8	E. Kisvarsanyi
Ocklawaha	-81.8659	29.09941	8	J. Cheney

CAMS-Florida consists of twenty-nine video cameras at five locations. The network employs an array of cameras based on the 1/2 inch chip (Watec 902H2 Ultimate) and 1/3 inch chip (Sony ICX 672 and ICX 810). Using 12mm f/1.2 lenses, the Watec cameras have a limiting meteor magnitude of +4, while the other cameras use 8mm f/1.0 lenses to achieve a meteor limiting magnitude of +3.5. Fields of view are 22° × 30° for the Watec cameras, and 26° × 34° for all others. For time-keeping, each CAMS-Florida station uses either a GPS time server or Network Time Protocol (NTP).

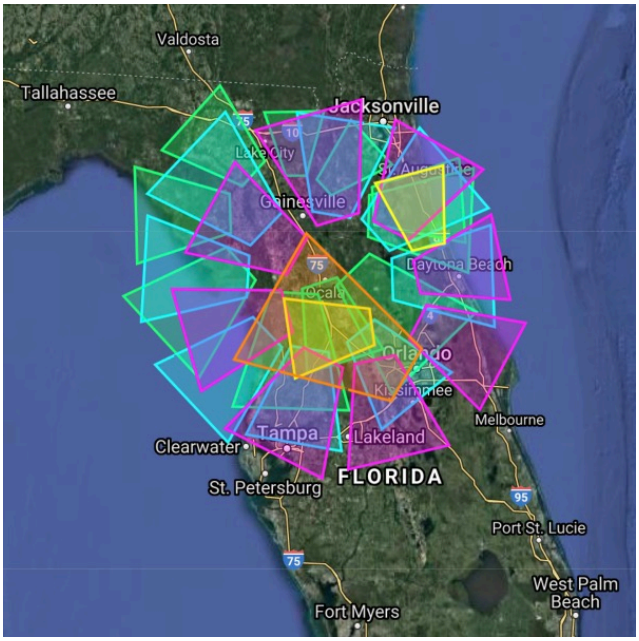

Figure 1 – CAMS-Florida Area Coverage.

3 Observing the AMO outburst

As the sky darkened above Florida on the evening of November 21–22, skies were mostly clear. Ten minutes before local midnight (21 November 23^h50^m EST = 22 November 04^h50^m UT), when the outburst was predicted to reach its peak, the radiant would be between 21 and 23 degrees above the eastern horizon. CAMS-Florida cameras operated without interruption during the night. UFOOrbit

software[3] was used the next morning to calculate radiants and orbital parameters. The results showed that CAMS-Florida had detected forty-four alpha Monocerotid meteors.

Table 2 lists the times, in order of appearance, of the forty-four coincident meteors. The outburst's first coincident meteor was spotted at $4^h38^m27.746^s$ UT, and the next-to-last was detected at $5^h36^m57.258^s$ UT. A lone straggler came into view 2 1/2 hours later at $7^h55^m40.143^s$ UT, yielding the night's final total of 44 confirmed meteors from the AMO outburst. Each meteor was seen by a minimum of two geographically separated sites.

Table 2 – Forty-four AMO meteors in order of appearance (UT Times).

(01) $04^h38^m27.746$	(16) $04^h58^m18.763$	(31) $05^h08^m33.820$
(02) $04^h39^m06.173$	(17) $04^h59^m30.117$	(32) $05^h08^m36.208$
(03) $04^h45^m38.553$	(18) $04^h59^m39.201$	(33) $05^h10^m02.467$
(04) $04^h45^m51.050$	(19) $04^h59^m58.872$	(34) $05^h10^m57.548$
(05) $04^h46^m06.777$	(20) $05^h01^m33.036$	(35) $05^h11^m48.137$
(06) $04^h46^m19.289$	(21) $05^h01^m45.301$	(36) $05^h13^m15.219$
(07) $04^h49^m07.775$	(22) $05^h02^m22.511$	(37) $05^h13^m54.659$
(08) $04^h49^m44.127$	(23) $05^h02^m26.832$	(38) $05^h18^m03.757$
(09) $04^h51^m14.843$	(24) $05^h04^m21.051$	(39) $05^h20^m22.182$
(10) $04^h51^m21.510$	(25) $05^h05^m26.889$	(40) $05^h23^m24.288$
(11) $04^h51^m36.248$	(26) $05^h07^m15.487$	(41) $05^h26^m25.138$
(12) $04^h53^m31.329$	(27) $05^h07^m17.999$	(42) $05^h30^m52.123$
(13) $04^h56^m35.504$	(28) $05^h07^m22.125$	(43) $05^h36^m57.258$
(14) $04^h57^m32.778$	(29) $05^h08^m07.771$	(44) $07^h55^m40.143$
(15) $04^h57^m43.983$	(30) $05^h08^m27.972$	

4 Interarrival time and the arrival rate of meteors

Meteor interarrival times provide a way to estimate a meteor shower's rate, event by event, as meteors come into view. Interarrival time is defined as $T_i = UT_i - UT_{i-1}$ for $i = 1,2,...,n$, where UT_i is the UT time of the i-th meteor, and n is the number of meteors seen.

Meteor arrival rate and interarrival time are inversely related. When interarrival time is short, the arrival rate of meteor arrivals is high. When interarrival time is long, the arrival rate of meteors is low. Low light-level video meteor cameras and GPS timing are ideally suited to measure interarrival time T with a precision of 30–40 milliseconds. The utility of interarrival times is that they give a nearly instantaneous reading of the level of meteor activity.

An intuitive method to estimate the meteor arrival rate, λ, is to take the reciprocal of interarrival time, $\hat{\lambda} = 1/T$. For example, if $T = 10$ seconds, then $\hat{\lambda} = 0.1$ second, equivalent to a rate of 360 meteors per hour.

[Note: $\hat{\lambda}$ is the statistical estimator of the parameter, λ, which is the "true" (but unknown) arrival rate of meteors. It can be shown that $\hat{\lambda} = 1/T$ is the maximum likelihood estimator of the arrival rate. (Ross, 2009, p. 267)]

The calculated value of meteor arrival rate $\hat{\lambda}$, is a point estimate. By itself, it gives no information about the precision of the estimate. For this reason, it is desirable to calculate upper and lower bounds that constrain, with a specified level of confidence, the likely range of λ.

5 Confidence interval of the arrival rate of meteors

The number of meteors seen during a specified time interval is often modeled as a Poisson process. The Poisson model has just one parameter, λ, the rate parameter. Three conditions are necessary for the Poisson model to apply[4]: (1) Events are independent of one each other; (2) The average rate (events per time period) is constant; (3) Two events cannot happen at the same time.

The Poisson model has a close connection with interarrival times. If the occurrence of meteors conforms to a Poisson process with parameter λ, then the distribution of interarrival times follows an exponential distribution with mean $1/\lambda$. (Ross, 2009, page 182).

The exponential distribution has the important property that it is "memoryless". That is, prior history does not affect the time until the next event (i.e., meteor arrival). The probability of seeing a meteor during the next period of time is the same regardless of how long one has already been waiting.

Suppose one has n observations of meteor interarrival time, whose sample mean is $\bar{T} = \sum_{i=1}^{n} T_i/n$. The reciprocal of this statistic yields the maximum likelihood estimator of the meteor arrival rate, $\hat{\lambda} = 1/\bar{T}$. From this, Ross (2009, p. 267) shows how to construct a $100(1-\alpha)\%$ confidence interval of λ, where α is the "miss rate" of the confidence interval. Downey (2011, p. 97)[5] presents an alternative form of the confidence interval:

$$\left(\hat{\lambda}\frac{\chi^2(2n, 1-\alpha/2)}{2n}, \hat{\lambda}\frac{\chi^2(2n, \alpha/2)}{2n}\right)$$

When analyzing a meteor shower's outburst, it's desirable to get the highest possible time resolution. For this purpose, set $n = 1$, which yields the confidence interval of meteor arrival rate from a single observation of meteor interarrival time:

[3] http://sonotaco.com/soft/e_index.html#ufoo
[4] https://towardsdatascience.com/the-poisson-distribution-and-poisson-process-explained-4e2cb17d459
[5] http://greenteapress.com/thinkstats/thinkstats.pdf

Table 3 – Instantaneous Hourly Rate (HR). Terminology: UT = time of meteor detection by the first camera to detect, T = interarrival time in seconds, 1/T = rate per second, HR = 3600/T = rate per hour, −1 S.E. = one standard error lower confidence limit of HR, +1 S.E. = one standard error upper confidence limit of HR.

UT	T	1/T	HR	−1 S.E.	+1 S.E.
$04^h38^m27.7^s$	—	—	—	—	—
$04^h39^m06.2^s$	38.427	0.026023	93.68	16.18	172.47
$04^h45^m38.6^s$	392.38	0.002549	9.17	1.58	16.89
$04^h45^m51.1^s$	12.497	0.080019	288.07	49.77	530.34
$04^h46^m06.8^s$	15.727	0.063585	228.91	39.54	421.42
$04^h46^m19.3^s$	12.512	0.079923	287.72	49.71	529.71
$04^h49^m07.8^s$	168.486	0.005935	21.37	3.69	39.34
$04^h49^m44.1^s$	36.352	0.027509	99.03	17.11	182.32
$04^h51^m14.8^s$	90.716	0.011023	39.68	6.86	73.06
$04^h51^m21.5^s$	6.667	0.149993	539.97	93.28	994.1
$04^h51^m36.2^s$	14.738	0.067852	244.27	42.2	449.7
$04^h53^m31.3^s$	115.081	0.00869	31.28	5.4	57.59
$04^h56^m35.5^s$	184.175	0.00543	19.55	3.38	35.99
$04^h57^m32.8^s$	57.274	0.01746	62.86	10.86	115.72
$04^h57^m44.0^s$	11.205	0.089246	321.29	55.5	591.49
$04^h58^m18.8^s$	34.78	0.028752	103.51	17.88	190.56
$04^h59^m30.1^s$	71.354	0.014015	50.45	8.72	92.88
$04^h59^m39.2^s$	9.084	0.110084	396.3	68.46	729.6
$04^h59^m58.9^s$	19.671	0.050836	183.01	31.62	336.93
$05^h01^m33.0^s$	94.164	0.01062	38.23	6.6	70.38
$05^h01^m45.3^s$	12.265	0.081533	293.52	50.71	540.37
$05^h02^m22.5^s$	37.21	0.026874	96.75	16.71	178.12
$05^h02^m26.8^s$	4.321	0.231428	833.14	143.93	1533.83
$05^h04^m21.1^s$	114.219	0.008755	31.52	5.44	58.03
$05^h05^m26.9^s$	65.838	0.015189	54.68	9.45	100.67
$05^h07^m15.5^s$	108.598	0.009208	33.15	5.73	61.03
$05^h07^m18.0^s$	2.512	0.398089	1433.12	247.58	2638.41
$05^h07^m22.1^s$	4.126	0.242365	872.52	150.73	1606.32
$05^h08^m07.8^s$	45.646	0.021908	78.87	13.62	145.2
$05^h08^m28.0^s$	20.201	0.049502	178.21	30.79	328.09
$05^h08^m33.8^s$	5.848	0.170999	615.6	106.35	1133.32
$05^h08^m36.2^s$	2.388	0.41876	1507.54	260.43	2775.41
$05^h10^m02.5^s$	86.259	0.011593	41.73	7.21	76.83
$05^h10^m57.5^s$	55.081	0.018155	65.36	11.29	120.33
$05^h11^m48.1^s$	50.589	0.019767	71.16	12.29	131.01
$05^h13^m15.2^s$	87.082	0.011483	41.34	7.14	76.11
$05^h13^m54.7^s$	39.44	0.025355	91.28	15.77	168.04
$05^h18^m03.8^s$	249.098	0.004014	14.45	2.5	26.61
$05^h20^m22.2^s$	138.425	0.007224	26.01	4.49	47.88
$05^h23^m24.3^s$	182.106	0.005491	19.77	3.42	36.39
$05^h26^m25.1^s$	180.85	0.005529	19.91	3.44	36.65
$05^h30^m52.1^s$	266.985	0.003746	13.48	2.33	24.82
$05^h36^m57.3^s$	365.135	0.002739	9.86	1.7	18.15
$07^h55^m40.1^s$	8322.885	0.00012	0.43	0.07	0.8

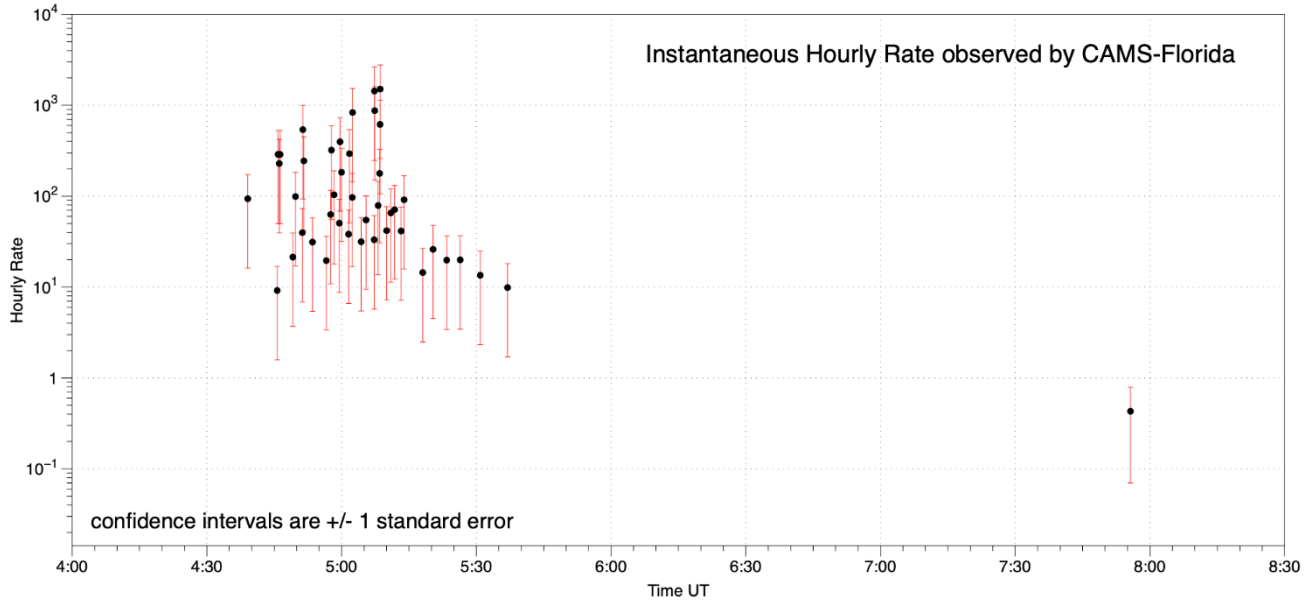

Figure 2 – Instantaneous hourly rate observed by CAMS-Florida.

$$\left(\hat{\lambda}\frac{\chi^2(2,1-\alpha/2)}{2},\hat{\lambda}\frac{\chi^2(2,\alpha/2)}{2}\right)$$

As before, $\hat{\lambda} = 1/\bar{T}$, which simplifies to $\hat{\lambda} = 1/T$, where T is the measured interarrival time. The chosen value of miss rate, α, determines the width of the confidence interval. A smaller α generates a wider confidence interval. Using the convention that the confidence interval encompasses ±1 standard error (S.E.), set $\alpha = 0.317$, which produces a $100(1-0.317)\% = 68.3\%$ confidence interval. ±1 standard error captures the central 68.3% of a normal distribution.

$$\left(\hat{\lambda} * 0.1728, \hat{\lambda} * 1.8410\right)$$

Simulations of interarrival time in an Excel spreadsheet show that the confidence interval calculated this way works as expected. The simulations tested meteor arrival rates λ=1, 10, 100, and 1000 per hour. In each of these trials, the calculated confidence intervals correctly captured the population parameter, λ, very nearly equal to the theoretical expectation of $100(1-\alpha)\%$. When the confidence interval did not include λ, the parameter landed with nearly equal frequency on both sides of the confidence interval.

6 Results

Instantaneous hourly rate of the AMO meteors

Table 3 presents the list of forty-four alpha Monocerotid meteors observed by CAMS-Florida. A minimum of two cameras at two different sites observed each meteor. The start time of each meteor's track varied slightly between cameras. For one-half (50%) of the observed meteors, the start times agreed within 38 milliseconds, and the average time difference was 78 milliseconds. The largest recorded time difference in start time was 324 milliseconds, which is explained by the time delay to enter a camera's field of view, whenever a meteor first appeared outside the field of view. The arrival time of each meteor was set equal to the time of earliest detection by the ensemble of cameras. See *Figure 2* for the instantaneous hourly rate of the AMO meteors.

Timeline of the alpha Monocerotid outburst

- 04^h38^m The AMO outburst begins with detection of the first coincident meteor, when the rate is about 10/hour.
- 04^h38^m–05^h08^m Rate increases steadily to a peak of 100–200/hour. Within the upward trend, there are indications of momentary surges to even higher rates.
- 05^h08^m Outburst peaks at 100–200/hour.
- 05^h13^m Rate is 40/hour.
- 05^h35^m Rate is 10/hour, signaling that the end of the outburst is near.
- 07^h55^m The last coincident AMO meteor is detected. Rate is below 1/hour.

7 Histogram of meteor absolute magnitudes

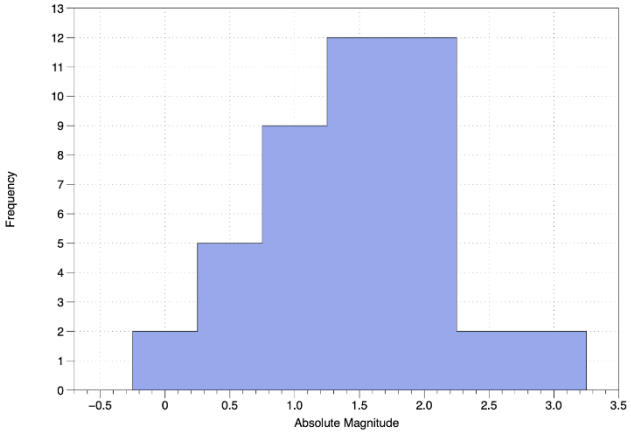

Figure 3 – A histogram of absolute magnitudes (at the standard altitude of 100 km). 90% of the forty-four AMO meteors observed by CAMS-Florida had an absolute magnitude between 0 and 2.

Figure 3 is a histogram of absolute magnitudes of the forty-four alpha Monocerotid meteors that were the subject of this report. 90% of the detected meteors had absolute magnitudes, which were computed by UFOOrbit, between 0 and + 2. The number of magnitude +1 meteors is 4.5 times greater than the number of magnitude 0 meteors. Similarly, the number of magnitude +2 meteors is 1.33 times greater than the number of magnitude +1 meteors. This suggests that the population index, *r*, is in the range of 1.33 to 4.5. The magnitude frequency distribution of alpha Monocerotid meteors from this outburst is planned as the subject of a future article in MeteorNews.

8 Discussion

This report gives a statistical method to estimate meteor arrival rate using interarrival times. Each new arrival of a meteor gives another measurement of the rate of a meteor shower. Measurements are inherently more powerful than the counting data that meteor observers have historically used.

The analysis of interarrival times of the AMO outburst shows that CAMS-Florida observed a peak hourly rate of 100–200 per hour, with possible short-lived spikes up to 1000 per hour. The duration of peak rate was short, lasting no more than 10–15 minutes.

The results reported by CAMS-Florida are apparent rates, not zenithal hourly rates (ZHR). Further work is needed to convert the observed rates to ZHR, accounting for such factors as (1) radiant elevation; (2) population index; (3) camera limiting magnitude; and (4) areal coverage of CAMS-Florida. Put another way, calibration of the measurement system is necessary before definitive conclusions can be made regarding zenithal hourly rate.

Acknowledgment

The author thanks Meteor News editors Adriana and Paul Roggemans for many improvements including a clearer presentation of the confidence interval of meteor arrival rate.

References

Downey Allen B. (2011) "Think Stats."

Koehrsen Will. "The Poisson Distribution and Poisson Process Explained." Towards Data Science Accessed 20 Jan 2020.

Lyytinen E. and Jenniskens P. (2020). "Likely alpha Monocerotids (AMO#246) outburst on the morning of November 22, 2019". *eMetN*, **5**, 11–12.

Ross Sheldon M. (2009). Introduction to Probability and Statistics for Engineers and Scientists. 4th Edition. Academic Press.

SonotaCo. "UFOOrbit." Accessed January 21, 2020.

Ursids (URS#015) in 2019

Paul Roggemans[1] **and Carl Johannink**[2]

[1] **Pijnboomstraat 25, 2800 Mechelen, Belgium**
paul.roggemans@gmail.com

[2] **Dutch Meteor Society, the Netherlands**
c.johannink@t-online.de

The United Arab Emirates Camera Network, UACN, registered a significant number of Ursid orbits during the night of 22-23 December 2019 between 20^h00^m and 02^h00^m UT. The CAMS-BeneLux network struggled with poor weather circumstances but still registered three Ursid orbits. When the sky conditions improved after 2^h UT, the number of Ursid orbits had decreased. The question arises if the Ursids should remain on the short list of annual major showers since the activity is comparable or inferior to several established minor showers. A -1 Ursid meteor recorded with RMS cameras allowed to calculate its orbit using three different orbit software solutions which resulted in three similar but nevertheless not identical orbits.

1 Introduction

The Ursid meteor stream is being listed since long time as one of the annual major showers. However, anyone who made attempts to observe this shower has been disappointed unless being lucky to observe during one of the rare outbursts of the Ursids. Most of the time low numbers of Ursid meteors are registered, not at all at the level of any of the major showers. The question arises if the Ursids should be rather qualified as a minor shower that may produce outbursts? Listing the Ursids as an annual major shower raises expectations that are most of the time not fulfilled. This is a good topic for a future case study.

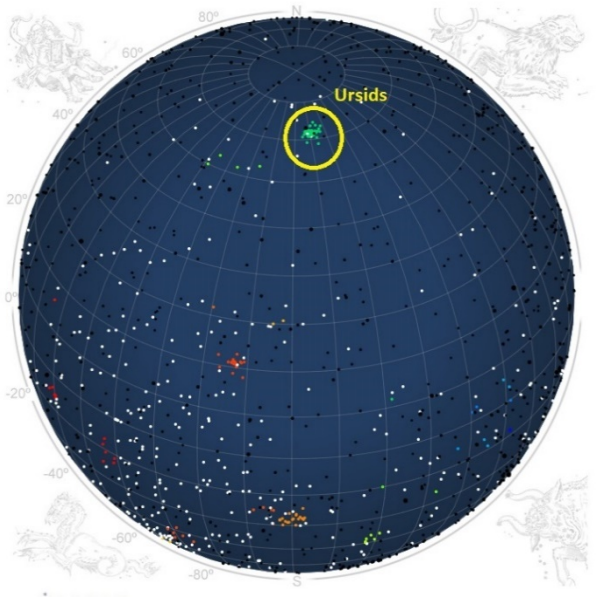

Figure 1 – Radiant map of CAMS for 2019 December 23 with the radiants of 46 Ursid orbits[6].

2 The Ursids in 2019

The United Arab Emirates Camera Network, UACN, registered a significant Ursid activity during the night of December 22–23. They collected a nice set of orbits during the time interval of $270.40° < \lambda_O < 270.65°$, corresponding to December 22–23, at about 20^h00^m–02^h00^m UT.

Table 1 – Number of orbits collected per night (24 hours) by CAMS worldwide in 2019 for the Ursids (URS#015). Hydrids (HYD#016), December Monocerotids (MON#019) and the December Comae Berenicids (COM#020). The time period covers the complete Ursid activity period.

Night	URS	HYD	MON	COM
December 11–12	1	48	28	12
December 12–13	2	64	34	18
December 13–14	2	47	37	16
December 14–15	1	56	32	29
December 15–16	2	49	37	62
December 16–17	3	29	11	27
December 17–18	3	30	14	31
December 18–19	11	63	11	66
December 19–20	10	57	16	62
December 20–21	17	21	2	39
December 21–22	13	23	4	27
December 22–23	46	20	1	24
December 23–24	3	11	3	29
December 24–25	2	9	1	30

The numbers of Ursid orbits depend upon the weather circumstances across the camera networks, but these numbers are very low. In *Table 1* we list the number of Ursid orbits registered by all CAMS networks together for each night. The first Ursid orbit was registered during the

[6] http://cams.seti.org/FDL/index.html

night December 11–12, the last one December 24–25, the sharp maximum occurred in the night of December 22–23 at about $\lambda_{\odot} = 270.52°$.

Table 1 also lists the number of orbits registered for three established minor showers: the sigma Hydrids (HYD#016), the December Monocerotids (MON#019) and the December Comae Berenicids (COM#020). If these are typical minor showers, then what are the Ursids?

3 Ursids by CAMS BeNeLux

Unfortunately, the CAMS BeNeLux region remained overcast at most places in the evening hours that night. Only three meteors, all Ursids, were collected before 2^h UT: one at 20^h14^m UT, one at 21^h13^m UT and another at 00^h24^m UT. No dust trails were expected to produce any enhanced activity in 2019.

Between 2^h00^m–3^h00^m UT two orbits were registered, once again both Ursids (02^h29^m and 02^h46^m UT). After 03^h00^m UT more and more regions in the BeNeLux got clear sky, but unfortunately the Ursid activity seemed to have weakened. Until twilight, another 31 meteor orbits were collected, including only 5 Ursids, even though the radiant was located higher in the sky.

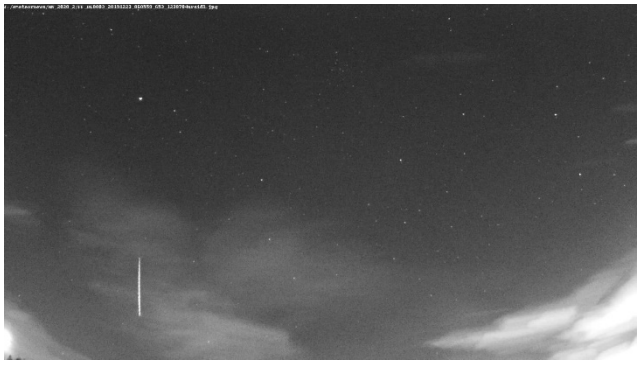

Figure 2 – The –1 magnitude Ursid meteor of 2019 December 23, $06^h06^m05.95^s$, registered by BE0003 (3815) at Cosmodrome, Genk, Belgium. RMS camera with f/0.95,3.6 mm lens (Adriana and Paul Roggemans).

Figure 3 – The –1 magnitude Ursid meteor of 2019 December 23, $06^h06^m05.95^s$, registered by BE0004 (3831) at Mechelen, Belgium. RMS camera with f/1.0,8 mm lens (Adriana and Paul Roggemans).

The orbital elements for all ten Ursids are listed in *Table 3*. The mean orbit (Jopek et al., 2006) was calculated using all these orbits except the Ursid registered at 06^h24^m which has a too high geocentric velocity. The result is shown in *Table 2* and compared with a reference from literature.

Table 2 – Mean orbit for 9 CAMS BeNeLux orbits compared to a reference orbit from literature.

	Mean orbit CAMS BeNeLux	Jenniskens et al. 2016
$\lambda_{\odot}$	270.7°	271.0°
α_g	218.5°	219.9°
δ_g	+75.2°	+75.4°
v_g	33.1 km/s	32.9 km/s
a	4.84 A.U.	4.87 A.U.
q	0.938 A.U.	0.940 A.U.
e	0.806	0.807
ω	206.0°	205.6°
Ω	270.6°	270.1°
i	53.0°	52.6°

The Ursid of December 23, 06^h06^m UT was recorded by two RMS cameras (see *Figure 2 and 3*). The orbits calculated by CAMS software are marked with 'C' in *Table 3*. The RMS camera data has also been analyzed by Denis Vida for the Global Meteor Network and since the RMS cameras provide also the detection info in UFO Capture format, Takashi Sekiguchi could compute the orbit with the UFO_orbit software of SonotaCo. This offers a unique possibility to compare the computational result for the orbit obtained by three different software solutions, based on identical measured positional data.

The results can be compared in *Table 3* with the three last mentioned orbits obtained for the same Ursid meteor, computed by Carl Johannink (C), by Denis Vida (G) and by Takashi Sekiguchi (S). The CAMS software and the SonotaCo software are well established, while the Global Meteor Network software is still being finetuned. SonotaCo uses only the position of the begin and end points of the meteor to compute the trajectory solution and the orbit. CAMS and GMN use all the measured positions on the meteor trail and take the deceleration into account.

The three solutions result in three similar orbits, but these orbits are not identical. CAMS gives the highest geocentric velocity v_g, eccentricity e, inclination i, and the lowest argument of perihelion ω. The GMN solution has the begin point H_e more than a kilometer lower in the atmosphere than CAMS, although the measured position used is identical.

These results provide us with an idea to which extent the method used to compute the orbit produces a slightly different result. The differences are larger than the error margins given and should be explained somehow. When the orbits depend so much on the method used to compute them, the resulting mean orbits that serve as references will also be different from each other. Another question arises as how many digits behind the comma are relevant to be listed for orbital elements?

Table 3 – The 10 orbits as obtained by CAMS BeNeLux (calculated by Carl Johannink). The Ursid of 2019 Dec. 23, $06^h06^m06^s$ UT, registered by BE0003 (003815) and BE0004 (003831), has also the orbit obtained for the Global Meteor Network (calculated by Denis Vida) and computed with the UFO_orbit software of SonotaCo (calculated by Takashi Sekiguchi).

	C 2019/12/22 $20^h14^m10.28^s$	C 2019/12/22 $21^h13^m22.29^s$	C 2019/12/23 $00^h24^m33.28^s$	C 2019/12/23 $02^h29^m52.41^s$
$\lambda_\odot$	270.407°	270.449°	270.584°	270.673°
α_g	217.42 ± 0.004°	214.29 ± 0.00°	215.12 ± 2.17°	217.68 ± 1.64°
δ_g	+75.34 ± 0.005°	+75.21 ± 0.00°	+75.63 ± 1.38°	+74.31 ± 0.48°
v_g	33.64 ± 0.00 km/s	33.10 ± 0.00 km/s	34.74 ± 0.21 km/s	33.29 ± 0.27 km/s
H_b	107.33 ± 0.00 km	104.53 ± 0.00 km	98.98 ± 0.02 km	101.35 ± 0.03 km
H_e	70.66 ± 0.01 km	92.31 ± 0.00 km	88.32 ± 0.07 km	91.50 ± 0.05 km
a	5.58 A.U.	4.27 A.U.	8.92 A.U.	4.37 A.U.
q	0.93778 ± 0.00001 A.U.	0.93267 ± 0.000 A.U.	0.93416 ± 0.0043 A.U.	0.94028 ± 0.00261 A.U.
e	0.8319 ± 0.0002	0.7814 ± 0.0000	0.8953 ± 0.0481	0.7850 ± 0.0248
ω	206.206 ± 0.003°	208.15 ± 0.00°	206.70 ± 1.11°	205.889 ± 0.890°
Ω	270.4048 ± 0.0000°	270.4470 ± 0.0000°	270.5835 ± 0.0002°	270.6729 ± 0.0001°
i	53.54 ± 0.004°	53.22 ± 0.00°	54.63 ± 0.81°	53.65 ± 0.40°

	C 2019/12/23 $02^h46^m03.34^s$	C 2019/12/23 $03^h15^m47.48^s$	C 2019/12/23 $04^h45^m31.94^s$	C 2019/12/23 $06^h24^m01.37^s$
$\lambda_\odot$	270.684°	270.705°	270.769°	270.839°
α_g	219.17 ± 2.03°	219.16 ± 1.24°	225.41 ± 0.46°	214.28 ± 0.80°
δ_g	+75.40 ± 1.63°	+75.13 ± 0.20°	+76.17 ± 0.21°	+74.91 ± 0.74°
v_g	33.14 ± 0.11 km/s	30.31 ± 0.15 km/s	32.84 ± 0.08 km/s	40.72 ± 0.18 km/s
H_b	98.86 ± 0.04 km	100.19 ± 0.02 km	99.73 ± 0.04 km	101.95 ± 0.04 km
H_e	89.33 ± 0.04 km	84.23 ± 0.09 km	90.34 ± 0.05 km	92.19 ± 0.04 km
a	5.12 A.U.	2.72 A.U.	6.62 A.U.	∞ A.U.
q	0.93975 ± 0.00507 A.U.	0.93850 ± 0.00165 A.U.	0.94558 ± 0.0058 A.U.	0.93746 ± 0.00210 A.U.
e	0.8163 ± 0.0490	0.6548 ± 0.0126	0.8571 ± 0.0087	1.2665 ± 0.0311
ω	205.762 ± 1.310°	207.882 ± 0.647°	203.638 ± 0.18°	203.659 ± 0.480°
Ω	270.6844 ± 0.0000°	270.7056 ± 0.0001°	270.7695 ± 0.0000°	270.8396 ± 0.0002°
i	52.82 ± 0.83°	49.82 ± 0.23°	51.69 ± 0.14°	60.58 ± 0.49°

	C 2019/12/23 $06^h34^m57.17^s$	C 2019/12/23 $06^h06^m05.95^s$ CAMS	G 2019/12/23 $06^h06^m08.21^s$ GMN	S 2019/12/23 $06^h08^m08^s$ SonotaCo
$\lambda_\odot$	270.846°	270.826°	270.826°	270.826°
α_g	219.88 ± 0.51°	218.50 ± 0.87°	218.07 ± 0.17°	218.56°
δ_g	+75.07 ± 0.38°	+74.11 ± 0.47°	+75.10 ± 0.30°	+74.87°
v_g	32.82 ± 0.11 km/s	34.21 ± 0.42 km/s	33.46 ± 0.04 km/s	33.27 km/s
H_b	100.59 ± 0.03 km	104.95 ± 0.05 km	103.76 ± 0.04 km	104.57 km
H_e	87.37 ± 0.03 km	81.86 ± 0.08 km	81.10 ± 0.03 km	81.80 km
a	4.57 A.U.	5.83 A.U.	5.26 ± 0.15 A.U.	4.87 A.U.
q	0.94130 ± 0.00110 A.U.	0.94249 ± 0.00049 A.U.	0.938929±0.0009 A.U.	0.940104 A.U.
e	0.7942 ± 0.0135	0.8384 ± 0.0286	0.8215 ± 0.0055	0.806835°
ω	205.480 ± 0.302°	204.74 ± 0.31°	205.95 ± 0.24°	205.73°
Ω	270.8472 ± 0.0001°	270.8268 ± 0.0004°	270.8268 ± 0.0000°	270.8258°
i	52.59 ± 0.23°	54.64 ± 0.57°	53.37 ± 0.19°	53.26°

4 Conclusion

The Ursids displayed a fair level of activity during about 6 hours in the night of 2019 December 22–23, 20^h to 2^h UT, but the number of orbits recorded for the Ursids remains rather modest compared to the numbers recorded for some minor showers that are active at the same time. The question arises if the Ursids should remain listed as an annual major shower, or be rather considered as a minor shower with periodic outbursts?

Computation of the orbit for an identical Ursid meteor using the CAMS software, the GMN software and the SonotaCo software results in similar but not identical orbits. The question if and to which extent orbits may differ depending on the software used requires further investigation.

Acknowledgment

The authors wish to thank Denis Vida for providing the GMN results and the Py program to compute average orbits according to the method of Jopek et al. (2006). We thank Takashi Sekiguchi for his computations with the SonotaCo software and Masahiro Koseki for his mediation.

Thanks to the CAMS BeNeLux team that provided the meteor video data for December 2019: *Hans Betlem* (Leiden, Netherlands, CAMS 371, 372 and 373), *Jean-Marie Biets* (Wilderen, Belgium, CAMS 379, 380, 381 and 382), *Martin Breukers* (Hengelo, Netherlands, CAMS 320, 321, 322, 323, 324, 325, 326 and 327, RMS 328 and 329), *Guiseppe Canonaco* (Genk, RMS 3815), *Bart Dessoy* (Zoersel, Belgium, CAMS 397, 398, 804, 805, 806 and 888), *Jean-Paul Dumoulin and Christian Walin* (Grapfontaine, Belgium, CAMS 814 and 815, RMS 003814), *Luc Gobin* (Mechelen, Belgium, CAMS 390, 391, 807 and 808), *Tioga Gulon* (Nancy, France, CAMS 3900 and 3901), *Robert Haas* (Alphen aan de Rijn, Netherlands, CAMS 3360, 3361, 3362, 3363, 3364, 3365, 3366 and 3367), *Robert Haas* (Texel, Netherlands, CAMS 810, 811, 812 and 813), *Robert Haas / Edwin van Dijk* (Burlage, Germany, CAMS 801, 802, 821 and 822), *Klaas Jobse* (Oostkapelle, Netherlands, CAMS 3030, 3031, 3032, 3033, 3034, 3037, 3038 and 3039), *Carl Johannink* (Gronau, Germany, CAMS 311, 312, 314, 315 and 316), *Hervé Lamy* (Dourbes, Belgium, CAMS 394 and 395), *Hervé Lamy* (Humain Belgium, CAMS 816), *Hervé Lamy* (Ukkel, Belgium, CAMS 393), *Koen Miskotte* (Ermelo, Netherlands, CAMS 351, 352, 353 and 354), *Tim Polfliet* (Gent, Belgium, CAMS 396), *Steve Rau* (Zillebeke, Belgium, CAMS 3850 and 3852), *Paul and Adriana Roggemans* (Mechelen, Belgium, CAMS 383, 384, 388, 389, 399 and 809, RMS 003830 and 003831), *Hans Schremmer* (Niederkruechten, Germany, CAMS 803) and *Erwin van Ballegoij* (Heesch, Netherlands,CAMS 347 and 348).

References

Jenniskens P., Nénon Q., Albers J., Gural P. S., Haberman B., Holman D., Morales R., Grigsby B. J., Samuels D. and Johannink C. (2016). "The established meteor showers as observed by CAMS". *Icarus*, **266**, 331–354.

Jopek T. J., Rudawska R. and Pretka-Ziomek H. (2006). "Calculation of the mean orbit of a meteoroid stream". *Monthly Notices of the Royal Astronomical Society*, **371**, 1367–1372.

December sigma Virginids (DSV) complex

Masahiro Koseki

NMS (The Nippon Meteor Society), 4-3-5 Annaka Annaka-shi, Gunma-ken, 379-0116 Japan
geh04301@nifty.ne.jp

The IAU MDC Meteor Shower Database (SD) contains many duplicate entries. The DSV complex is one of these examples and contains DSV#428, EPV#513 and JPV#500. The COM complex and the STA complex are well known and beyond these we find a new complex. This complex may consist of several components like the COM complex and more research is needed by using more abundant data.

1 Introduction

We know several discrepancies and confusions in the IAU MDC Meteor Shower Database (SD)[7]. The case of the 'December sigma Virginids (DSV) complex' (Koseki, 2020) is very interesting to study. This complex includes three showers from the Shower Database listed in *Table 1*: 0428DSV00 (December sigma Virginids, DSV#428), 0500JPV01 (January phi Virginids, JPV#500) and 0513EPV00 (epsilon Virginids, EPV#513). These look like different showers when simply looking at their radiant point RP in equatorial coordinates (α, δ). However, when looking at their Sun centered ecliptic coordinate radiants ($\lambda - \lambda_\odot$, β) these are close although the $\lambda_\odot$ values are somewhat apart. We investigate the details of this 'DSV complex' using video observations mainly by SonotaCo (2009) and compare this with the results from EDMOND[8] (Kornoš et al., 2014a, 2014b) and CAMS[9] (Jenniskens et al., 2018).

Table 1 – The December sigma Virginids (DSV) complex and its related showers.

Code	α (°)	δ (°)	v_g (km/s)	$\lambda_\odot$ (°)	$\lambda-\lambda_\odot$ (°)	β (°)
0428DSV00	205	+5.5	66	267.4	293.7	14.8
0500JPV01	221.9	+1.2	65.1	288.2	290.9	16.5
0513EPV00	197	+7.2	66.4	258	294.8	13.3

2 Relationship of the three showers

Although the difference in $\lambda_\odot$ seems too large to identify a shower activity, *Figure 1* strongly suggests these three activities may be connected. This figure counts the number of meteors within 3 degrees from the Sun centered ecliptic radiant point ($\lambda - \lambda_\odot$, β) listed in *Table 1* and shows some additional indexes (see for details in the caption of the figure). The DSV activity begins before $\lambda_\odot < 260°$ and continues to be active after $\lambda_\odot > 280°$. JPV is active around $\lambda_\odot = 275°$ and the activity of EPV continues beyond the DSV activity.

Figure 2 gives the radiant distributions of these three showers and suggests the radiant drift likewise. It is interesting to combine the radiant distribution over a longer period than what is shown in *Figure 2* ($\Delta\lambda_\odot = 20°$). *Figure 3* represents the radiant distributions centered on the DSV radiant position during a 30 degrees period before and after $\lambda_\odot$ (*Table 1*), i.e., $\Delta\lambda_\odot = 60°$. *Figure 3* (bottom right) gives the distribution of the radiants of the Shower Database meteor streams within the same period. *Table 2* shows the reference data used in *Figure 3* (bottom right). We can easily conclude that these three activities are related to each other. *Figure 4* is based on SonotaCo, EDMOND and CAMS data and confirms that this combination is reasonable. The three independent observations also show that the activity period is longer than previously assumed.

Table 2 – Reference data for Figure 3 (bottom right). The coordinates (x, y) represent each shower.

Code	$\lambda_\odot$ (°)	$\lambda-\lambda_\odot$ (°)	β (°)	x	y
0502DRV00	252.5	287	13.8	6.6	–0.8
0502DRV01	253.2	286.5	13.3	7	–1.4
0502DRV02	256	285.6	14.9	7.8	0.2
0513EPV00	258	294.8	13.3	–1.1	–1.5
0502DRV03	258.4	285.7	15.5	7.7	0.9
0428DSV01	262	295	13.5	–1.2	–1.3
0428DSV00	267.414	293.7	14.8	0	0
0428DSV02	278.8	292.2	16	1.4	1.2
0731JZB00	282	290.7	22.2	2.8	7.4
0500JPV00	285.6	291.5	17.3	2.2	2.5
0500JPV01	288.2	290.9	16.5	2.7	1.8
0500JPV02	289	291.3	16.9	2.3	2.1
0972JGL00	295.8	298.8	7.3	–5	–7.4

[7] IAUMDC meteor shower database, https://www.ta3.sk/IAUC22DB/MDC2007/

[8] https://fmph.uniba.sk/en/microsites/daa/division-of-astronomy-and-astrophysics/research/meteors/edmond/ or https://www.meteornews.net/edmond/edmond/

[9] http://cams.seti.org/

3 Radiant drift and final results

A meteor shower radiant usually shifts with time and its movement is expressed in equatorial coordinates in general by $\Delta\alpha$ and $\Delta\delta$. This expression is sufficient for showers near the equator and of short duration, but if the radiant moves on a great circle, the drift moves along a curve on the equatorial sphere in case of long duration or high declination showers. The radiant shift can be represented as a short line in the orthographic projection for the Sun centered ecliptic coordinates ($\lambda - \lambda_\odot$, β) (*Figure 3* top and bottom left) and it can be more accurately expressed by the linear regression rather than as $\Delta\alpha$ and $\Delta\delta$.

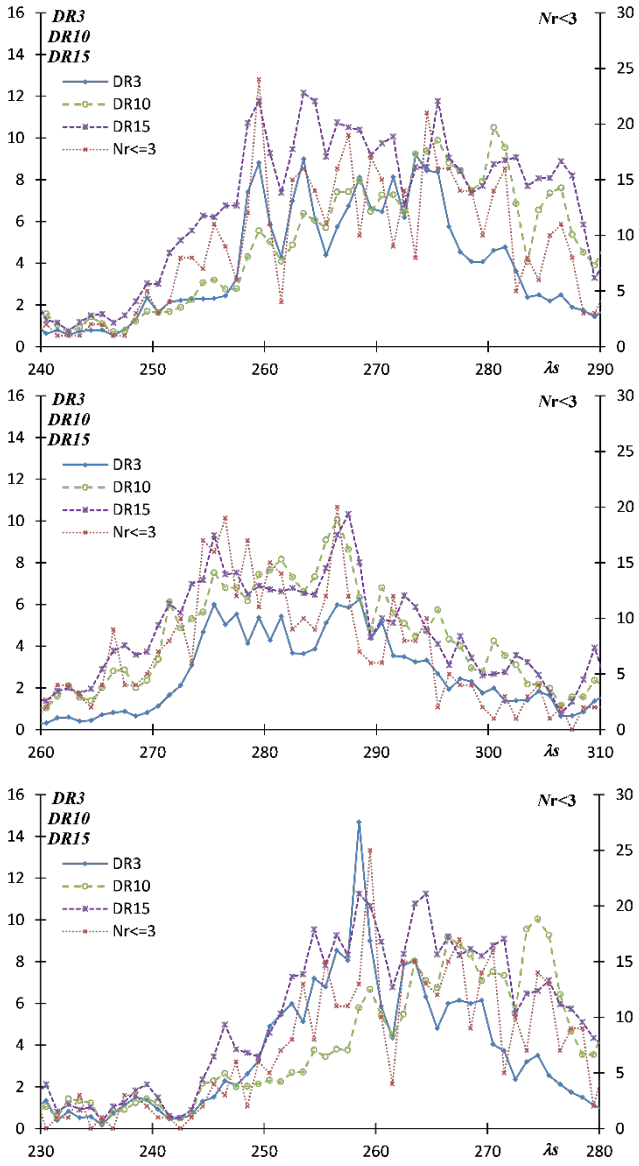

Figure 1 – Activity profiles based on SonotaCo observations. Top: DSV#428, middle: JPV#500 and bottom: EPV#513. Nr<3 is the number of meteors within 3 degrees from the radiant point ($\lambda - \lambda_\odot$, β) listed in Table 1. DR3, DR10 and DR15 are the sliding mean of the radiant density ratios within bins of 3 degrees in $\lambda_\odot$. DR3 is the density ratio within a circle of 3 degrees relative to a ring of 3~6 degrees. DR10 is the density ratio within a circle of 3 degrees relative to a ring of 6~10 degrees. DR15 is the density ratio within a circle of 3 degrees relative to a ring of 10~15 degrees.

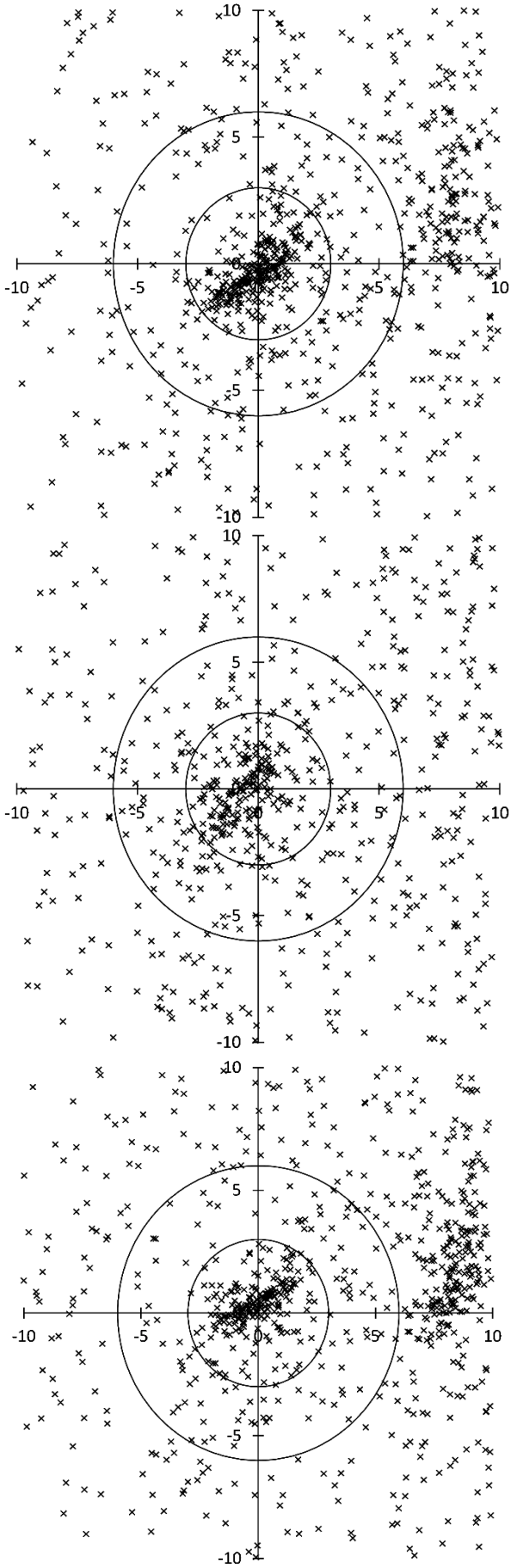

Figure 2 – Radiant distributions centered at each radiant point ($\lambda - \lambda_\odot$, β) of Table 1, within 10 degrees both sides of $\lambda_\odot$. Top: DSV#428, middle: JPV#500 and bottom: EPV#513. The y-axis runs through each ecliptic longitude of $\lambda - \lambda_\odot$, the scale is in degrees. The two circles represent the distance from the center at 3 degrees and at 6 degrees.

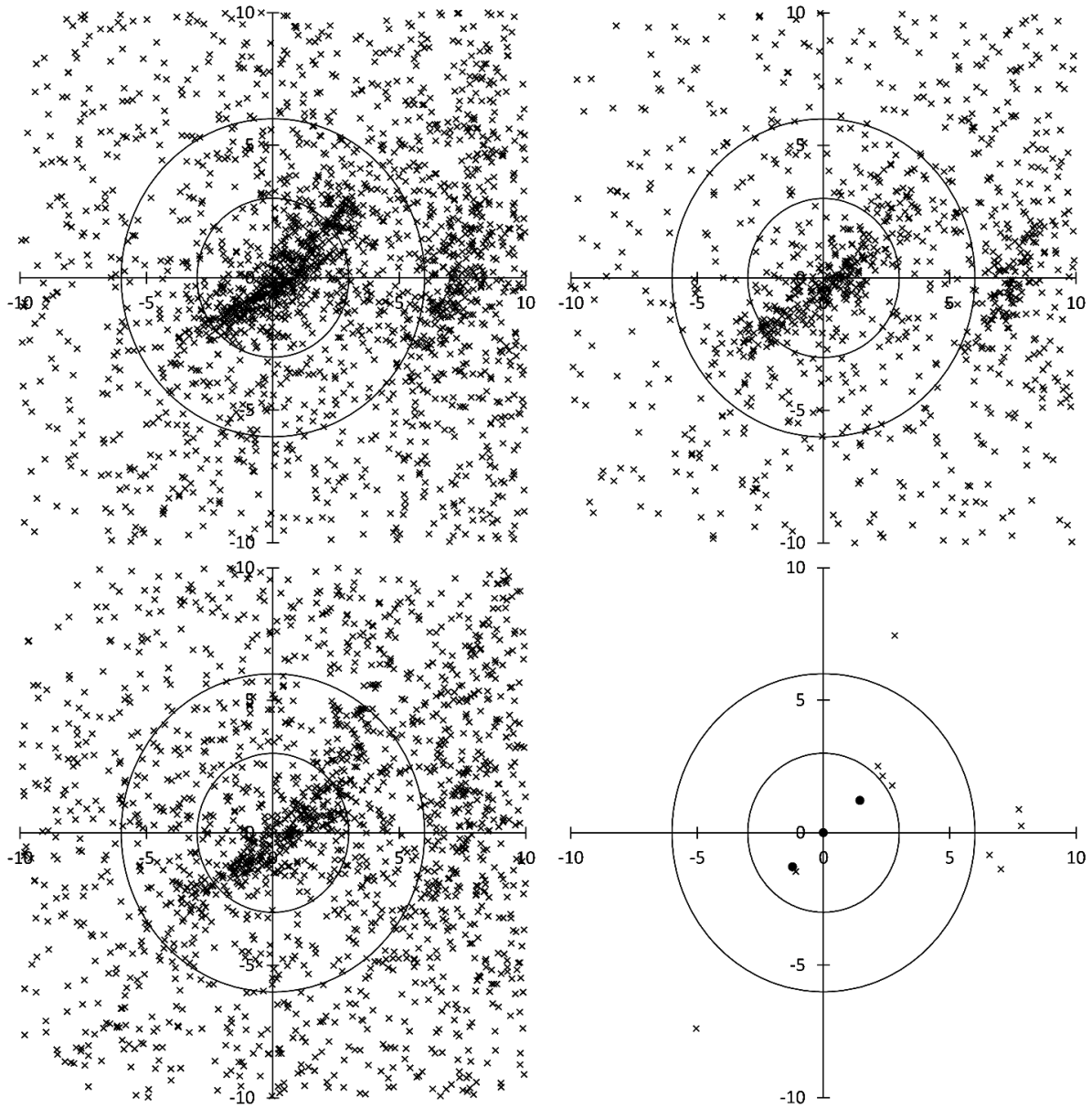

Figure 3 – The radiant distribution centered at the DSV radiant within a period of $\Delta\lambda_\odot = 30°$ before and after $\lambda_\odot$. Top left: SonotaCo, top right: EDMOND, bottom left: CAMS, bottom right: the Shower Database meteor streams. The scale and the circles are the same as in Figure 2.

Table 3 – Estimated radiant drift for the 'DSV complex'.

$\lambda_\odot$ (°)	$\lambda-\lambda_\odot$ (°)	β (°)	α (°)	δ (°)	v_g (km/s)
240	297.4	11.6	182.3	11.7	66.1
245	296.7	12.1	186.5	10.4	66.1
250	296.1	12.7	190.6	9.2	66.1
255	295.4	13.2	194.8	8	66.1
260	294.8	13.7	198.9	6.8	66.1
265	294.1	14.3	203	5.7	66.1
270	293.5	14.8	207.2	4.6	66.1
275	292.8	15.3	211.3	3.6	66.1
280	292.2	15.8	215.4	2.7	66.1
285	291.5	16.3	219.5	1.8	66.1
290	290.9	16.9	223.6	1	66.1
295	290.2	17.4	227.7	0.3	66.1
300	289.5	17.9	231.8	-0.4	66.1

We calculate the linear regression of ($\lambda_\odot$, x) and ($\lambda_\odot$, y) where (x, y) are the coordinates of radiant distribution centered at the shower radiant such as displayed in *Figure 3* top left. The regression calculations were repeated 5 times to become stable. We applied the regression calculations on the SonotaCo, EDMOND and CAMS data separately and all the results coincide very well with each other. Therefore, it is sufficient to show the final results obtained with the SonotaCo data.

Figure 5 gives the radiant distribution for the period of $240 < \lambda_\odot < 300$. The radiants are concentrated within a surprisingly small area. The concentration at the right side is caused by DSV#428 (see *Table 2*). DSV, JPV and EPV are expressed as a single activity.

Table 3 shows the radiant drift of the 'DSV complex' and it is clear that the radiant follows a curve in the equatorial coordinates. The estimated radiant drifts obtained from EDMOND and CAMS agree within 1 degree.

4 Discussions

We can compute the orbital elements based on *Table 3*. The results are shown in *Table 4*. *Table 5* lists the Shower Database meteor streams for comparison. We find some differences between *Table 4* and *Table 5* but these are small enough to identify them as one and the same activity.

Figure 6 shows the activity profile of the 'DSV complex'. The curve of DR10 before $\lambda_O < 260°$ seems to be lower than DR3 and DR15, because the DRV activity between 6 to 10 degrees from the center affects the results. *Figure 7* compares the final results of the SonotaCo, the EDMOND and the CAMS datasets. The total number of meteors differ: SonotaCo (284273), EDMOND (317689) and CAMS (471582). It is interesting to see that *Figure 7* (left) indicates that SonotaCo net captured more meteors than the other two datasets. This is partially caused by the observational years. SonotaCo data covers the period 2007–2018 almost evenly but the other two datasets are biased by the observations in later years. SonotaCo net may capture higher velocity meteors than the other two. *Figure 7* (right) shows the compensated profiles, because DR15 represents the radiant density ratios and not the observed meteor rates. The profiles are alike except for the increase around $\lambda_O = 267°$ in the EDMOND data. This difference can be explained by the decrease in the number of meteors in the EDMOND data between 10 to 15 degrees from the center of this period. This peak may be apparent though it is unclear why the decrease occurred.

We have found no trace of the 'DSV complex' neither in the photographic meteor listings nor in the catalogues of meteor streams. The 'DSV complex' may be a newborn or video favorable event. All the DSV related entries in the IAU MDC Meteor Shower Database are reported by video observations.

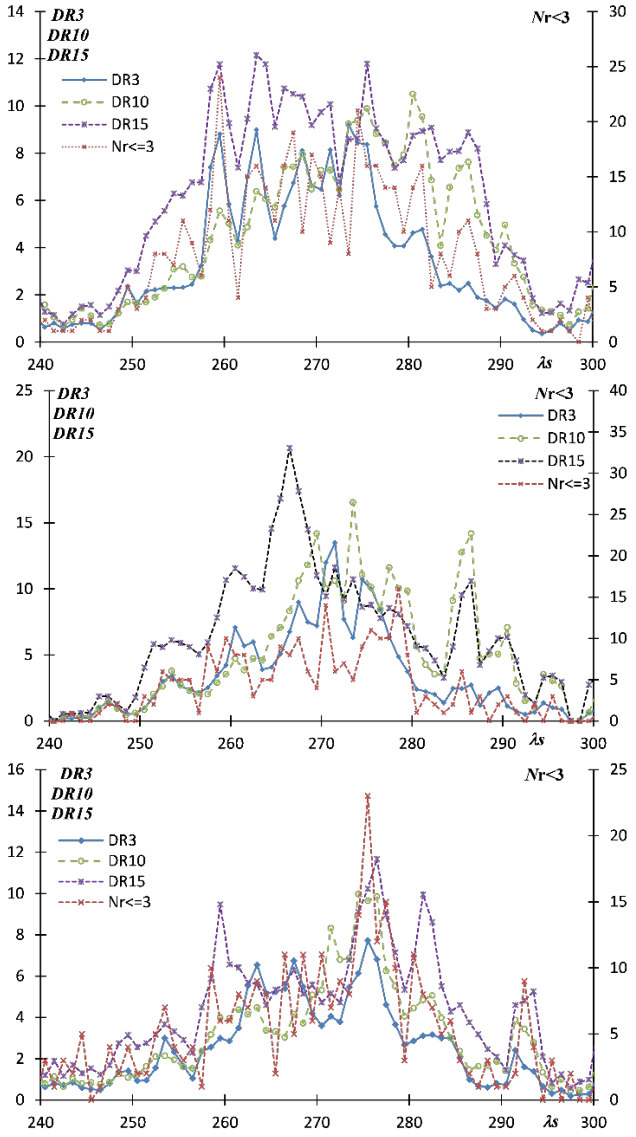

Figure 4 – The activity profiles of the DSV centered activity. Top: SonotaCo (same as in Figure 2 top, except for the x-axis), middle: EDMOND, bottom: CAMS. The explanation for the axis is the same as in Figure 1.

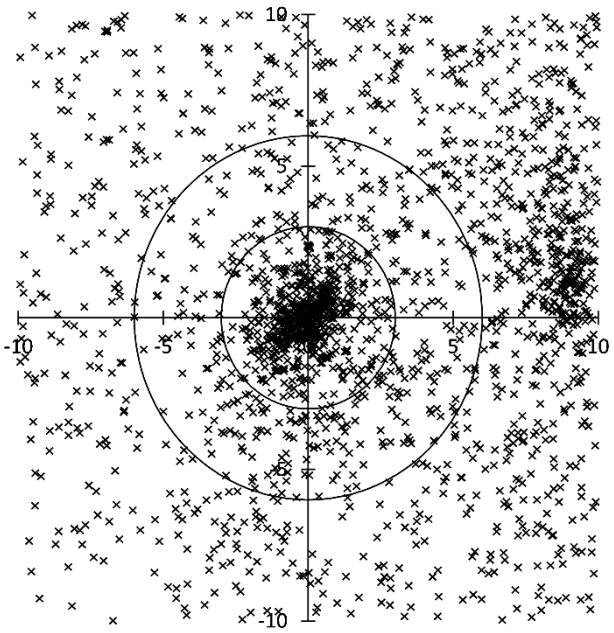

Figure 5 – The radiant distribution of the 'DSV complex' during the period of 240°< λ_O <300° taking the radiant drift into account. The scale and the circles are the same as in Figures 2 and 3.

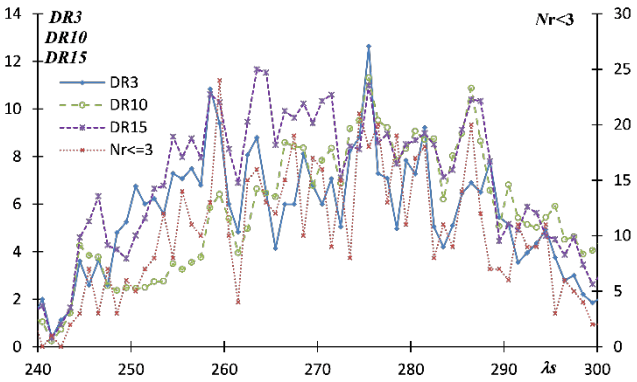

Figure 6 – The activity profile of 'DSV complex' taking the radiant drift into account. The scales of two axes are the same as in Figures 1 and 4.

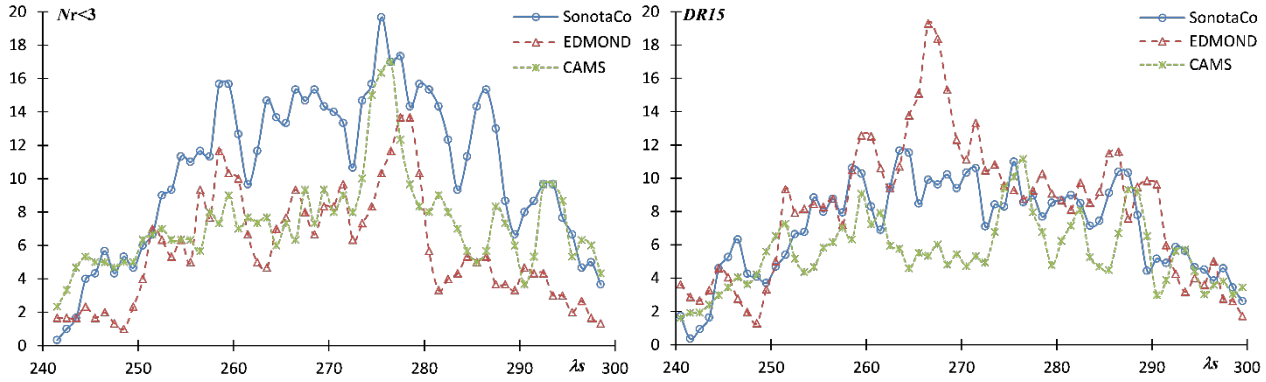

Figure 7 – Comparison of the activity profiles between the three data sets. Left: sliding mean meteor number within 3 degrees from the center with bins of 3 degrees in $\lambda_\odot$. Right: adjusted profile according to DR15.

Table 4 – The change of the orbital elements of the 'DSV complex' based on Table 3; each line refers to the corresponding line in Table 3. λ_Π and β_Π are the ecliptic coordinates of the perihelion.

e	q A.U.	i (°)	ω (°)	Ω (°)	a A.U.	λ_Π (°)	β_Π (°)
0.996	0.509	154.1	91.7	240	138.3	148.1	25.9
0.988	0.525	153.2	93.4	245	44.8	151.2	26.7
0.98	0.541	152.4	95.1	250	27.6	154.2	27.5
0.973	0.558	151.6	96.9	255	20.4	157.2	28.2
0.965	0.575	150.8	98.7	260	16.6	160	28.8
0.958	0.591	150	100.6	265	14.2	162.8	29.4
0.952	0.609	149.3	102.6	270	12.6	165.4	29.9
0.945	0.626	148.5	104.6	275	11.4	168	30.4
0.94	0.643	147.8	106.6	280	10.6	170.5	30.7
0.934	0.661	147.1	108.8	285	10.1	173	31
0.93	0.679	146.4	110.9	290	9.6	175.4	31.1
0.926	0.697	145.7	113.1	295	9.4	177.7	31.2
0.922	0.714	145.1	115.4	300	9.2	179.9	31.2

Table 5 – Orbital elements for all entries of DSV#428, JPV#500 and EPV#513 in the IAU MDC Meteor Shower Database.

Code	e	q A.U.	i (°)	ω (°)	Ω (°)	a A.U.	λ_Π (°)	β_Π (°)
0428DSV00	0.974	0.605	149.64	102.7	267.4	23.3	162.8	29.5
0428DSV01	0.971	0.565	151.5	97.9	261.8	8.2	162.8	28.2
0428DSV02	0.989	0.647	148.3	108	278.8	43.3	167.9	30
0500JPV00	0.95	0.669	145.3	110.3	285.6	13.4	171.4	32.3
0500JPV01	0.866	0.657	146.5	106.6	288.2	4.9	178.5	31.9
0500JPV02	0.966	0.677	146.6	111.2	290.1	6.5	175.2	30.9
0513EPV00	0.98	0.573	151	99	258	28	157.7	28.6

5 Conclusion

The final results indicate that the DSV, JPV and EPV compose a widespread complex. The activity profile shows a plateau with several peaks. The computed orbital elements differ widely and suggest that this complex may come from different sources.

References

Kornoš L., Koukal J., Piffl R. and Tóth J. (2014a). "EDMOND Meteor Database". In, Gyssens M., Roggemans P., Zoladek, P., editors, Proceedings of the International Meteor Conference, Poznań, Poland, August 22–25, 2013. International Meteor Organization, pages 23–25

Kornoš L., Matlovič P., Rudawska R., Tóth J., Hajduková M. Jr., Koukal J. and Piffl R. (2014b). "Confirmation and characterization of IAU temporary meteor showers in EDMOND database." In Jopek T.J., Rietmeijer F.J.M., Watanabe J., Williams I.P., editors, Proceedings of the Meteoroids 2013 Conference, A.M. University, Poznań, Poland, August 26–30, 2013, pages 225–233

Koseki M. (2020). "Confusions in IAUMDC Meteor Shower Database (SD)". *eMetN*, **5**, 93–111.

Jenniskens P., Baggaley J., Crumpton I., Aldous P., Pokorny P., Janches D., Gural P. S., Samuels D., Albers J., Howell A., Johannink C., Breukers M., Odeh M., Moskovitz N., Collison J. and Ganjuag S. (2018). "A survey of southern hemisphere meteor showers". *Planetary Space Science*, **154**, 21–29.

SonotaCo (2009). "A meteor shower catalog based on video observations in 2007-2008". *WGN, the Journal of the IMO*, **37**, 55–62.

December 2019 report CAMS BeNeLux

Paul Roggemans

Pijnboomstraat 25, 2800 Mechelen, Belgium
paul.roggemans@gmail.com

A summary of the activity of the CAMS BeNeLux network during the month of December 2019 is presented. 22591 meteors were recorded, 12329 of which proved multiple station, or 55%. Weather remained relative favorable; 28 nights allowed to collect some orbits with as many as 13 nights with more than 100 orbits. In total 4124 orbits were added to the CAMS BeNeLux database.

1 Introduction

With more than 14 hours observing time to capture meteors each night, December could be the most rewarding meteor month of the year. The richest annual shower, the Geminids has a broad maximum on December 13–14 while also 12–13 and even 14–15 December produce large numbers of meteors. However, the reason why December in generally disappoints is the most unfavorable weather this time of the year. What would 2019 bring?

2 December 2019 statistics

CAMS BeNeLux collected 22591 meteors of which 12329 or 55% were multi-station, good for 4124 orbits (compared to 25912 meteors, 13220 or 51% multi-station and 4908 orbits in December 2018). This month counted 13 nights with more than 100 orbits and only 3 nights without any orbits. Not any single night remained without some meteors being recorded at some stations. The weather circumstances were definitely better this year than in December 2018. The main reason why less meteors and less orbits were collected in 2019 is the bad luck during the main Geminid activity nights, 12–13 and 13–14. The nice score in orbits in December 2018 was thanks to a lucky coincidence that some of the very few clear nights happened during the best Geminid activity nights. During most nights of December 2019, the network had to function with less cameras since two cornerstone CAMS stations, Gronau and Terschelling, were not available and some other stations suffered technical problems.

The statistics of December 2019 are compared in *Figure 1* and *Table 1* with the same month in previous years since the start of CAMS BeNeLux in 2012. In 8 years, 182 December nights allowed to obtain orbits with a grand total of 19627 orbits collected during December during all these years together.

While December 2017 had a maximum of 86 cameras, 68.9 on average available, December 2018 had 78 cameras at best and 69.8 on average, in 2019 the network had 82 cameras operational on some nights, 72.8 on average. The role of AutoCams is essential to take advantage of the unpredictable nature of the weather during the long winter nights. In spite of what most amateurs expect with our very mediocre weather circumstances, there are rather few nights without any clear spans. It is often remarkable how many meteors can be registered during unpredicted moments with some clear sky. The chances to have multi-station events are modest with such variable cloud cover, but the more stations that function 7/7 with AutoCams, the better the chances to obtain more orbits.

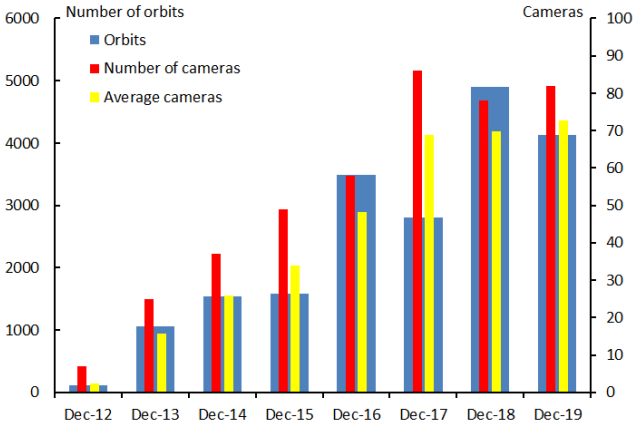

Figure 1 – Comparing December 2019 to previous months of December in the CAMS BeNeLux history. The blue bars represent the number of orbits, the red bars the maximum number of cameras running in a single night and the yellow bar the average number of cameras running per night.

Table 1 – December 2019 compared to previous months of December.

Year	Nights	Orbits	Stations	Max. Cams	Min. Cams	Mean Cams
2012	12	117	6	7	-	2.4
2013	23	1053	10	25	-	15.7
2014	19	1540	14	37	-	25.8
2015	27	1589	15	49	8	33.8
2016	25	3492	21	58	25	48.3
2017	25	2804	22	86	49	68.9
2018	23	4908	21	78	52	69.8
2019	28	4124	21	82	64	72.8
Total	182	19627				

3 Conclusion

December 2019 brought relatively good observing conditions, but no luck with the best Geminid nights this year. All in all, the harvest in number of orbits is an excellent result.

Acknowledgment

Many thanks to all participants in the CAMS BeNeLux network for their dedicated efforts. Thanks to *Carl Johannink* for providing all the data on which this report is based. The CAMS BeNeLux team was operated by the following volunteers during the month of December 2019:

Hans Betlem (Leiden, Netherlands, CAMS 371, 372 and 373), *Jean-Marie Biets* (Wilderen, Belgium, CAMS 379, 380, 381 and 382), *Martin Breukers* (Hengelo, Netherlands, CAMS 320, 321, 322, 323, 324, 325, 326 and 327, RMS 328 and 329), *Guiseppe Canonaco* (Genk, RMS 3815), *Bart Dessoy* (Zoersel, Belgium, CAMS 397, 398, 804, 805, 806 and 888), *Jean-Paul Dumoulin and Christian Walin* (Grapfontaine, Belgium, CAMS 814 and 815, RMS 003814), *Luc Gobin* (Mechelen, Belgium, CAMS 390, 391, 807 and 808), *Tioga Gulon* (Nancy, France, CAMS 3900 and 3901), *Robert Haas* (Alphen aan de Rijn, Netherlands, CAMS 3360, 3361, 3362, 3363, 3364, 3365, 3366 and 3367), *Robert Haas* (Texel, Netherlands, CAMS 810, 811, 812 and 813), *Robert Haas / Edwin van Dijk* (Burlage, Germany, CAMS 801, 802, 821 and 822), *Klaas Jobse* (Oostkapelle, Netherlands, CAMS 3030, 3031, 3032, 3033, 3034, 3037, 3038 and 3039), *Carl Johannink* (Gronau, Germany, CAMS 311, 312, 314, 315 and 316), *Hervé Lamy* (Dourbes, Belgium, CAMS 394 and 395), *Hervé Lamy* (Humain Belgium, CAMS 816), *Hervé Lamy* (Ukkel, Belgium, CAMS 393), *Koen Miskotte* (Ermelo, Netherlands, CAMS 351, 352, 353 and 354), *Tim Polfliet* (Gent, Belgium, CAMS 396), *Steve Rau* (Zillebeke, Belgium, CAMS 3850 and 3852), *Paul and Adriana Roggemans* (Mechelen, Belgium, CAMS 383, 384, 388, 389, 399 and 809, RMS 003830 and 003831), *Hans Schremmer* (Niederkruechten, Germany, CAMS 803) and *Erwin van Ballegoij* (Heesch, Netherlands,CAMS 347 and 348).

Annual report 2019 CAMS BeNeLux

Paul Roggemans

Pijnboomstraat 25, 2800 Mechelen, Belgium
paul.roggemans@gmail.com

A summary of the activity of the CAMS BeNeLux network during the year 2019 is presented. The year 2019 offered unusual good weather for astronomical observations with many clear nights during the period of April until September. 42749 orbits could be computed during 333 different nights which corresponds to 91% of all 365 nights in 2019. The months October and November 2019 were much worse than in 2018, reason why 2019 remained far below the record number of 49627 orbits recorded in 2018.

1 Introduction

The CAMS project started in 2010 with its first two camera stations in California, U.S.A. Already in its early stage single-CAMS was developed to allow amateur astronomers to participate in the project. When the CAMS principal investigator, Dr. Peter Jenniskens, came to Europe with part of the CAMS equipment to monitor the predicted 2011 Draconid outburst, he invited some amateurs of the Dutch Meteor Society to operate a set of CAMS equipment during a so-called crash expedition in function of weather forecasts. Hunting for clear skies, the observers then are dropped 'somewhere' last minute to install and to operate the equipment while observing visually. Such last-minute dropping campaigns are adventurous but very demanding, requiring a lot of improvisation and flexibility. After the Draconid expedition, the CAMS equipment remained a while in the Netherlands allowing some amateurs to get familiar with the procedures while being lucky with the weather during the 2011 Orionids and Taurids.

The results of the 2011 Draconid project and the tests during Orionids and Taurids were presented during a meeting of Belgian and Dutch amateurs on 29 October 2011 in Heesch, the Netherlands with Dr. Peter Jenniskens as guest speaker. The CAMS project was introduced, the required equipment exposed. Several amateurs returned home inspired to acquire the CAMS equipment. It took a few months before the first CAMS BeNeLux stations got operational at Oostkapelle and Ooltgenplaat. The first night 13–14 March 2012 resulted in the very first orbits for the CAMS BeNeLux network.

More amateurs joined in and step-by-step the CAMS network expanded in number of cameras and camera stations until in 2017 the entire atmosphere above the BeNeLux got well covered. The CAMS BeNeLux got developed into one of the most successful amateur astronomy projects ever in the BeNeLux. The network depends 100% on volunteers, amateur astronomers who dedicate some of their free time to operate cameras, taking care of the daily task to confirm real meteors, deleting false detections and to report the meteor data to the CAMS network coordinator. The auto-financed basis of CAMS BeNeLux goes with a much stronger commitment compared to similar projects financed by subsides.

The CAMS BeNeLux network results are submitted to the CAMS project scientist Dr. P. Jenniskens at the Seti Institute. Results are published in refereed papers, presented at scientific conferences and results are online available[10]. The CAMS software developer, Pete Gural, keeps in touch and provides feedback to the networks involved to adapt the software for new developments. The CAMS software is made available to all participating networks and technical support is provided by Steve Rau to implement the CAMS software and to configure Auto-Cams.

2 CAMS BeNeLux 2019 statistics

The year started with a rather poor month of January, the weather was unfavorable, and the network had to do with less operational cameras than one year before.

Table 1 – Total numbers of nights (D) with orbits, number of orbits, number of camera stations (S), maximum of cameras available (M_x), minimum of cameras available (M_i), average number of cameras (M_m), total number of meteors and percentage of multiple station meteors.

M	D	Orbits	S	M_x	M_i	M_m	Meteors	%
Jan	22	1857	22	76	54	64.1	10943	47%
Feb	24	3485	22	74	50	68.8	17784	59%
Mar	29	1217	22	78	54	64.4	–	–
Apr	29	2534	21	80	44	67.7	14667	54%
May	29	1825	21	84	52	72.3	–	–
Jun	28	2457	21	84	63	75.5	–	–
Jul	30	4139	19	86	63	75.2	–	–
Aug	29	9921	19	87	65	79.0	55335	60%
Sep	29	4609	20	79	64	72.3	30389	49%
Oct	29	3344	21	76	47	67.5	–	–
Nov	27	3237	21	77	60	71.1	21143	44%
Dec	28	4124	21	82	64	72.8	22591	55%
	333	42749						

[10] http://www.cams.seti.org

Since CAMS station Ooltgenplaat quit in June 2018 after being damaged by fire, the CAMS network was suddenly left with poor coverage for several cameras elsewhere. This loss did not get compensated during 2019. To make things worse, the most northern CAMS station Terschelling got a computer failure at the begin of 2019 and remained out of service the rest of the year. Another major drawback was the non-availability of the cornerstone CAMS station in Gronau after mid-August until end 2019.

With several cameras being unavailable, the network dropped at about 80% of the capacity it had end 2017. This is visible in *Figure 1*, as a drop in the maximum (green line) and the average number (red line) of cameras available each month since 2018. The many technical problems prevented any recovery and the capacity in terms of number of cameras remained at the same level in 2019.

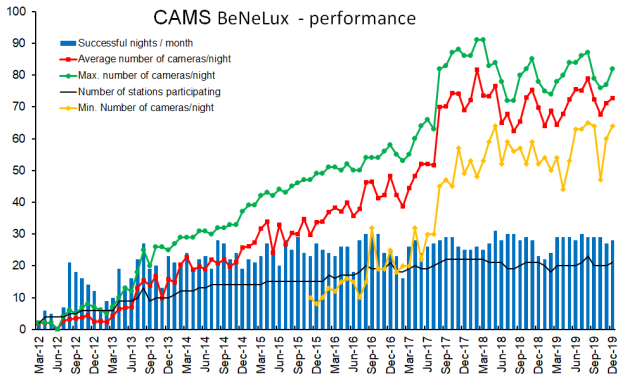

Figure 1 – Cams BeNeLux performance at a glimpse. The blue bars represent the number of nights with orbits for each month. The black line is the number of operational Cams stations, the green line the maximum number of operational cameras, the red line the average number of operational cameras and the yellow line the minimum number of operational cameras.

With the network functioning some years now, several stations suffered technical problems. For instance, the EzCap 116 framegrabbers proved to be rather poor quality and required many replacements. In some cases, the camera operators were not aware of any problems until some cameras turned out to have no orbits during some clear nights. One particular phenomenon in 2019 were the so-called “Zebrids”, meteor trails with irregular interruptions caused by dropped frames during the capture of the appearance of the meteor. Therefore, the measurement of the time duration of the meteor and its velocity are corrupted. The CAMS trajectory and orbit solving app Coincidence rejects such meteors because of the erroneous velocity measurement. This reduced the chance for double station meteors and accumulated in a loss of many hundreds of double station events that could not be used to obtain a reliable orbit.

Some new cameras were added to the CAMS BeNeLux network (see also *Figure 7*):

- CAMS 816 at the new CAMS station in Humain, Belgium, became operational 19 February;
- CAMS 328 and 329 in Hengelo, formerly Watecs, were replaced by RMS cameras;
- CAMS 003830 (BE0002) is a new RMS camera installed in Mechelen and pointed low to cover most of the eastern part of the Netherlands with a FOV of 22.5 × 41.4°;
- CAMS 003814 (BE0001) another new RMS camera was moved from Mechelen where its optics proved too bright for the light polluted region, to the very dark site Grapfontaine. Pointed at azimuth 350.0° and elevation 37.0° with its large FoV of 47.0 × 88.3°, this single camera covers about two thirds of the CAMS BeNeLux region and overlaps with as many as 62 cameras at other stations;
- CAMS 3901 got operational at the most southern station of the network in Nancy, France;
- CAMS 379 was added at the CAMS station in Wilderen, Belgium, dedicated to give coverage over Luxembourg.
- CAMS 3815 (BE0003) is another RMS camera installed at the new CAMS station in Genk, Belgium, pointed south to give coverage on the Ardennes, Luxembourg and North-East of France;
- CAMS 3831 (BE0004) a fourth RMS installed in Mechelen, pointed low to cover Luxembourg, the Ardennes and North-East of France with a FOV of 22.5 × 41.4°;

After the disappointing month of January, February brought a major improvement, just like in 2018, although the harvest in orbits was less impressive than previous year. Apart from slightly less favorable weather, the smaller number of operational stations and cameras kept the scores lower (3485 orbits against 4147 in 2018).

Just like in 2018, weather deteriorated in March resulting in slightly less orbits in 2019. A major weather improvement happened in April, just in time for the coverage of the Lyrids and a new record number of orbits for the month of April. On April 22 CAMS BeNeLux detected an outburst of the shower 15 Bootids (FBO#923) (Johannink, 2019; Roggemans, 2019a). May brought less favorable weather and less orbits while June 2019 resulted in a record number of orbits collected during the short nights of the month of June. Another outburst was detected on June 24 by different CAMS networks: June epsilon Ophiuchids (JEO#459) (Roggemans, 2019b).

July 2019 became the best month of July ever, just in time when the nights got longer, and the meteor activity picked up. August 2019 became another record month, the best month ever in the history of CAMS BeNeLux with as many as 9921 orbits. August broke the previous record of October 2018 when the Draconids outburst boosted the number of orbits. The success of August 2019 is remarkable in the sense that Moonlight interfered a lot during the best Perseids nights. Autumn came with deteriorating weather during the last week of September. October became a poor month with no chance for a good Orionid coverage. Poor weather ruled November and December, missing the main

Geminid activity. Still the results obtained under these unfavorable circumstances are excellent. *Figure 2* shows the monthly scores in numbers of orbits.

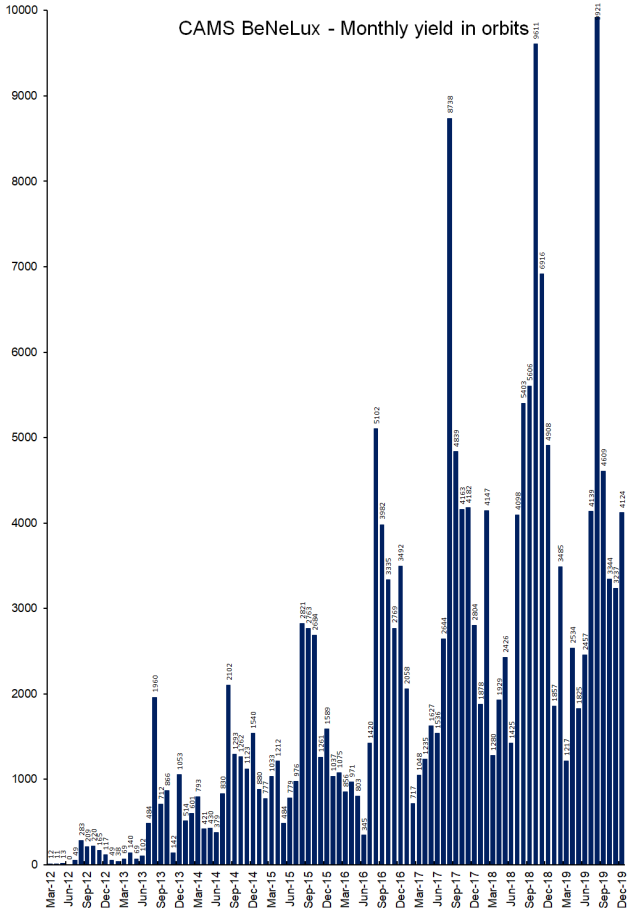

Figure 2 – The total number of orbits collected per month. August 2019 has the record with 9921 orbits in a single month.

3 2019 compared to previous years

Figure 3 shows the accumulated number of orbits. With 42749 orbits, 2019 was another excellent year for CAMS BeNeLux, bringing the total score at 188464 orbits. The total numbers of orbits are far higher than the most optimistic estimates anybody had expected in the past. The good result for 2019 is mainly due to the overall exceptional number of clear nights this year, combined with the use of Auto-CAMS and the still large number of operational cameras, although up to 20% of the equipment remained unavailable during much of 2019.

Comparing 2019 with previous years the highest average number of nights per month with orbits, 27.8, was better than ever before. 333 of the 365 nights of 2019 allowed to collect orbits, only 32 nights had zero orbits. The success is mainly the result of exceptional good weather. The expansion of the network covering a larger surface than few years ago offered better chances for local clear sky in some regions while the rest of the network remained 100% cloudy. Amateurs who operate their cameras only during predicted clear sky are missing all the unforeseen periods with clear sky. It is very recommended to run AutoCAMS 7/7 to cover these nights with unexpected clear sky. Some statistics are shown in *Table 2* and in *Figure 4*.

The number of operational cameras got at full strength in August 2017 while AutoCAMS was introduced in November 2015. The result in terms of orbits per year depends on being lucky with weather circumstances during the major showers.

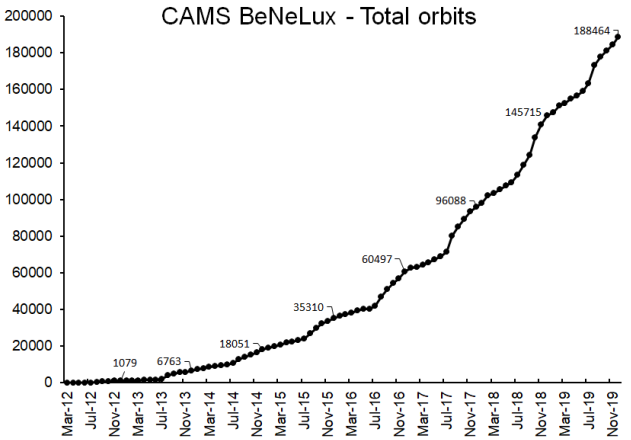

Figure 3 – The evolution of the number of orbits collected by the CAMS BeNeLux network.

Table 2 – Total numbers per year: average number of nights with orbits per month (D_m), orbits, average number of cameras per month (C_m), maximum number of operational cameras (C_{max}), number of operational sites and total number of nights with orbits.

Year	D_m	Orbits	C_m	C_{max}	Sites	Nights
2012	10.1	1079	2.6	8	6	101
2013	16.5	5684	9.5	26	13	198
2014	22.4	11288	20.6	37	14	269
2015	24.5	17259	30.1	49	15	294
2016	25.8	25187	40.3	58	21	309
2017	25.6	35591	57.2	86	22	307
2018	27.5	49627	71.3	91	22	330
2019	27.8	42749	70.9	91	23	333
		188454				2141

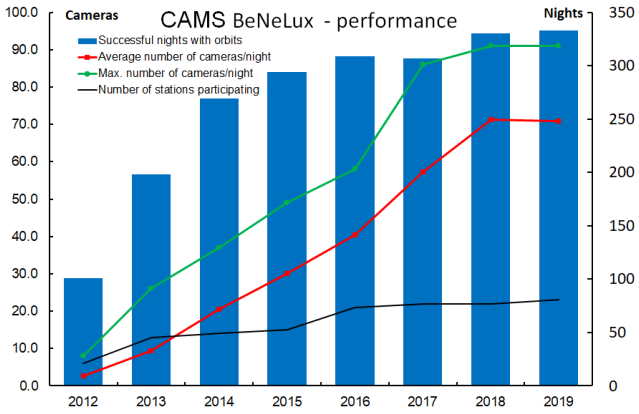

Figure 4 – The performance of the CAMS BeNeLux network from year to year. The blue bars represent the total number of nights during which orbits were obtained. The black line is the number of Cams stations, the green line the maximum number of cameras available and the red line the average number of cameras available.

TOTAL	01-02	02-03	03-04	04-05	05-06	06-07	07-08	08-09	09-10	10-11	11-12	12-13	13-14	14-15	15-16	16-17	17-18	18-19	19-20	20-21	21-22	22-23	23-24	24-25	25-26	26-27	27-28	28-29	29-30	30-31	31-01	
January	33	374	590	312	386	181	333	290	69	172	75	21	191	155	159	186	224	308	378	472	387	131	5	57	197	234	55	73	204	51	113	6416
February	76	158	151	140	316	395	135	192	32	59	107	606	569	142	594	181	299	181	86	193	359	314	435	566	234	246	359	150	80			7355
March	53	111	182	169	150	124	270	227	194	196	333	304	239	190	148	180	114	104	118	154	130	158	80	224	202	189	198	81	83	93	93	5091
April	128	66	112	103	203	210	119	224	115	174	172	165	188	94	125	236	409	341	556	430	307	294	319	34	102	166	153	160	95	119		5919
May	248	109	327	282	378	300	266	356	178	328	86	157	134	298	155	88	200	69	170	247	171	62	185	153	195	217	54	101	33	123	182	5852
June	111	68	110	142	201	166	73	67	235	193	165	103	191	174	166	137	167	186	111	170	199	98	80	34	168	248	211	157	236	199		4566
July	290	388	330	194	400	354	232	439	151	263	227	341	317	465	270	210	593	558	355	295	351	275	447	239	378	153	410	167	218	530	661	10501
August	664	643	653	865	1494	1597	450	748	669	861	890	3866	1461	954	1133	510	799	736	418	422	527	865	398	524	763	420	593	805	362	377	942	26409
Septembe	806	813	284	200	280	340	617	388	991	527	529	473	661	716	498	779	785	588	494	398	589	570	885	1084	695	1192	635	1135	800	652		19404
October	505	599	410	1047	935	168	621	1712	778	963	752	796	1122	1084	1005	468	597	912	860	924	469	644	144	51	217	711	1040	315	710	715	867	22141
November	790	940	776	354	658	1010	630	204	160	455	347	327	1001	620	421	1114	995	595	241	133	242	702	216	696	461	219	623	791	475	362		16558
December	52	434	607	796	430	236	752	331	851	775	1118	2182	1985	568	289	438	78	142	416	242	8	141	127	180	200	313	599	370	545	28	270	15503
																																145715
0 orbits:		0																														
>0 orbits:		366																														
>100 orbits		325																														
>500 orbits:		104																														
>1000 orbits:		20																														

TOTAL	01-02	02-03	03-04	04-05	05-06	06-07	07-08	08-09	09-10	10-11	11-12	12-13	13-14	14-15	15-16	16-17	17-18	18-19	19-20	20-21	21-22	22-23	23-24	24-25	25-26	26-27	27-28	28-29	29-30	30-31	31-01	
January	99	400	716	312	386	204	438	358	149	172	75	21	212	171	159	203	414	434	667	818	506	132	5	69	198	234	55	214	206	126	120	8273
February	77	247	343	140	352	395	184	226	32	173	210	648	708	458	920	376	549	197	109	304	365	476	698	818	488	522	595	150	80			10840
March	55	114	183	198	159	124	271	232	194	231	356	346	240	216	153	181	182	246	145	194	164	181	145	325	218	198	200	227	248	155	227	6308
April	224	79	178	183	203	244	152	261	213	321	222	276	287	169	260	255	456	451	733	643	514	661	387	96	115	223	155	253	101	138		8453
May	308	127	334	372	440	319	276	456	179	369	240	335	320	439	248	91	207	75	171	247	189	152	249	244	279	220	63	251	33	143	301	7677
June	222	86	158	171	201	268	74	177	244	198	168	222	260	174	247	301	268	276	121	270	338	252	168	110	253	314	334	361	459	328		7023
July	417	548	516	218	504	384	332	559	281	268	274	365	317	540	299	411	633	565	412	509	415	599	652	459	518	208	470	458	722	872	915	14640
August	978	801	898	867	1668	1738	965	1028	1110	1553	1760	4252	2636	955	1425	510	799	1036	732	750	917	1312	814	954	1106	683	808	822	700	764	989	36330
September	1121	951	458	393	613	369	692	657	1301	645	535	492	928	1073	542	868	1043	787	871	854	957	570	920	1111	700	1237	728	1142	802	653		24013
October	530	738	411	1102	936	271	621	1865	872	997	905	864	1194	1113	1106	468	646	937	883	925	471	656	234	123	417	722	1558	435	1197	1230	1058	25485
November	790	943	806	380	660	1026	1132	334	441	576	391	375	1051	633	536	1349	995	680	672	339	341	736	466	788	494	220	623	837	734	447		19795
December	375	599	1035	1157	432	236	752	364	1160	775	1233	2188	2038	991	397	457	117	342	456	567	24	177	167	184	297	346	690	631	838	324	278	19627
																																188464
0 orbits:		0																														
>0 orbits:		366																														
>100 orbits		347																														
>500 orbits:		143																														
>1000 orbits:		38																														

Figure 5 – Day-by-day tally of the cumulated number of orbits per calendar day collected by CAMS-BeNeLux. Top: the overview up to 31 December 2018, bottom: the situation on 31 December 2019.

10 years ago, at the start of the CAMS project, the purpose of the project was to collect at least a hundred orbits for each calendar date to detect unknown minor showers caused by weak dust trails. This initial target proved to be too modest as meanwhile the BeNeLux Cams network alone almost accomplished this purpose. CAMS proved much more successful than ever expected and meanwhile many hundreds of orbits are available for all nights of the year. *Figure 5* shows the number of orbits collected per calendar date by CAMS BeNeLux alone, which is about 15% of the global CAMS collection of orbits.

Figure 6 displays the location of the CAMS stations and cameras which contributed orbits in 2019. Framegrabbers and computer problems were responsible for the non-availability of some cameras at several occasions. Therefore, some extra cameras and stations would be very welcome to guarantee good coverage when somewhere technical problems occur. The situation at each CAMS station was discussed during the 2019 CAMS meeting which took place on 10 March 2019. A report about this CAMS meeting can be read in the March 2019 CAMS report (Roggemans, 2019c).

Since end 2018 some experiments have been made with the new RMS cameras. In 2019 the first RMS cameras were effectively used to provide extra coverage to the network.

Figure 6 – Location of all the active CAMS BeNeLux stations and cameras during 2019.

The results exceeded all expectations in spite of numerous technical problems. The number of orbits for each camera depends mainly upon the coverage provided by other camera stations. However, the scores obtained by the RMS cameras listed in *Table 3* are remarkable although these have been less nights in service during 2019 than most of the Watecs.

Table 3 – Selection of 20 cameras with the highest scores in orbits.

Camera	Total orbits	nights active	nights with orbits
003814 (RMS Grapfontaine B)	5573	222	154
003830 (RMS Mechelen B)	3448	275	183
000384 (Watec Mechelen B)	3023	365	263
000399 (Watec Mechelen B)	2724	365	256
000388 (Watec Mechelen B)	2503	365	249
000816 (Watec Humain B)	2391	316	210
003035 (Watec Oostkapelle Nl)	2388	218	200
000391 (Watec Mechelen B)	2388	353	229
000383 (Watec Mechelen B)	2322	365	250
000395 (Watec Dourbes B)	2320	354	216
000380 (Watec Wilderen B)	2293	365	227
003900 (Watec Nancy F)	2197	306	173
000353 (Watec Ermelo Nl)	2186	175	155
000814 (Watec Grapfontaine B)	2183	359	193
000812 (Watec Texel Nl)	2061	363	239
000390 (Watec Mechelen B)	2021	359	217
003815 (RMS Genk B)	2021	157	94
000809 (Watec Mechelen B)	1997	365	241
000393 (Watec Ukkel B)	1958	361	228
000394 (Watec Dourbes B)	1942	251	153

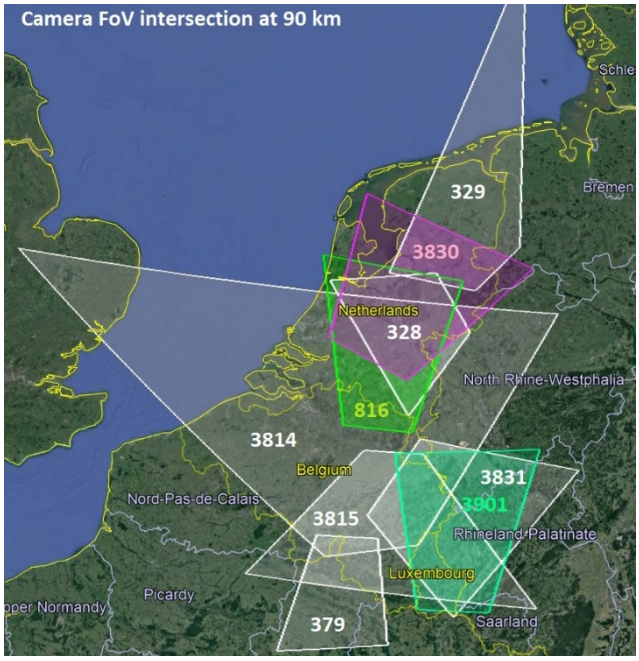

Figure 7 – Fields of View (FoV) of the new cameras started during 2019. 328, 329, 3814, 3815, 3830 and 3831 are RMS cameras.

4 CAMS BeNeLux in the world

CAMS is a global project in which different networks around the world participate all using the same CAMS software. The 16th century emperor Charles V claimed that the Sun never set in his empire, the opposite is true for CAMS. The Sun never rises as there is always some network with nighttime allowing to collect video meteor orbits 24/24 if weather permits.

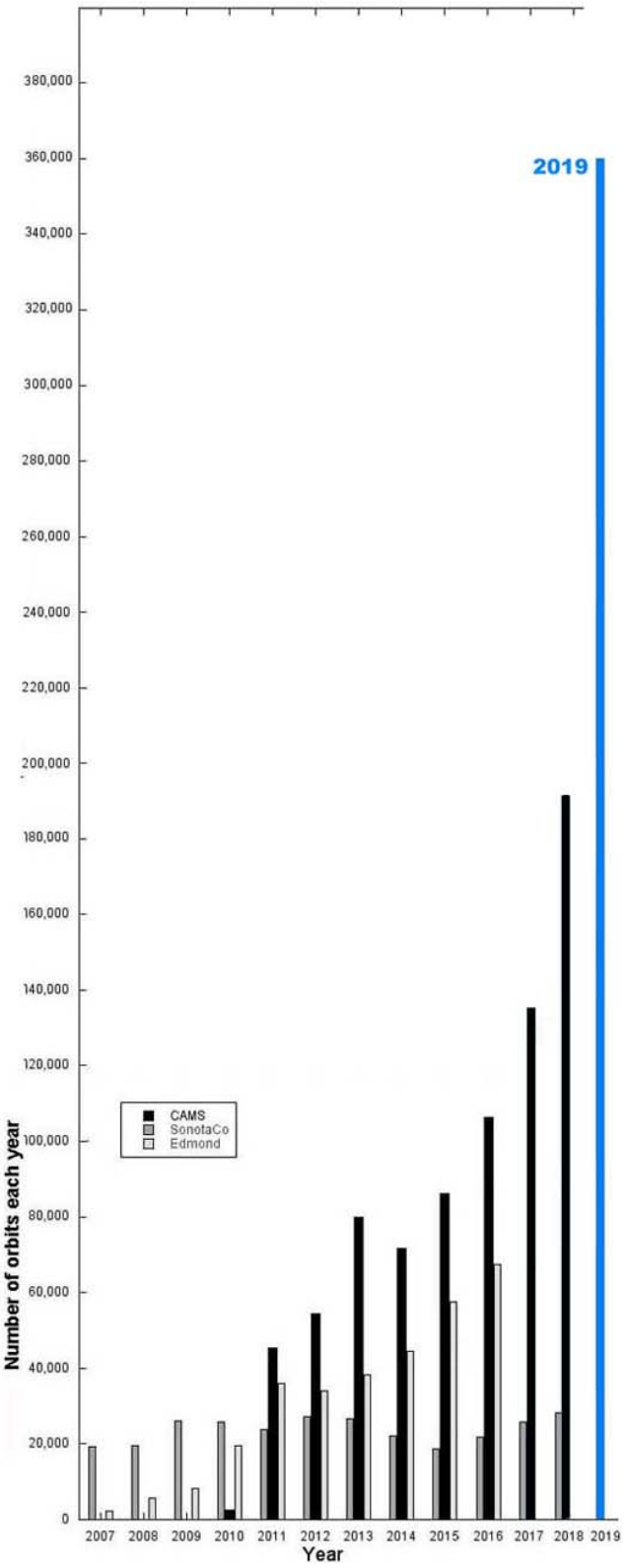

Figure 8 – CAMS BeNeLux within the global CAMS project compared to the other major video networks.

Altogether the CAMS networks collected about 364000 orbits in 2019, almost twice as much as the year before (see *Figure 8*). The different CAMS networks had the following numbers of orbits (raw data):

- CAMS Arkansas 13630 (2595 in 2018)
- CAMS Australia 37837 (new since June 2019)
- CAMS BeNeLux 42749 (49627 in 2018)
- CAMS California 69924 (68329 in 2018)
- CAMS Chile 51700 (new since July 2019)
- EXOSS Brazil 342 (400 in 2018)
- CAMS Florida 24944 (5654 in 2018)
- LOCAMS Arizona 49748 (45230 in 2018)
- CAMS Namibia 18875 (new since September 2019)
- CAMS New Zealand 23806 (3201 in 2018)
- CAMS Northern California 4582 (818 in 2018)
- CAMS South Africa 9640 (new since June 2019)
- UAZ-CN 16085 (10583 in 2018)
- Total 2019~364000 orbits (186500 in 2018)

CAMS BeNeLux contributed almost 12% of the total score for 2019. Since the start of the CAMS project more than 1100000 video meteor orbits have been collected of which 188454 orbits by CAMS BeNeLux. This is currently the largest collection of optical orbits and the project is expected to be continued for years with more networks involved than previous years.

Acknowledgment

Many thanks to all participants in the CAMS BeNeLux network for their dedicated efforts. Thanks to *Martin Breukers* and *Carl Johannink* for providing all the data on which this report is based. The CAMS BeNeLux team is operated by the following volunteers:

Hans Betlem (Leiden, CAMS 371, 372 and 373), *Jean-Marie Biets* (Wilderen, CAMS 379, 380, 381 and 382), *Martin Breukers* (Hengelo, CAMS 320, 321, 322, 323, 324, 325, 326, 327, RMS 328 and 329), *Bart Dessoy* (Zoersel, CAMS 397, 398, 804, 805, 806 and 888), *Jean-Paul Dumoulin / Christian Wanlin* (Grapfontaine, CAMS 814 and 815, RMS 003814), *Luc Gobin* (Mechelen, CAMS 390, 391, 807 and 808), *Tioga Gulon* (Nancy, France, CAMS 3900 and 3901), *Robert Haas* (Alphen aan de Rijn, CAMS 3160, 3161, 3162, 3163, 3164, 3165, 3166 and 3167), *Robert Haas / Edwin van Dijk* (Burlage, CAMS 801, 802, 821 and 822) , *Robert Haas* (Texel, CAMS 810, 811, 812 and 813), *Klaas Jobse* (Oostkapelle, CAMS 3030, 3031, 3032, 3033, 3034, 3035, 3036 and 3037), *Carl Johannink* (Gronau, CAMS 311, 312, 313, 314, 315, 316, 317 and 318), *Hervé Lamy* (Ukkel, CAMS 393), *Hervé Lamy* (Dourbes, CAMS 394 and 395), *Hervé Lamy* (Humain, CAMS 816), *Koen Miskotte* (Ermelo, CAMS 351, 352, 353 and 354) , *Jos Nijland* (Terschelling, CAMS 841, 842, 843 and 844), *Tim Polfliet* (Gent, CAMS 396), *Steve Rau* (Zillebeke, CAMS 3850 and 3852), *Adriana en Paul Roggemans* (Mechelen, CAMS 383, 384, 388, 389, 399 and 809, RMS 003830 and 003831), *Adriana en Paul Roggemans* (Genk, RMS 3815), *Hans Schremmer* (Niederkruechten, CAMS 803), *Erwin van Ballegoij* (Heesch, CAMS 347 and 348)) and *Marco Van der Weide* (Hengelo, CAMS 3110).

References

Johannink C. (2019). “Activity of the 15 Bootids (FBO#923) observed by CAMS BeNeLux”. *eMetN*, **4**, 213–215.

Roggemans P. (2019a). “Outburst 15 Bootids (FBO#923)”. *eMetN*, **4**, 216–219.

Roggemans P. (2019b). “June epsilon Ophiuchids (JEO#459), 2019 outburst and an impactor?”. *eMetN*, **4**, 201–206.

Roggemans P. (2019c). “March 2019 report CAMS BeNeLux”. *eMetN*, **4**, 246–248.

January 2020 report CAMS BeNeLux

Paul Roggemans

Pijnboomstraat 25, 2800 Mechelen, Belgium
paul.roggemans@gmail.com

A summary of the activity of the CAMS BeNeLux network during the month of January 2020 is presented. January 2020 was a typical winter month with mostly unfavorable weather circumstances. 12997 meteors were recorded, 6045 of which proved multiple station, or 47%, good for 2075 orbits. The Quadrantid maximum night January 3-4 was the most successful night with as many as 660 orbits in this single night.

1 Introduction

January tends to be one of the worst months for astronomy in the BeNeLux with mostly overcast sky. During the 8 past years the CAMS BeNeLux network did not have any single month of January with favorable weather circumstances. After 8 years, the night of January 23–24 with only 5 orbits collected remains the poorest calendar date on the CAMS BeNeLux orbit tally. Would 2020 bring us finally better luck for January?

2 January 2020 statistics

The first month of 2020 continued the unfavorable weather reputation for January with not a single perfect clear night. The best we got were nights with some clear spans. As many as 8 nights ended without any single orbit. Luckily, one of these partial clear nights occurred during the Quadrantid maximum which was favorably timed this year.

CAMS BeNeLux managed to register 12997 meteors (10943 in 2019) with a maximum of 83 operational cameras (75 in 2019) at 21 participating stations, with 6045 or 47% multi-station meteors (5124 or 47% in 2019) good for 2075 orbits (1857 in 2019). The total number of orbits is a new record number for the month of January. This good result is entirely due to the Quadrantid night of 3–4 January when as many as 660 orbits were collected. Without this lucky night, January 2020 would have been the worst January since 2016.

At best 83 of the 92 operational cameras were active during some nights in January 2020. On average 72.9 cameras were capturing per night. Only 8–9 January did not have any meteor registered. Thanks to AutoCAMS the surveillance of the BeNeLux sky was guaranteed with a minimum of 64 active cameras on all nights. On 23 nights orbits have been collected. The long winter nights may often start with an overcast sky looking hopeless to get anything like clear sky, but nights with up to 14 hours of dark sky often prove to have time spans with unpredicted clear sky. Casual observers often remain unaware of such clear periods while the AutoCAMS observers get happily surprised when confirming unexpected meteors. A substantial part of the January 2020 orbits comes from this permanent alertness provided by AutoCAMS. *Figure 1* and *Table 1* show the evolution compared to the previous months of January.

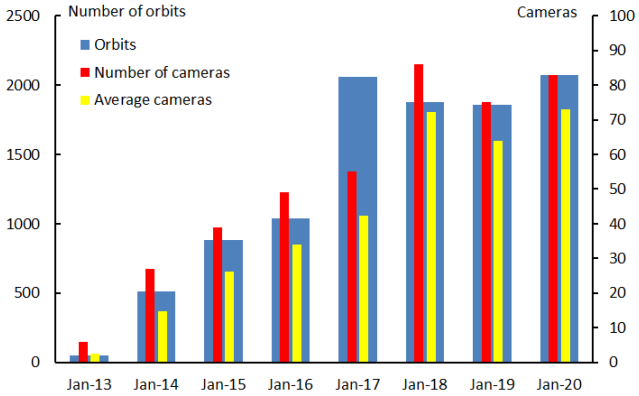

Figure 1 – Comparing January 2020 to previous months of January in the CAMS BeNeLux history. The blue bars represent the number of orbits, the red bars the maximum number of cameras running in a single night and the yellow bars the average number of cameras running per night.

Table 1 – January 2020 compared to previous months of January.

Year	Nights	Orbits	Stations	Max. Cams	Min. Cams	Mean Cams
2013	7	49	6	6	-	2.6
2014	21	514	11	27	-	14.8
2015	22	880	14	39	-	26.1
2016	25	1037	15	49	10	34.0
2017	23	2058	18	55	18	42.3
2018	25	1878	22	86	53	72.0
2019	22	1857	20	75	54	64.0
2020	23	2075	21	83	64	72.9
Tot.	168	10348				

A positive note for January 2020 is that less technical failures were reported.

3 Conclusion

The team members spent a lot of efforts to get some results out of mostly cloudy nights. Despite the bad weather still a very nice result has been obtained. The variable weather combined with long winter nights produces often some short intervals with clear skies. AutoCAMS is recommended to have all cameras running whenever unexpected clear sky occurs.

Acknowledgment

Many thanks to all participants in the CAMS BeNeLux network for their dedicated efforts. Thanks to *Carl Johannink* for providing all the data on which this report is based. The CAMS BeNeLux team is operated by the following volunteers:

Hans Betlem (Leiden, Netherlands, CAMS 371, 372 and 373), *Jean-Marie Biets* (Wilderen, Belgium, CAMS 379, 380, 381 and 382), *Martin Breukers* (Hengelo, Netherlands, CAMS 320, 321, 322, 323, 324, 325, 326 and 327, RMS 328 and 329), *Guiseppe Canonaco* (Genk, RMS 3815), *Bart Dessoy* (Zoersel, Belgium, CAMS 397, 398, 804, 805, 806 and 888), *Jean-Paul Dumoulin and Christian Walin* (Grapfontaine, Belgium, CAMS 814 and 815, RMS 003814), *Luc Gobin* (Mechelen, Belgium, CAMS 390, 391, 807 and 808), *Tioga Gulon* (Nancy, France, CAMS 3900 and 3901), *Robert Haas* (Alphen aan de Rijn, Netherlands, CAMS 3160, 3161, 3162, 3163, 3164, 3165, 3166 and 3167), *Robert Haas* (Texel, Netherlands, CAMS 810, 811, 812 and 813), *Robert Haas / Edwin van Dijk* (Burlage, Germany, CAMS 801, 802, 821 and 822), *Klaas Jobse* (Oostkapelle, Netherlands, CAMS 3030, 3031, 3032, 3033, 3034, 3035, 3036 and 3037), *Carl Johannink* (Gronau, Germany, CAMS 311, 312, 314, 315 and 316), *Hervé Lamy* (Dourbes, Belgium, CAMS 394 and 395), *Hervé Lamy* (Humain Belgium, CAMS 816), *Hervé Lamy* (Ukkel, Belgium, CAMS 393), *Koen Miskotte* (Ermelo, Netherlands, CAMS 351, 352, 353 and 354), *Tim Polfliet* (Gent, Belgium, CAMS 396), *Steve Rau* (Zillebeke, Belgium, CAMS 3850 and 3852), *Paul and Adriana Roggemans* (Mechelen, Belgium, CAMS 383, 384, 388, 389, 399 and 809, RMS 003830 and 003831), *Hans Schremmer* (Niederkruechten, Germany, CAMS 803) and *Erwin van Ballegoij* (Heesch, Netherlands,CAMS 347 and 348).

Winter and Ursids observations 2019

Pierre Martin

Ottowa, Canada
meteorshowersca@yahoo.ca

An overview is given of the 2019 December meteor observations by the author, covering the Ursid meteor shower.

1 December 22–23, 2019

Here's my report on the Ursids. Raymond Dubois joined me for an outing to the L&A Dark Sky Site, located about 190km south-west of Ottawa. The weather forecasts were most promising for this area, although the unseasonably mild temperature created a widespread haze of humidity in the atmosphere. Raymond and I travelled together with all our gear and we arrived at the L&A site near suppertime. My goal was to start observing as soon as possible to catch the Ursids near the possible timing of the dust filament. Unfortunately, there were some early frustrations. A number of people were at the site already and doing a campfire (not allowed I think). Also, a few issues setting up camera equipment. A nice long yellow Ursid of mag +2 was seen in the north-east. Eventually, I signed on at 7pm, and I observed for 42 minutes before cutting the hour short to attend my cameras. I resumed observing a half hour later and went on for an hour and a half. The sky was okay, but hazy and not optimal. Ursids were active in small numbers. After another short break, I observed for the next two hours, seeing 6 Ursids. At that point, a very heavy fog materialized, and gradually forced me to stop observing. It was thick enough to block the view of all but the brightest stars. I decided to go for a nap but I kept my cameras running. I woke up after 1:30am and the sky improved somewhat. I made an attempt to observe but it only lasted 17 minutes before heavy fog rolled in again. After another snooze, I woke up just before 4:30am, and the sky was crystal clear. I could watch for one more hour, and during that time, only one Ursid was seen among other meteors. All in all, in a total of about 5 hours, I saw 37 meteors (14 Ursids, 4 antihelions, 3 December Leo Minorids, 3 Coma Berenicids, 1 Quadrantid and 12 sporadics). It certainly felt like the Ursids were more active in the early part of the night and winding down towards the end.

The nicest meteor was a +1 green December Leo Minorid that shot swiftly in the north, leaving a 2 sec train.

At one point, a young couple joined us, and they enjoyed sitting back to watch the sky with us.

Observation December 22–23 2019, 00^h00^m–10^h40^m UT (19^h00^m–05^h40^m EST)

Location: L&A County Public Dark Site, Ontario, Canada, (Long: -77.116 West; Lat: 44.559 North) Observed showers:

- Anthelion (ANT) – 06:53 (103) +23
- Monocerotids (MON) – 07:28 (112) +07
- alpha Hydrids (AHY) – 07:46 (117) -06
- December Leonis Minorids (DLM) – 10:44 (161) +29
- Comae Berenicids (COM) – 12:11 (183) +14
- Ursids (URS) – 14:30 (218) +75
- Quadrantids (QUA) – 14:54 (224) +53

Figure 1 – Composite image of 9 Ursids and 3 sporadic meteors. Canon 6D, Sigma 35mm f/1.4 lens.

00^h00^m–00^h42^m UT (19^h00^m–19^h42^m EST); clear; 2/5 trans; F 1.11; LM 6.18; facing NNE60 deg; t_{eff} 0.70 hr

- URS: one: +4
- ANT: one: +3
- Sporadics: one: +4
- Total meteors: Three

01^h12^m–02^h12^m UT (20^h12^m–21^h12^m EST); clear; 2/5 trans; F 1.00; LM 6.20; facing NNE60 deg; t_{eff} 1.00 hr

- URS: five: +2(2); +3(2); +5
- ANT: two: +1; +4
- Sporadics: one: +1
- Total meteors: Eight

02^h12^m–02^h28^m UT (21^h12^m–21^h28^m EST); clear; 2/5 trans; F 1.00; LM 6.20; facing NNE60 deg; t_{eff} 0.266 hr

- URS: one: +5
- Total meteors: One

02^h57^m–03^h57^m UT (21^h57^m–22^h57^m EST); clear; 2/5 trans; F 1.00; LM 6.18; facing NNE60 deg; t_{eff} 1.00 hr

- URS: three: +3; +4(2)
- DLM: one: +1
- Sporadics: one: +5
- Total meteors: Five

03^h57^m–04^h45^m UT (22^h57^m–23^h45^m EST); clear; 1/5 trans; F 1.04; LM 5.63; facing NNE60 deg; t_{eff} 0.80 hr

- URS: three: +1; +3(2)
- ANT: one: +5
- Sporadics: four: +1; +4(2); +5
- Total meteors: Eight

06^h40^m–06^h57^m UT (01^h40^m–01^h57^m EST); clear; 1/5 trans; F 1.00; LM 5.90; facing NNE60 deg; t_{eff} 0.283 hr

- Sporadics: two: +5(2)
- Total meteors: Two

09^h25^m–10^h40^m UT (04^h25^m–05^h40^m EST); clear; 2/5 trans; F 1.00; LM 6.25; facing NNE60 deg; t_{eff} 1.25 hr

- COM: three: +4(3)
- DLM: two: +3; +5
- URS: one: +5
- QUA: one: +4
- Sporadics: three: +3(2); +4
- Total meteors: Ten
-

Figure 2 – Composite image of 3 Ursids and 4 sporadic meteors. Canon 5D, Rokinon 24mm f/1.4 lens.

Radio observations in December 2019

Ivan Sergei

Mira Str.40-2, 222307, Molodechno Belarus
seriv76@tut.by

The results of the author's radio meteor observations for December 2019 are presented, as well as the observing results of the meteor shower of the Geminids according to the Canadian Meteor Orbit Radar, (CMOR).

1 December observations

The observations were carried out at a private astronomical observatory near the town of Molodechno (Belarus) at the place of Polyani. A 5 element-antenna directed to the west was used, a car FM-receiver was connected to a laptop with as processor an Intel Atom CPU N2600 (1.6 GHz). The software to detect signals is Metan (author – Carol from Poland).

In the first week of December meteor activity was higher due to the combined activity of many minor streams, on top of the main Geminid meteor stream. The total activity with the Chi Orionids on December 2 reached about 45 signals per hour. The peak activity of the Geminids was recorded during 05^h00^m–07^h00^m UT on December 14, while the visual peak occurred around 23^h40^m UT on December 14 (according to imo.net). The difference in time can be explained by the difference in the observing methods. The Earth first encounters the smaller meteoroids (radio observations) and a bit later the larger particles being recorded visually. The second reason is the radiant reaching the optimal reflection geometry of the antenna's directional pattern.

In the first half of the month, according to the recorded activity of CMOR (identification of radar images) the following minor streams displayed activity: NOO, DPC, QUA, DGE, ZLE, DTH, HYD, ACA, DSA, DTA, DNA, DEL, DRV, DEC, ORN, DAD, DCC, KLI, SSE, ORS, GCM, RLE, MON, PUP, PHO, Chi Orionids, GEM, DMT. In the second half of the month there were less minor streams, so the total activity was less: MON, ACA, HYD, SSE, DHY, ORS, DLM, QUA, DMT, DMH, ALY, DLN, DCM, AHY, DDL, GEM, URS, COM. Noticeable activity around December 4 and 5 seems to confirm the activity of the meteor streams GEM and NOO (the total activity of these two showers was the same as that of the GEM stream alone in the period from December 9 to 11). *Figure 1* shows the maxima of minor meteor showers in black, medium activity showers in blue, variable activity showers in green and the major meteor shower in red.

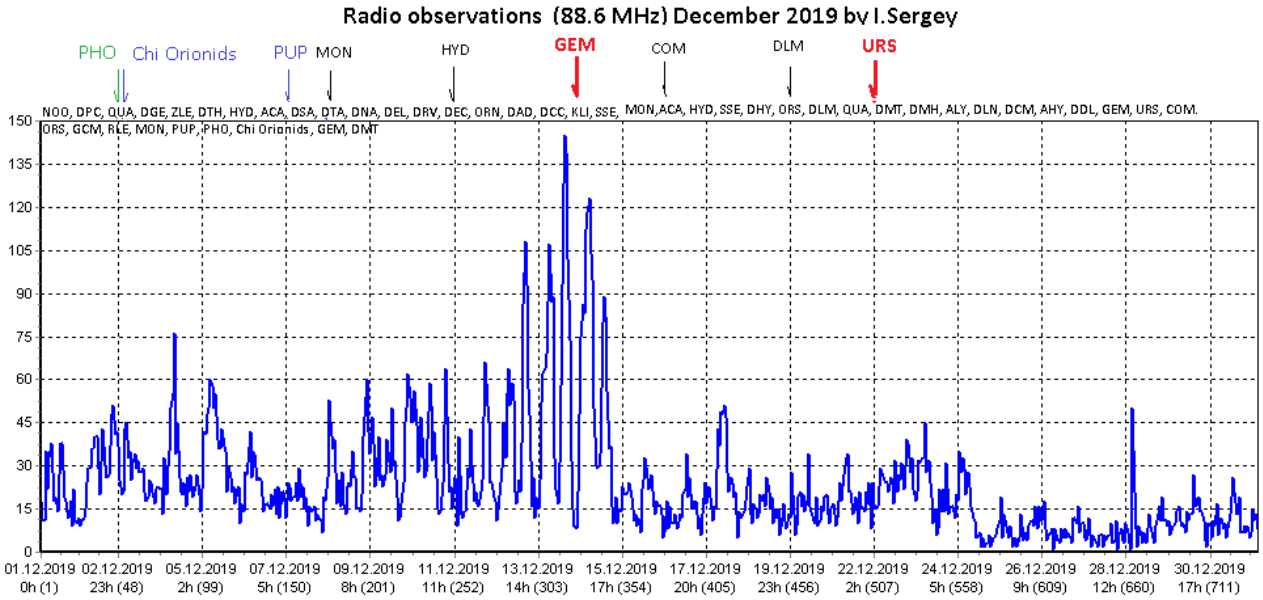

Figure 1 – Radio Meteor echo counts at 88.6 MHz for December 2019.

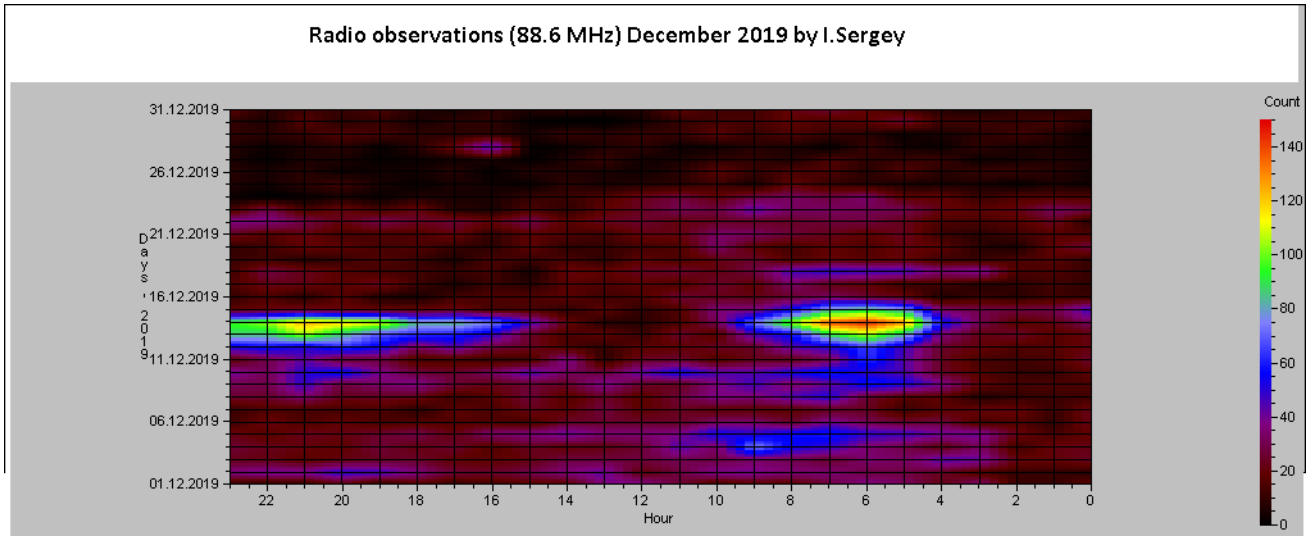

Figure 2 – Heatmap for radio meteor echo counts at 88.6 MHz for December 2019.

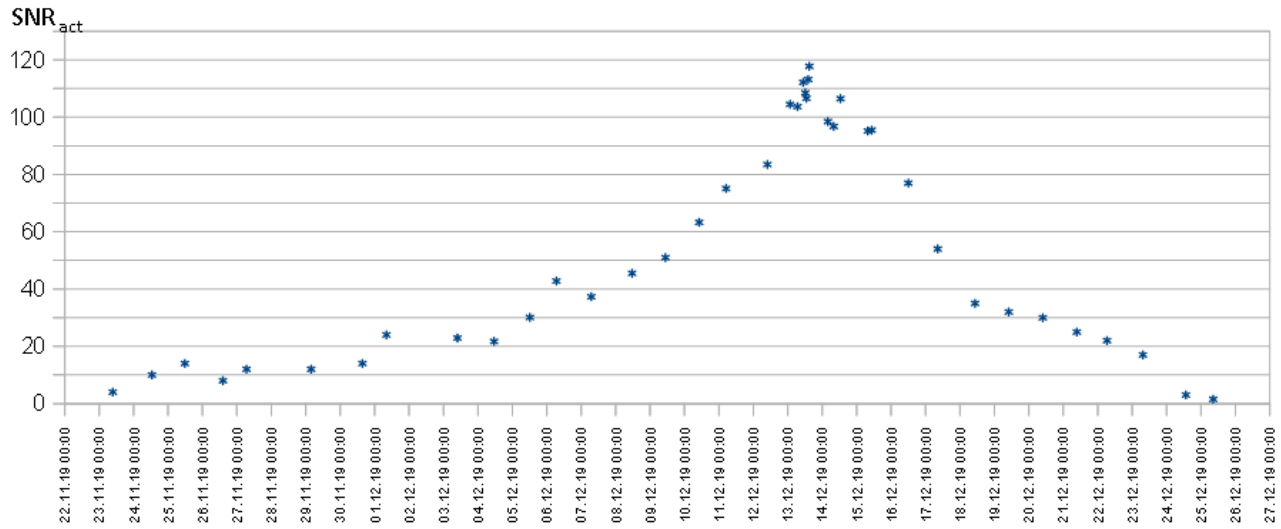

Figure 3 – The Geminid activity according to CMOR. (Signal -to-Noise Ratio – SNR is defined as the ratio of signal power to the background noise power).

The Geminid meteor shower has been detected on radar maps from November 23 onward. Confident identification of the shower occurs from November 24. However, according to IMO's visual data, the meteor stream starts later – on December 4. On December 1, for the first time there was a noticeable "redness" of the radiant, i.e. the activity of the stream then became stable and evident. The discrepancy with my data can be explained by the higher sensitivity of the radar, which causes the peak activity to occur about 15 hours earlier. December 23 is the last date when the radiant of this stream is identified on radar maps. The shower activity ends around December 25th.

The SNR value determined by the MaximDL photometry software with correction modifications (R,Y,G) was used to determine the activity level. A manual search was performed to detect the most optimal SNR value. SNR values were obtained by moving the cursor over the radiant image on the radar maps. General formula for calculating the shower activity level:

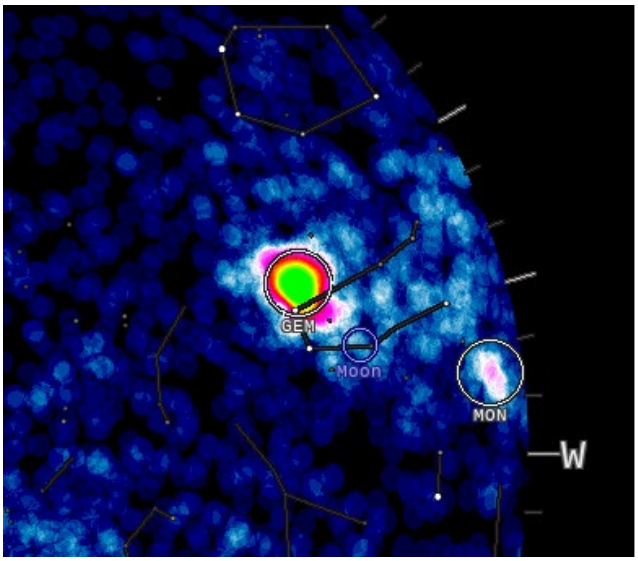

Figure 4 – Geminid radiant position 14 December 2019 12^h45^m UT according to CMOR.

SNRact = *SNR1* + *R* + *Y* + *G*, where *SNR1* is the total SNR level of the white and pink radiant area, *R* is the size in pixels of the radiation area on the radar maps, marked in red, *Y* is the size in pixels of the radiation area, marked in yellow on the radar maps, *G* is the size in pixels of the radiation area, marked in green on the radar maps.

According to the CMOR data, peak activity of the stream was maintained at a high level during the period from 13 December 2019 around 01^h00^m UT until 14 December 2019 around 13^h00^m UT. The probable peak of activity of the stream occurred around 15^h00^m UT 13 December 2019.

Acknowledgment

I would like to thank Sergey Dubrovsky for the software they developed for data analysis and processing of radio observations. Thanks to Paul Roggemans for his help in the lay-out and the correction of this article.

References

Jones J., Brown P., Ellis K. J., Webster A. R., Campbell-Brown M., Krzemenski Z., and Weryk R. J. (2005). "The Canadian Meteor Orbit Radar: system overview and preliminary results". *Planetary and Space Science*, **53**, 413–421.

Rendtel Jurgen (2019). "Meteor Shower Calendar". IMO.

Radio meteors December 2019

Felix Verbelen

Vereniging voor Sterrenkunde & Volkssterrenwacht MIRA, Grimbergen, Belgium
felix.verbelen@skynet.be

An overview of the radio observations during December 2019 is given.

1 Introduction

The graphs show both the daily totals (*Figure 1 and 2*) and the hourly numbers (*Figure 3 and 4*) of "all" reflections counted automatically, and of manually counted "overdense" reflections, overdense reflections longer than 10 seconds and longer than 1 minute, as observed here at Kampenhout (BE) on the frequency of our VVS-beacon (49.99 MHz) during the month of December 2019.

The hourly numbers, for echoes shorter than 1 minute, are weighted averages derived from:

$$N(h) = \frac{n(h-1)}{4} + \frac{n(h)}{2} + \frac{n(h+1)}{4}$$

During this month there was little local interference (apart from sometimes quite strong background noise), no registered "sporadic E" (Es) nor was there lightning activity. The automatic counts were corrected manually to eliminate as much as possible the effects of the interference.

The Geminids were, as expected, the eye-catchers of the month. The general structure of the shower is interesting: fairly slow increase of the activity if "all" Geminids are considered, while "long overdense reflections" reach a maximum more rapidly. Moreover, in the period before the maximum, the total number of meteors is strikingly larger than afterwards. This is best seen in the graphs of "all reflections"

The Ursids were rather weak this year. The graph with the hour counts of "all reflections" shows a small but clear peak at the expected time on December 23rd. However, overdense reflections longer than 10 seconds are evident on December 21–22–23, which is easily seen in the daily totals. Possibly the increase on December 21 is (partly) caused by another shower (? December Leonis Minorids = DLM).

Various other showers were active, especially in the first half of the month. To be further investigated.

Some screen-dumps of a selection of eye-catching long duration reflections are displayed (*Figures 5 to 14*).

If you are interested in the actual figures, please send me an e-mail: felix.verbelen at skynet.be.

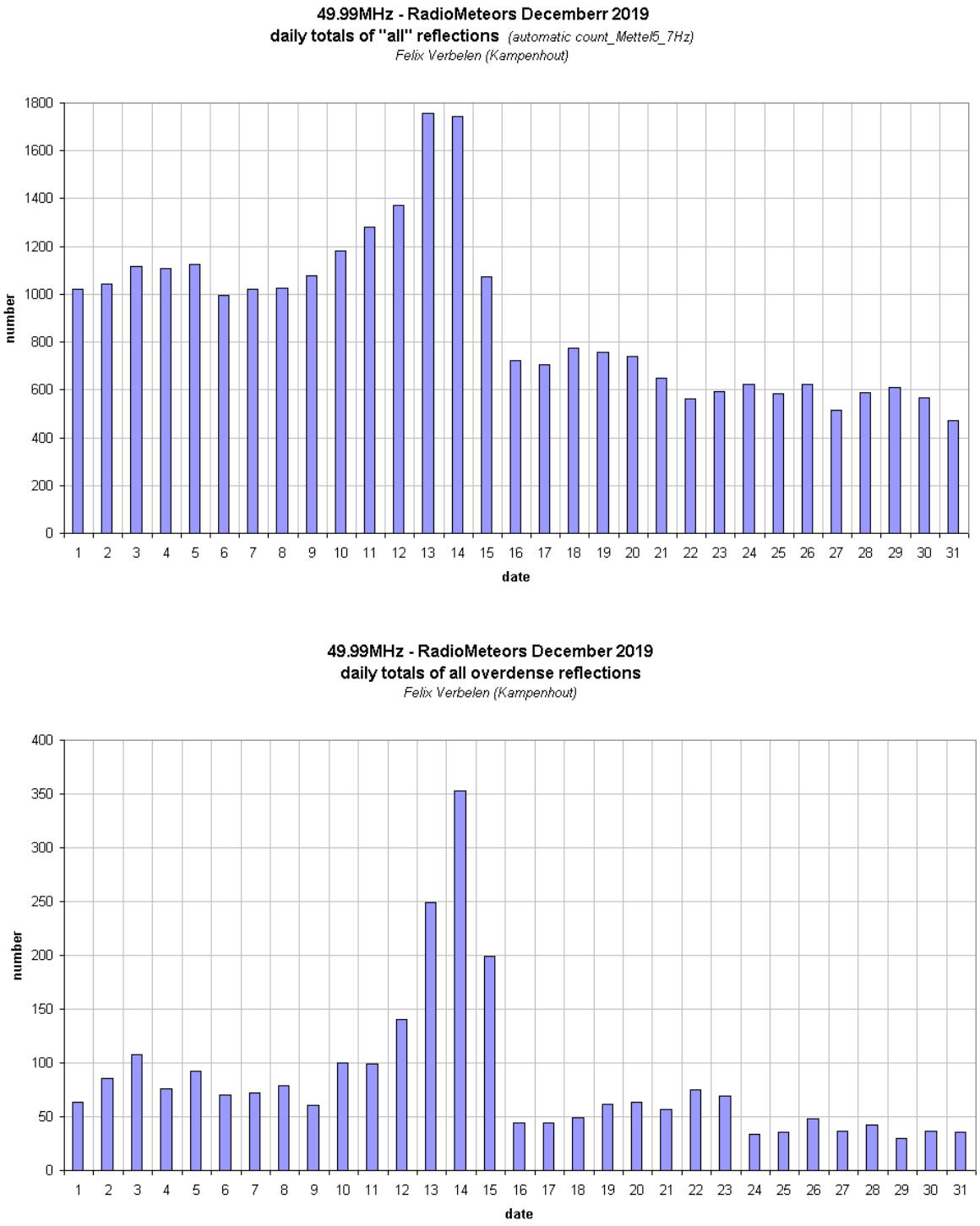

Figure 1 – The daily totals of "all" reflections counted automatically, and of manually counted "overdense" reflections, as observed here at Kampenhout (BE) on the frequency of our VVS-beacon (49.99 MHz) during December 2019.

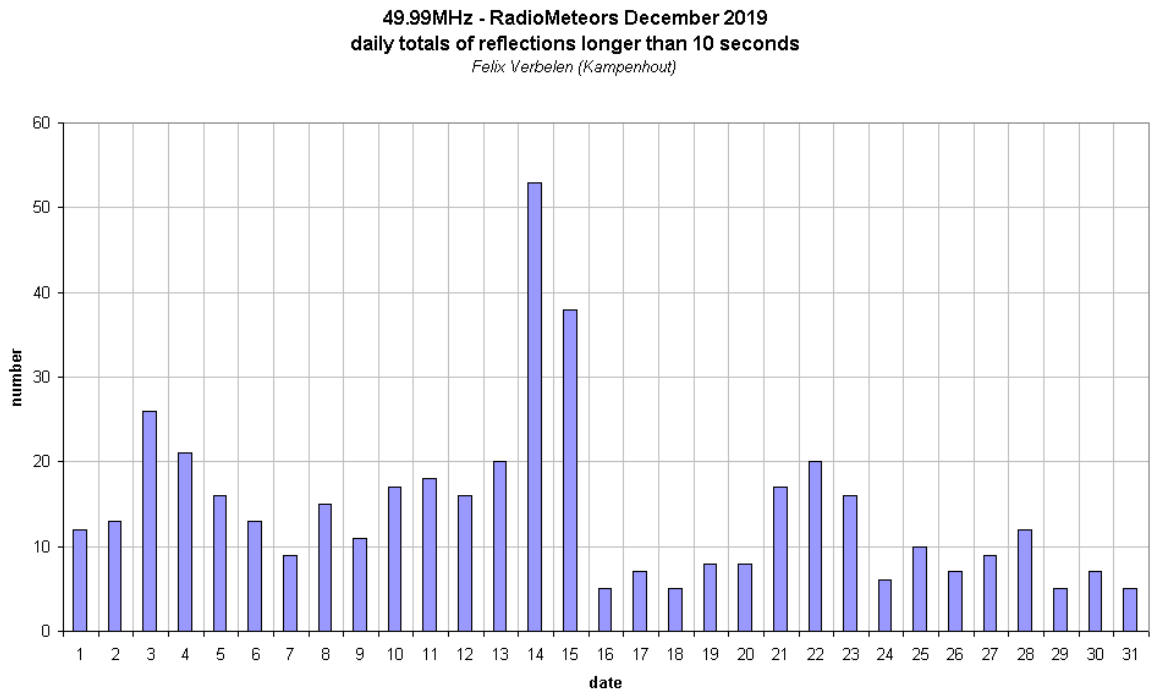

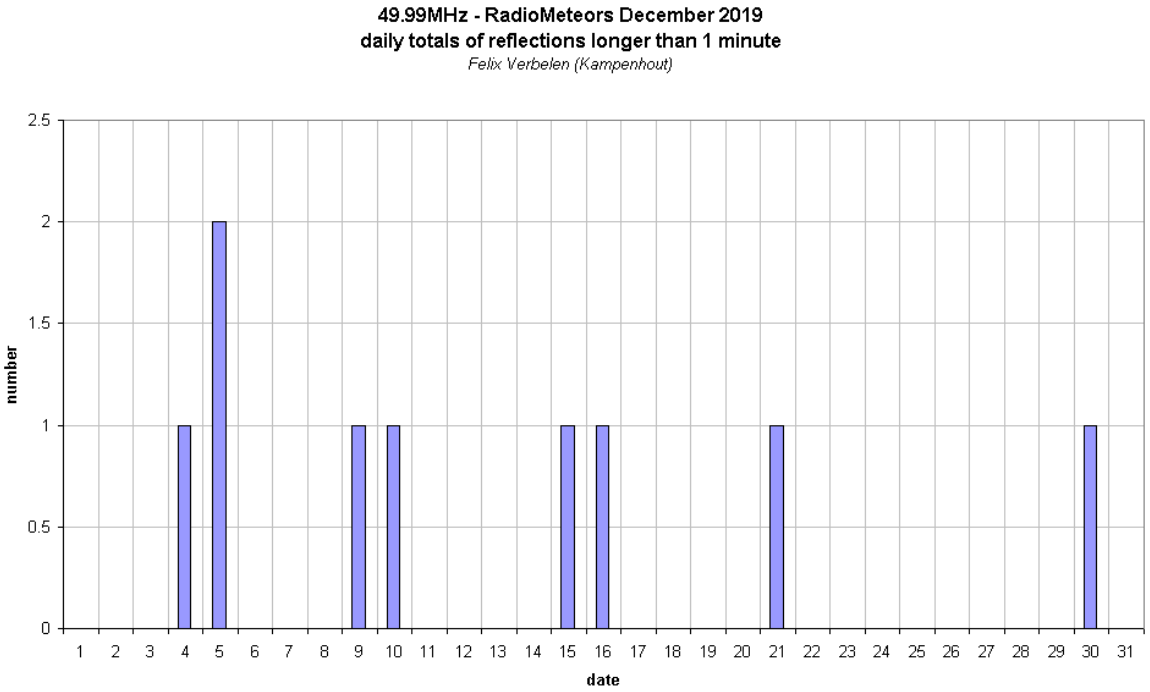

Figure 2 – The daily totals of overdense reflections longer than 10 seconds and longer than 1 minute, as observed here at Kampenhout (BE) on the frequency of our VVS-beacon (49.99 MHz) during December 2019.

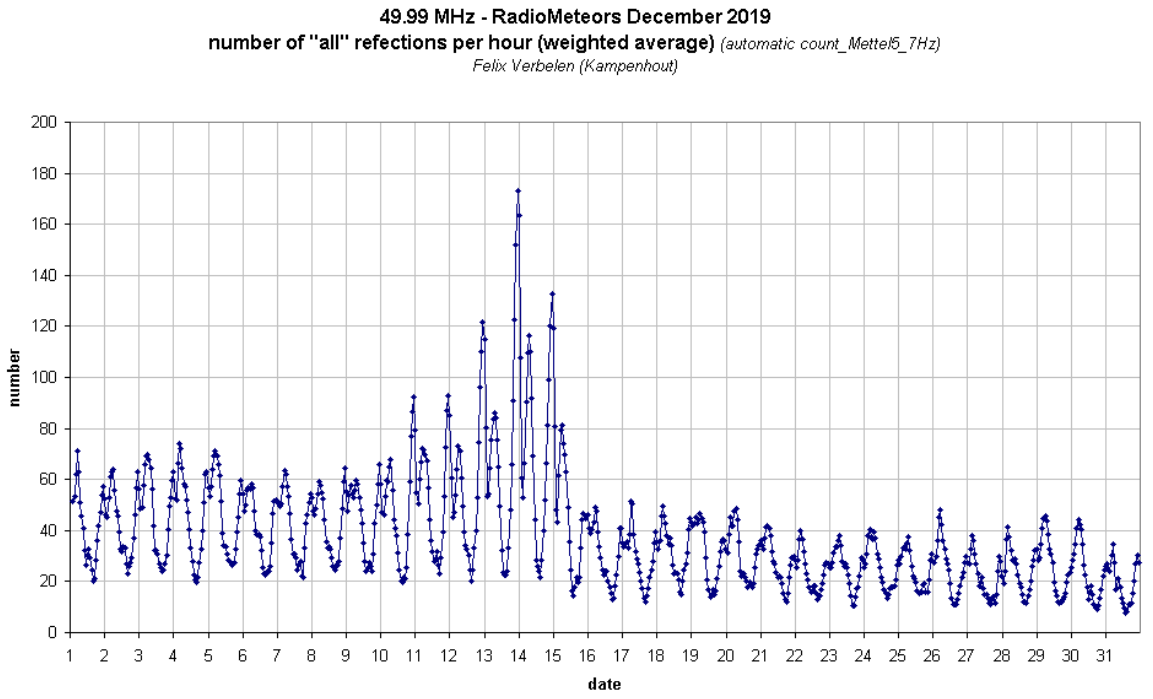

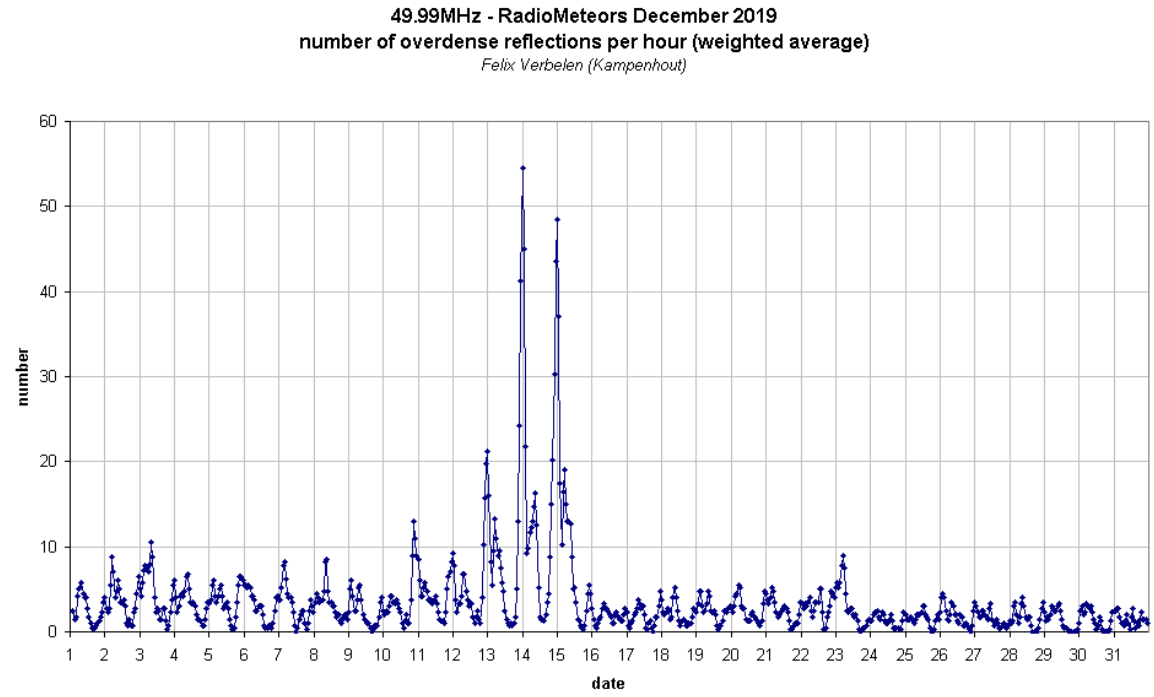

Figure 3 – The hourly numbers of "all" reflections counted automatically, and of manually counted "overdense" reflections, as observed here at Kampenhout (BE) on the frequency of our VVS-beacon (49.99 MHz) during December 2019.

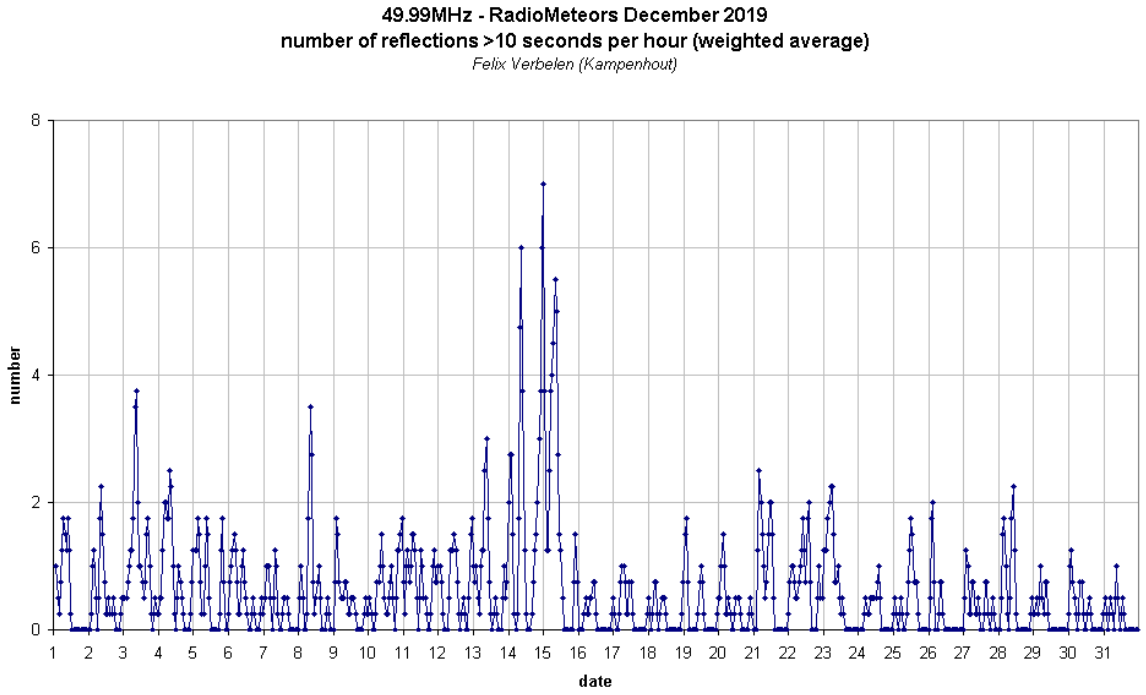

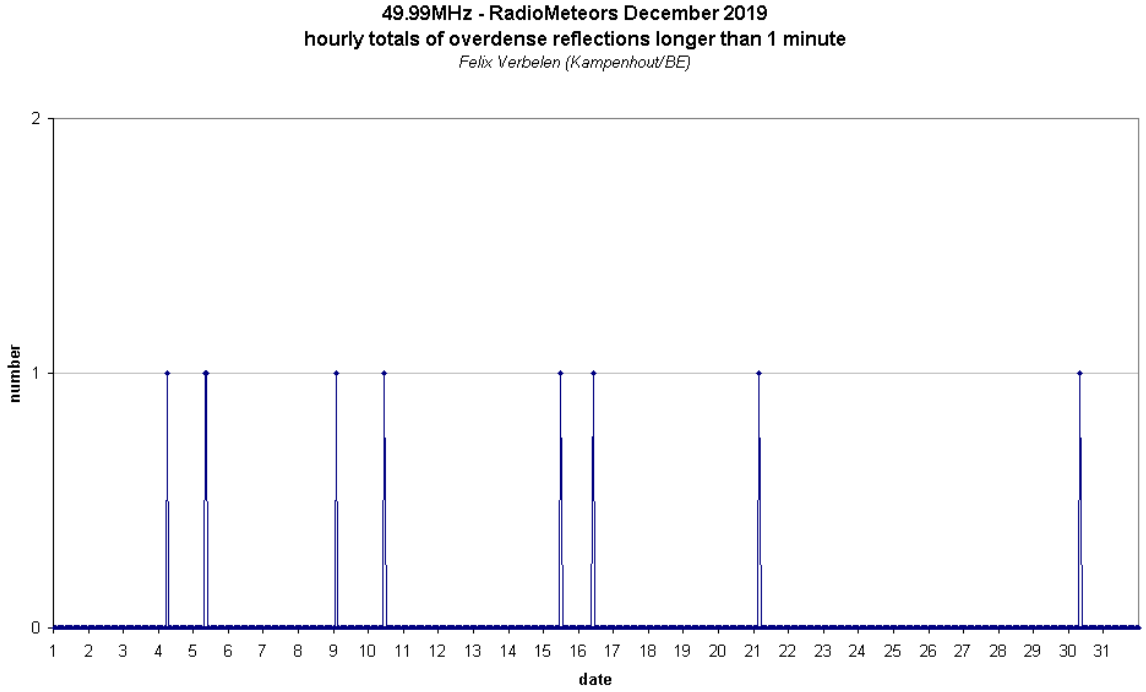

Figure 4 – The hourly numbers of overdense reflections longer than 10 seconds and longer than 1 minute, as observed here at Kampenhout (BE) on the frequency of our VVS-beacon (49.99 MHz) during December 2019.

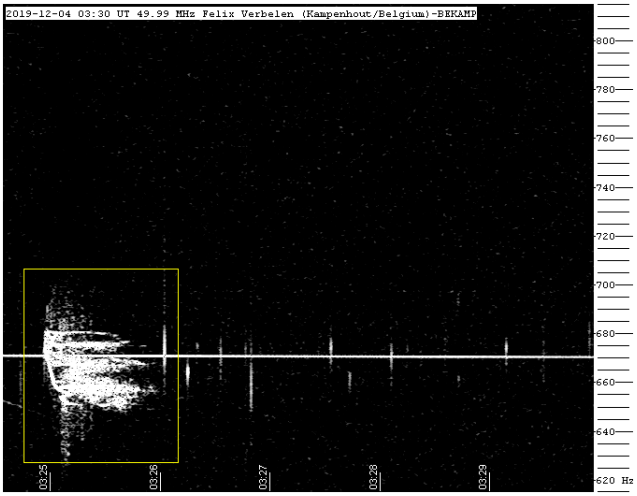

Figure 5 – 2019 December 04 at 03^h30^m UT.

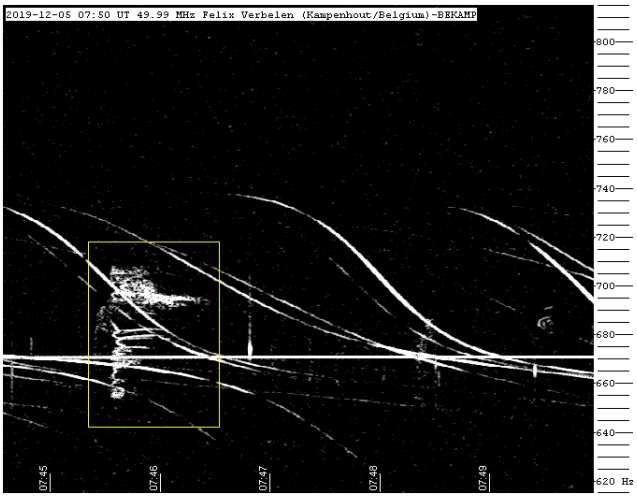

Figure 6– 2019 December 05 at 07^h50^m UT.

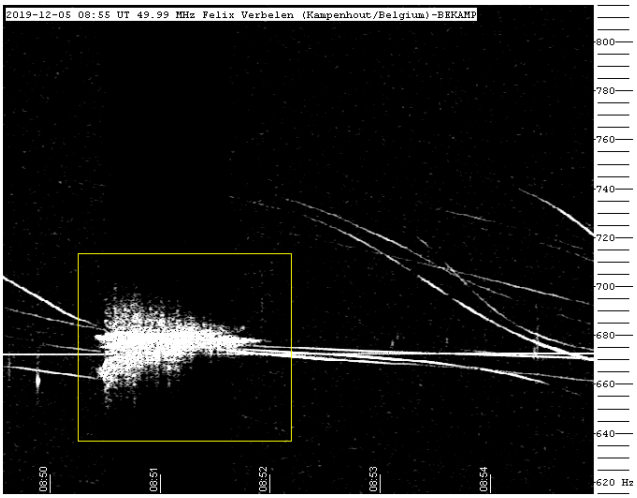

Figure 7 – 2019 December 05 at 08^h55^m UT.

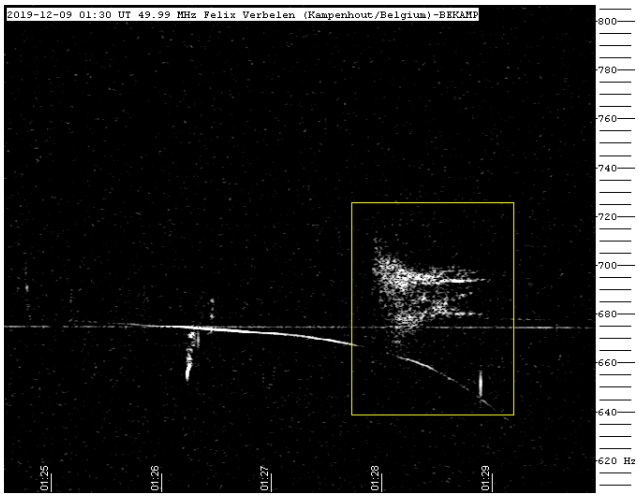

Figure 8 – 2019 December 09 at 01^h30^m UT.

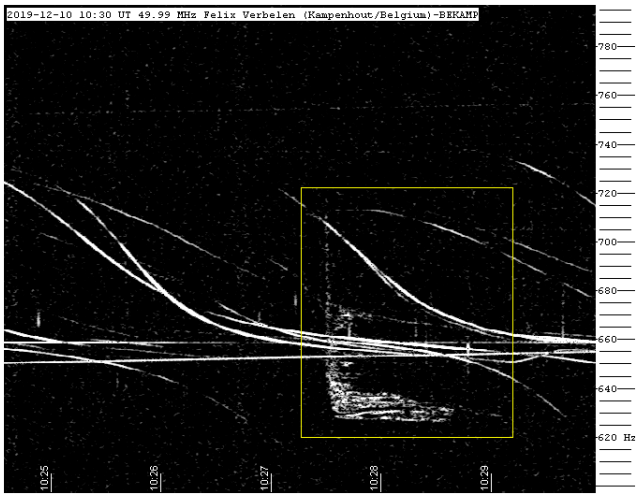

Figure 9 – 2019 December 10 at 10^h30^m UT.

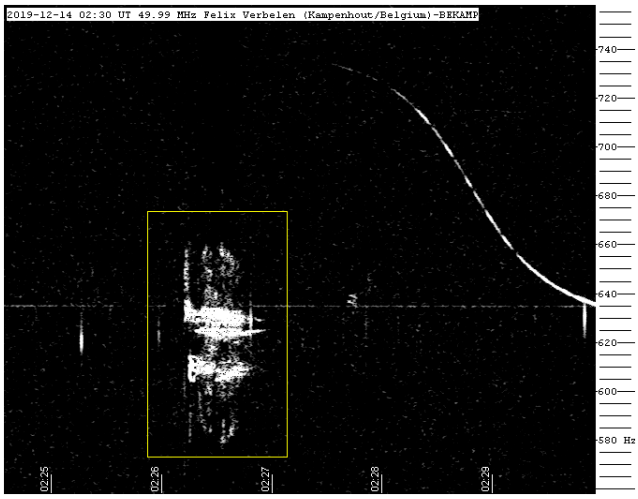

Figure 10 – 2019 December 14 at 02^h30^m UT.

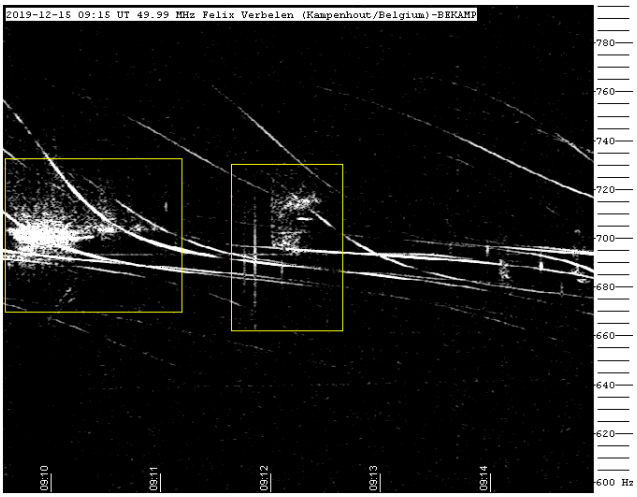

Figure 11 – 2019 December 15 at 09^{h}15^{m} UT.

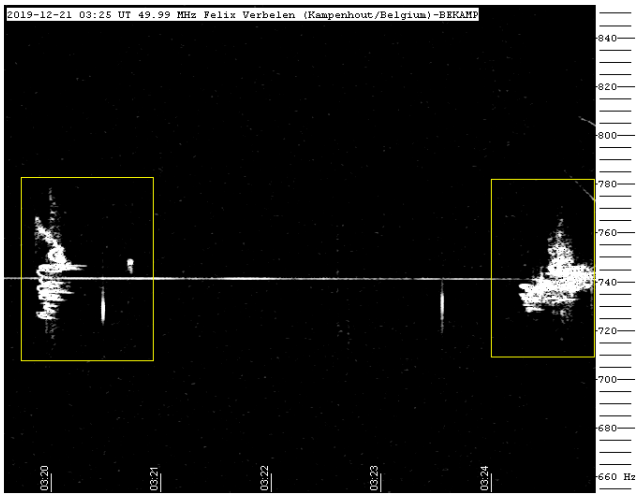

Figure 13 – 2019 December 21 at 03^{h}25^{m} UT.

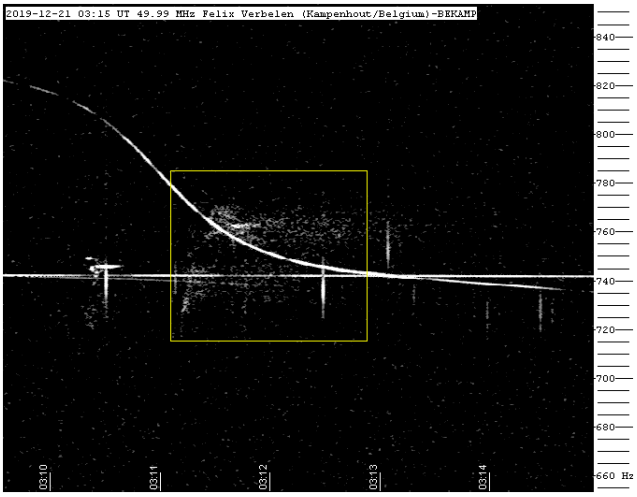

Figure 12 – 2019 December 21 at 03^{h}15^{m} UT.

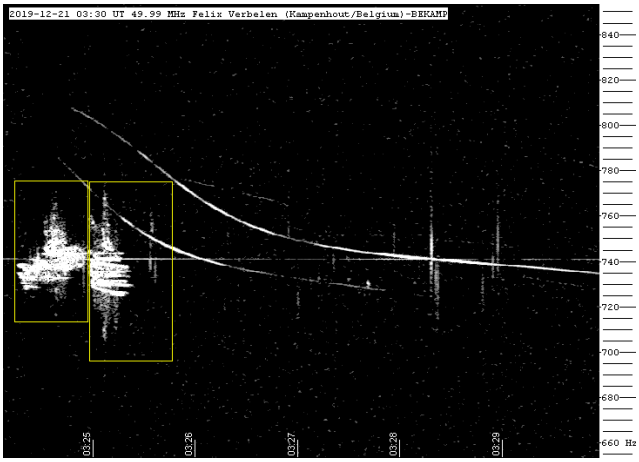

Figure 14 – 2019 December 21 at 03^{h}30^{m} UT.

Radio meteors January 2020

Felix Verbelen

Vereniging voor Sterrenkunde & Volkssterrenwacht MIRA, Grimbergen, Belgium
felix.verbelen@skynet.be

An overview of the radio observations during January 2020 is given.

1 Introduction

The graphs show both the daily totals (*Figure 1 and 2*) and the hourly numbers (*Figure 3 and 4*) of "all" reflections counted automatically, and of manually counted "overdense" reflections, overdense reflections longer than 10 seconds and longer than 1 minute, as observed here at Kampenhout (BE) on the frequency of our VVS-beacon (49.99 MHz) during the month of January 2020.

The hourly numbers, for echoes shorter than 1 minute, are weighted averages derived from:

$$N(h) = \frac{n(h-1)}{4} + \frac{n(h)}{2} + \frac{n(h+1)}{4}$$

During this month there were few local disturbances, no registered "sporadic E" and lightning activity on just 1 day (28 January).

Highlights of the month were of course the Quadrantids, peaking on January 4th. Compared to previous years, the shower was less active than expected. The rest of the month was fairly calm, but with nevertheless a number of nice smaller meteor showers, to be further analyzed in detail.

If you are interested in the actual figures, please send me an e-mail: felix.verbelen at skynet.be.

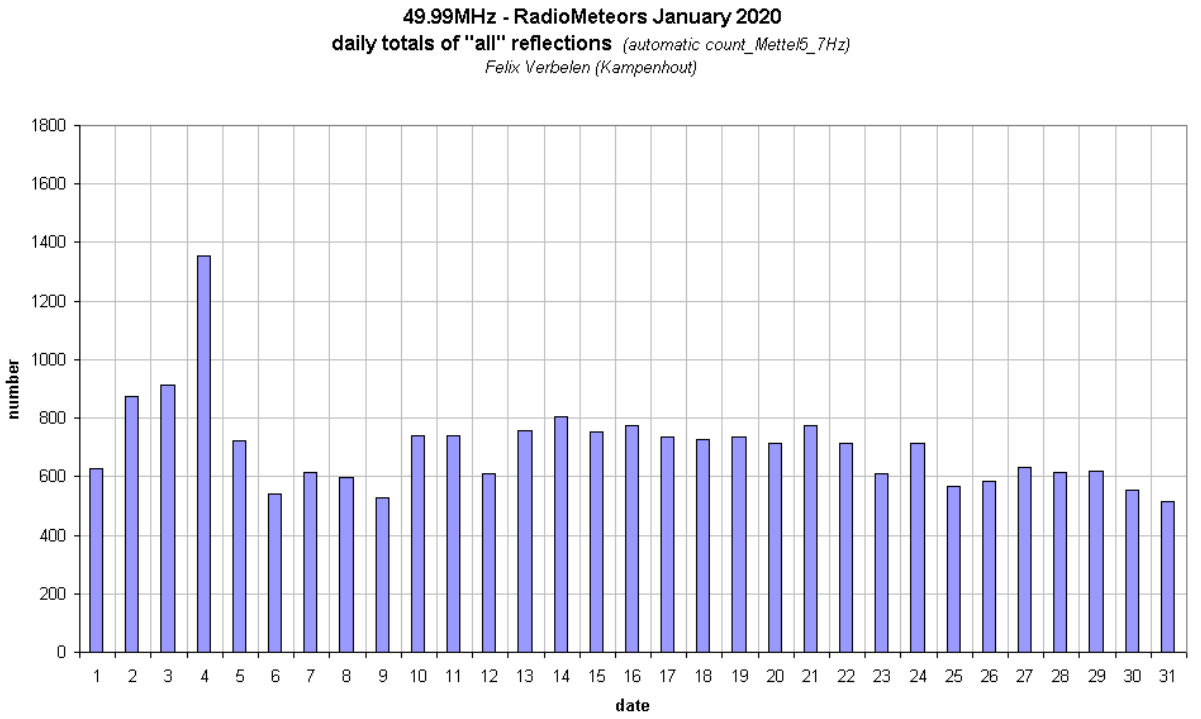

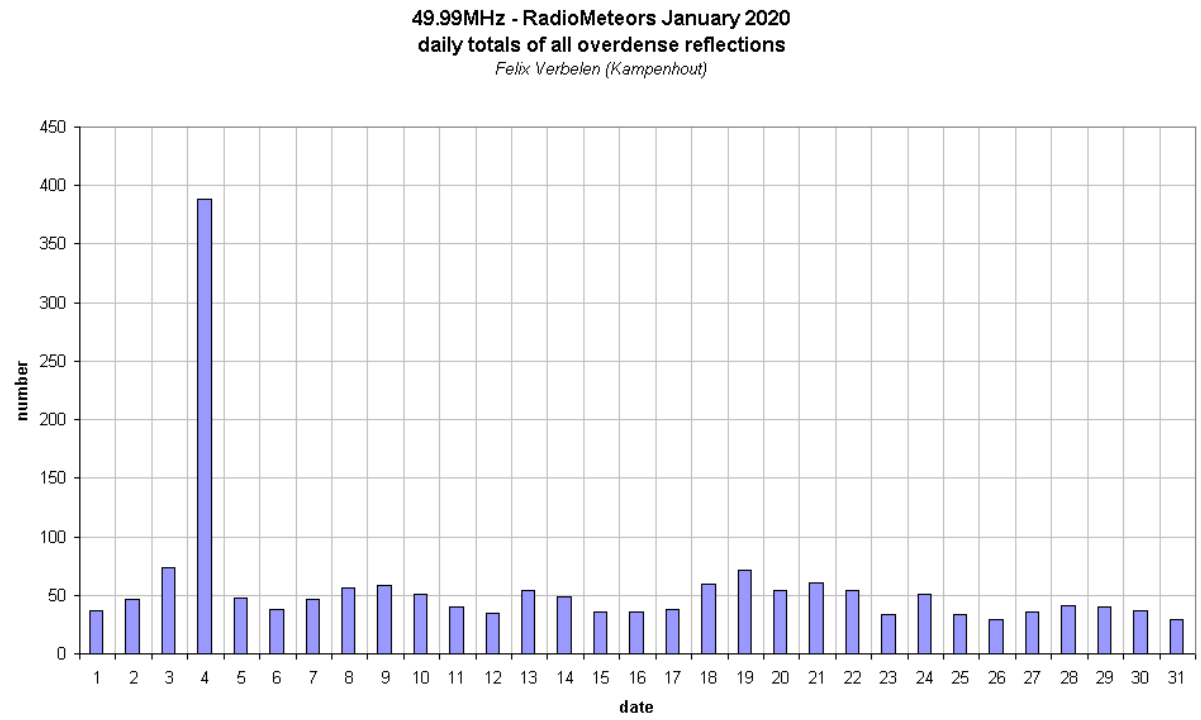

Figure 1 – The daily totals of "all" reflections counted automatically, and of manually counted "overdense" reflections, as observed here at Kampenhout (BE) on the frequency of our VVS-beacon (49.99 MHz) during January 2020.

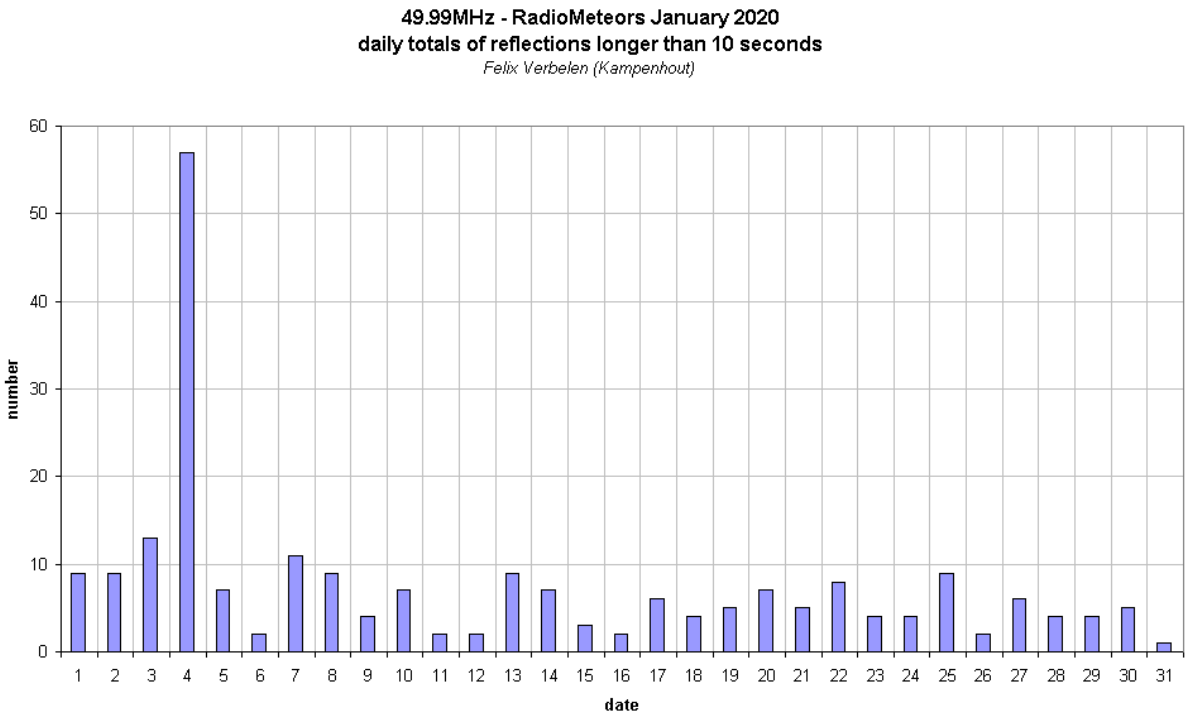

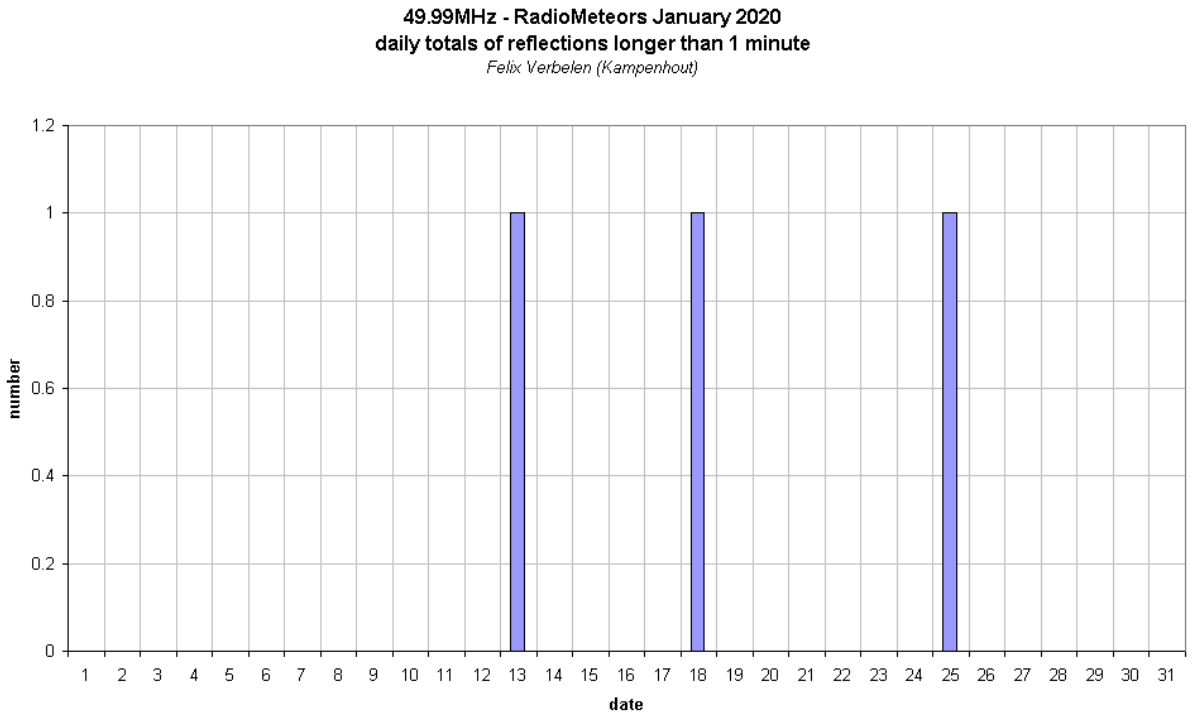

Figure 2 – The daily totals of overdense reflections longer than 10 seconds and longer than 1 minute, as observed here at Kampenhout (BE) on the frequency of our VVS-beacon (49.99 MHz) during January 2020.

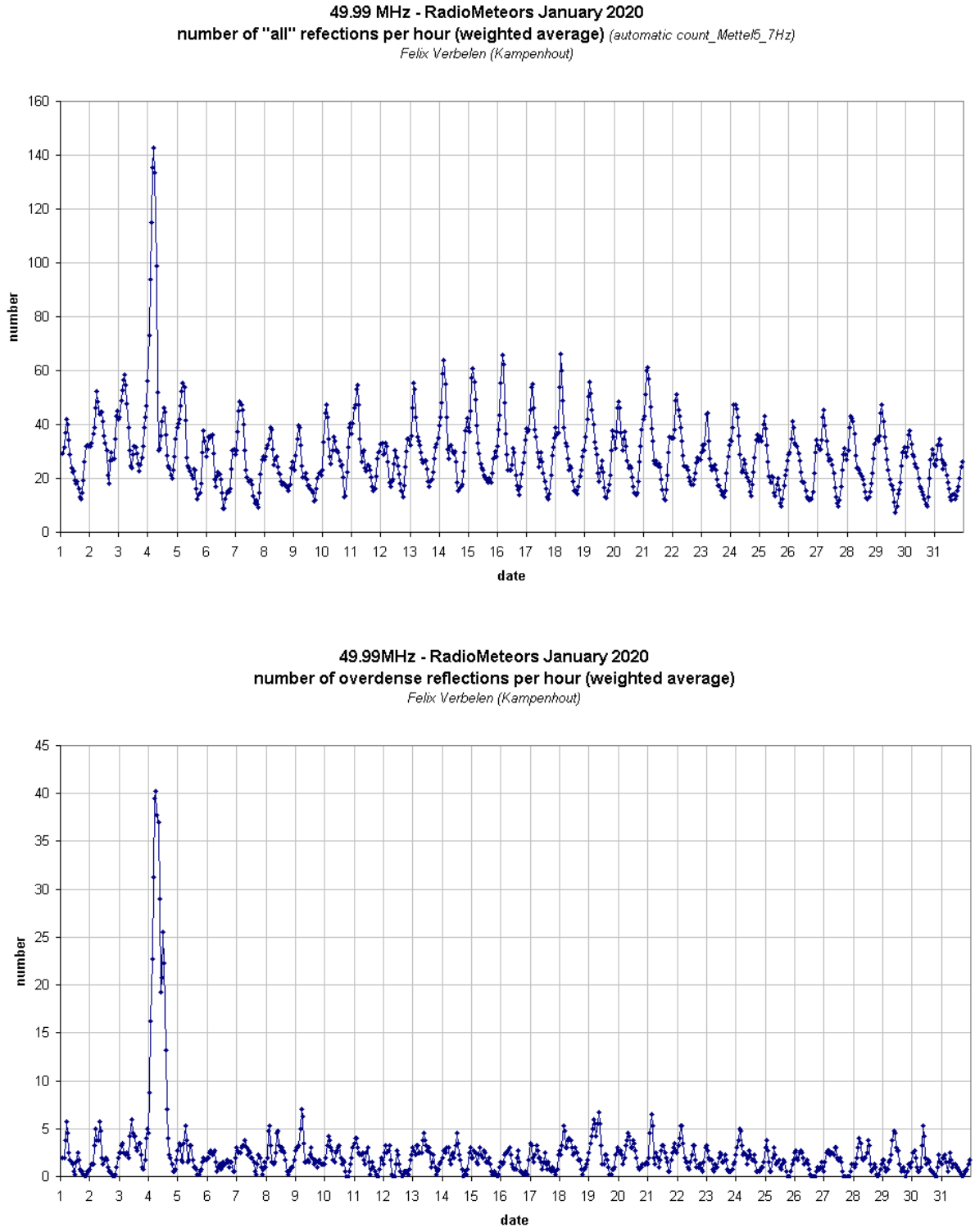

Figure 3 – The hourly numbers of "all" reflections counted automatically, and of manually counted "overdense" reflections, as observed here at Kampenhout (BE) on the frequency of our VVS-beacon (49.99 MHz) during January 2020.

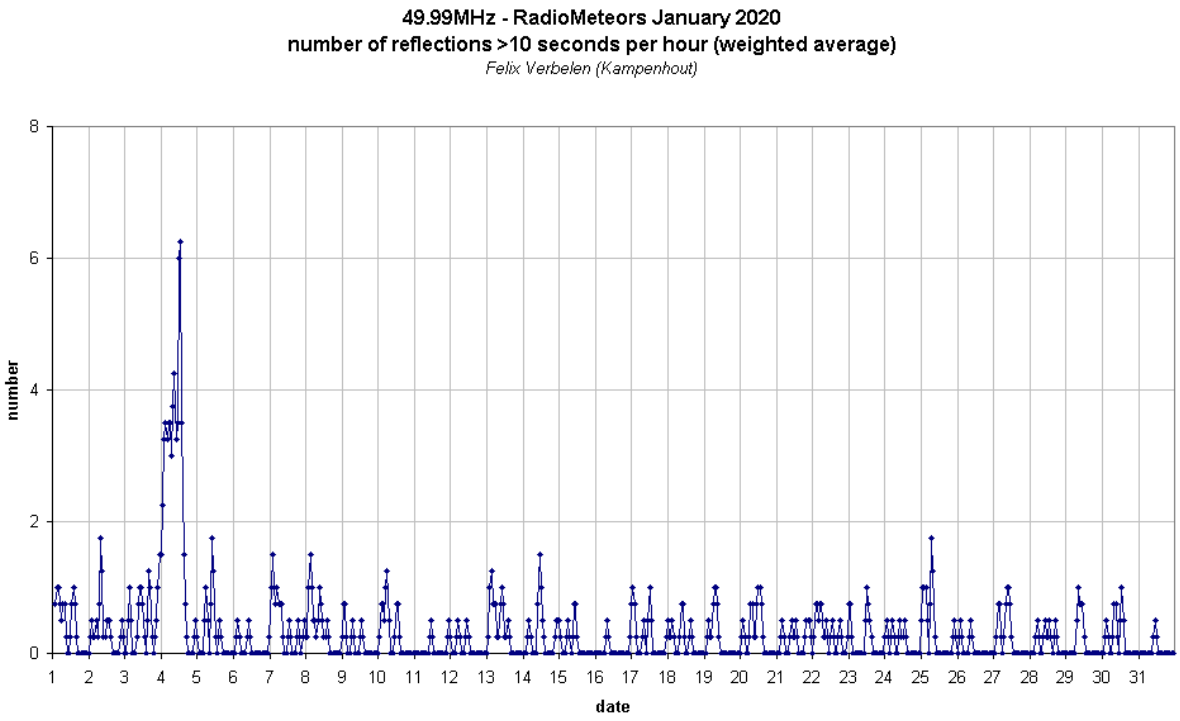

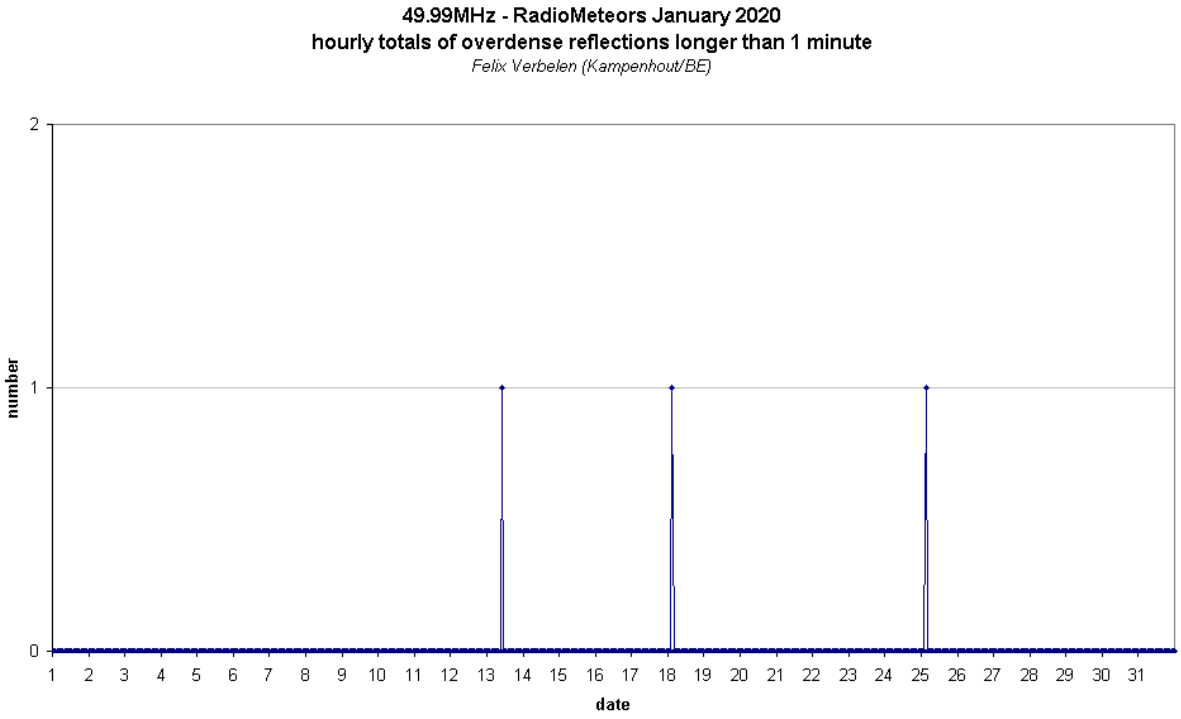

Figure 4 – The hourly numbers of overdense reflections longer than 10 seconds and longer than 1 minute, as observed here at Kampenhout (BE) on the frequency of our VVS-beacon (49.99 MHz) during January 2020.

Meteorite dropping fireball 8 April 2018

Gábor Kővágó

fotospentax@gmail.com

On 8 April 2018 at 18h47m33s UT a Full Moon bright bolide exploded over Hungary. Lots of meteorological camera caught the light of the fireball. Fortunately, three dedicated meteor cameras could also register the atmospheric trajectory. One of them was directly under the final phase of the fall and was able to take great pictures of it. The preliminary calculation shows that this event produced a meteorite fall in Croatia.

1 Initial data

As always, I tried to collect every online available picture about this event. Among the first there was a great photo of Landy-Gyebnár Mónika which has been published on Facebook (*Figure 1*).

Figure 1 – The bolide's photo from Veszprém, Hungary (Landy-Gyebnár Mónika's picture).

On the same day another lucky catch turned up, Pócsai Sándor's picture about the very end of the fall from Dávod. (*Figure 2*) The photo's fine resolution was a great help to measure the end of the trajectory accurately.

Figure 2 – Pócsai Sándor's photo about the fireball form Dávod, Hungary.

After a thorough search I could find numerous snapshots about the fireball (or at least its trail) among meteorological camera pictures. Because of licensing issues, I cannot publish any of them here, but this does not prevent the scientific use and measurement of the images.

Three dedicated meteor cameras could also observe the event (*Figure 3, 4 and 5*) moreover one of them was directly under the bolide's flight path. This camera's video offered a good opportunity to measure in detail the formed debris cloud's size and deceleration.

Figure 3 – The bolide's snapshot from Sárrét, (Slovakia).

Figure 4 – The bolide's snapshot from Soroksár, (Hungary).

Figure 5 – The bolide's snapshot from Becsehely, (Hungary).

The picture of Sárrét contains only the beginning part of the fall. Soroksár's picture didn't include the brightest phase of the fall, so the end of the trajectory is missing because of a software issue of Metrec. Becsehely's camera (also running with Metrec) somehow missed the first half of the fall but could catch the brightest phase – for that reason highly saturated – and the fragmentation.

2 Trajectory

I have seven observations all around the meteor trajectory, four of them are calibrated manually and three were made by dedicated meteor cameras.

Working with Metrec's data I noticed that the imprinted timestamps of the video frames were shifted, I had to take this into account when I was calculating with them.

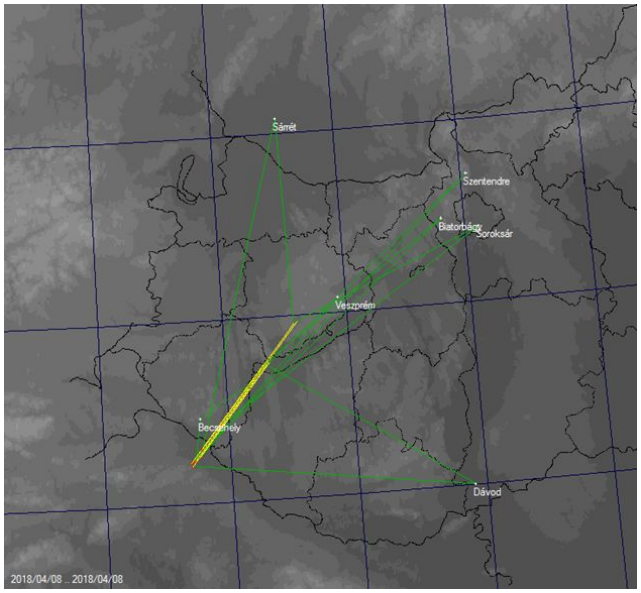

Figure 6 – UFOOrbit calculated trajectory based on seven calibrated observations.

I also had to manually measure begin- and endpoints in UFOAnalyzer, (SonotaCo, 2009) because the software calculation depends on detection's thresholds omitting frames, especially from the beginning of a fall. I used UFOOrbit's (SonotaCo, 2009) import function to deal with the measured points.

The meteor started its luminous path at 88.7±1.5 km reaching the atmosphere with 29.5±0.2 degrees inclination. It flew with an average speed of 15.7±0.5 km/s from Kapolcs (Hungary) to Cvetkovec (Croatia) during more than 6 seconds. The fireball's body fell apart above Becsehely reaching its peak brightness around –12±0.8 magnitude and formed a 6 km long cloud of debris. The meteor's fragments decelerated a lot in this phase until less than 4.8 km/s. I could calculate the deceleration by doing frame by frame measurement on the Becsehely's video for different heights during the fall. It also contains information about the initial velocity which was greater than 20.7 km/s. Luckily, the end of the trajectory was caught on fine resolution photos, so its accuracy is better than that at the beginning. The last fragments of the body could penetrate 27.2±0.7 km deep into the Earth's atmosphere.

Table 1 – Measured velocity at different heights from Becsehely.

Height (km)	Velocity (km/s)
63	20.71
31.6	5.08
29.9	4.846
29.6	4.8

3 Orbit

I used the three dedicated meteor cameras' observations to calculate the orbit of the fireball with the help of UFOOrbit, taking into consideration the deceleration. I matched the measured values with the already known fireballs' velocity curves and I changed manually the meteor velocity for the deduced entry value (21.5 km/s) in the imported data. I would draw attention to the fact that without error spread calculations the resulted orbit is just a rough estimate. Strangely, the resulting orbit – within its error boundaries – is very near or intersects the orbit of Mars.

The resulting orbital elements are:

- $\alpha = 246.6°$
- $\delta = +51.9°$
- $a = 1.3$ A.U.
- $q = 0.945$ A.U.
- $e = 0.265$
- $\omega = 223°$
- $\Omega = 18.6°$
- $i = 31.9°$

Figure 7 – Solid fragments in the wake at 29 km elevation.

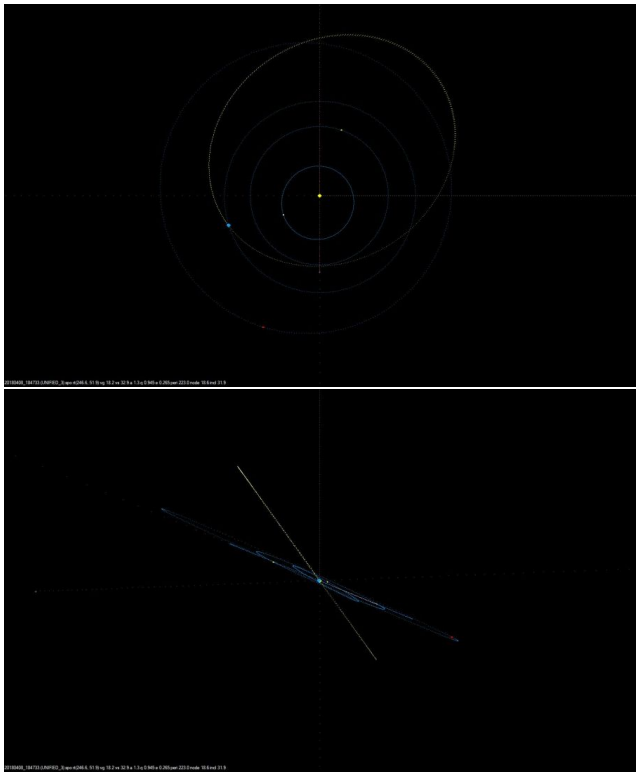

Figure 8– UFOOrbit calculated orbits, upper and lower image, with subtle differences between the observations.

4 Light and mass

After the event I found several visual observations online, in general they compared the fireball's brightness to the Full Moon. Especially those who were under the final phase of the fall.

As seen above, we have some very good photos for this event, but because of the unique settings and physical configuration of the machines, it is difficult to determine a reliable brightness from them.

Metrec isn't the finest tool either to measure precise light curve of a meteor. In this case, before the brightest phase – at around –3 magnitude – the software couldn't follow the meteor's trajectory for calculating its brightness because of the highly saturated images. I had to estimate its peak brightness with the aid of an old picture of the Full Moon with the same camera. It was in the same category or brighter as seen from Becsehely.

I calculated the photometric mass from the basic parameters of the event, absolute magnitude, velocity and zenith angle. (Jones et al., 1989) Insufficient knowledge about the brightness and the ablation coefficient increased the error margins greatly. The original mass was 1500±1000kg, which corresponds to a one-meter sized spherical body, assuming a density of an ordinary chondrite. After reaching the trajectory's terminal point, a total mass of about 1 kg began its dark flight.

5 Dark flight and strewn field

According to observations – while watching TV – people came out to the sound of explosion on the western part of the country. There was a double sonic boom which sounds like a distant thunder. Knowing this, seen the calculated residual mass and the deep penetration into the atmosphere there is a decent chance that some meteorites reached the ground.

I used a self-developed program called MetLab to calculate dark flight and the resulting strewn field. Wind and atmospheric data can be retrieved from the University of Wyoming (Department of Atmospheric Science) website[11]. In this case Zagreb's radiosonde measurement was 70 km away from the terminal phase of the fall. I started the Monte Carlo simulation with 100 pieces of 100–300 grams meteorites from the last three km of the trajectory assuming a density of an ordinary chondrite. (Brown circles) After that I added another 100 pieces with any known errors. (Red circles).

References

SonotaCo (2009). "A meteor shower catalog based on video observations in 2007-2008". *WGN, Journal of the International Meteor Organization*, **37**, 55–62.

Jones J., McIntosh B. A. and Hawkes R. L. (1989). "The age of the Orionid meteoroid stream". *Monthly Notices of the Royal Astronomical Society*, **238**, 179–191.

[11] http://weather.uwyo.edu/upperair/sounding.html

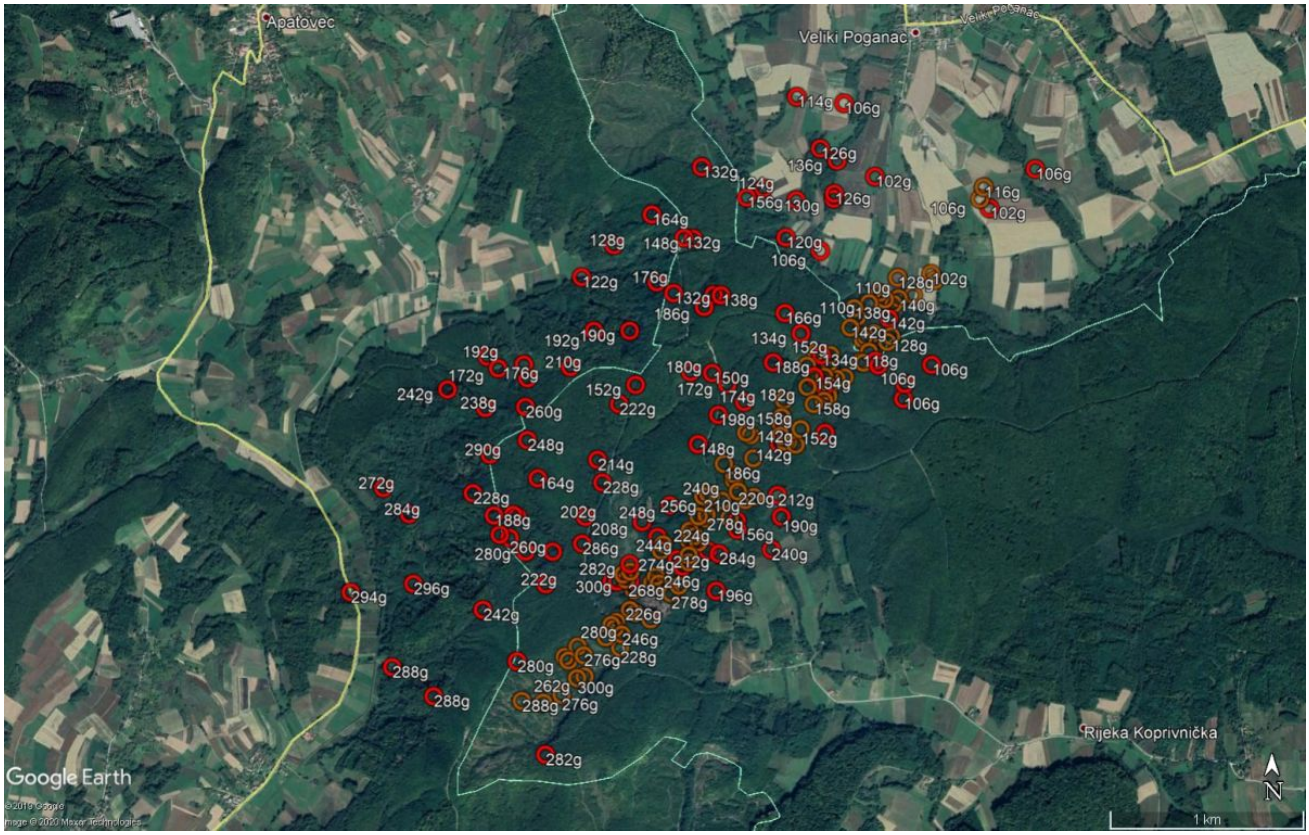

Figure 9 – The calculated strewn field is in a forested area among rural villages in Croatia.

Fireball events over Spain in January and February 2020

José María Madiedo

Instituto de Astrofísica de Andalucía
madiedo@iaa.es

An overview is presented of the exceptional fireball events by the meteor observing stations operated by the SMART Project from Sevilla and Huelva during January and February 2020.

1 2020 January 28

On 2020 January 28 at 23^h08^m UT, a rock from an asteroid entered the atmosphere at about 17 km/s and generated a mag. –14 fireball that overflew the south of Spain[12]. The event was recorded by the cameras operated in the framework of the SMART project. This project is being conducted by the Southwestern Europe Meteor Network (SWEMN), which in turn is leaded by the Institute of Astrophysics of Andalusia (IAA-CSIC). SMART obtained footage of the fireball from the astronomical observatories of Calar Alto (Almeria), La Sagra (Granada) and Seville.

The analysis of this sporadic event reveals that the fireball began at a height of about 91 km over the province of Cadiz (SW of Spain). It moved northeastwards and ended at a height of around 20 km over the province of Seville. The terminal point of the luminous trajectory was located almost over Arahal, a small town in Seville. The meteoroid was not completely destroyed at that point, which implies that this was a meteorite-producing fireball.

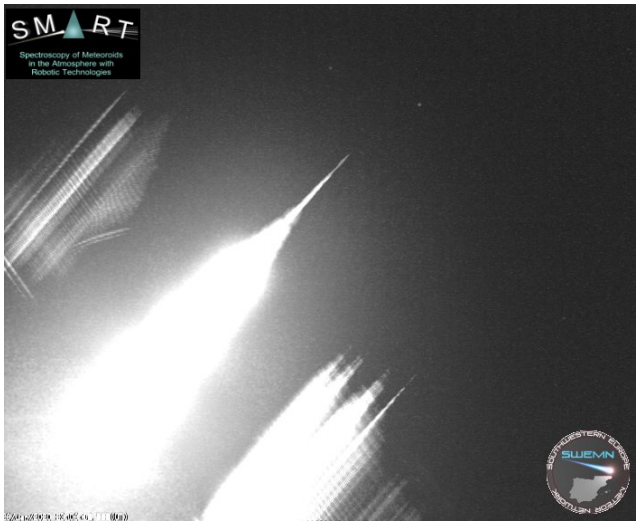

Figure 1 – Fireball of 2020 January 28 at 23^h08^m UT.

2 2020 February 19

This stunning fireball overflew the Mediterranean Sea[13] on 2020 February 19 at 3^h31^m UT. It was generated by a sporadic meteoroid moving on an asteroid-like orbit that hit the atmosphere at about 126000 km/h. The meteor reached a peak magnitude of -9 ± 1. It began at an altitude of about 99 km over the sea and ended at a height of around 31 km after traveling about 81 km in the Earth's atmosphere between the coasts of Spain and Algeria.

The event was recorded in the framework of the SMART project, operated by the Southwestern Europe Meteor Network (SWEMN), from the meteor-observing stations located at Calar Alto (Almería), Sierra Nevada (Granada), and Sevilla. The event has been analyzed by the principal investigator of the SMART project: Dr. Jose M. Madiedo, from the Institute of Astrophysics of Andalusia (IAA-CSIC).

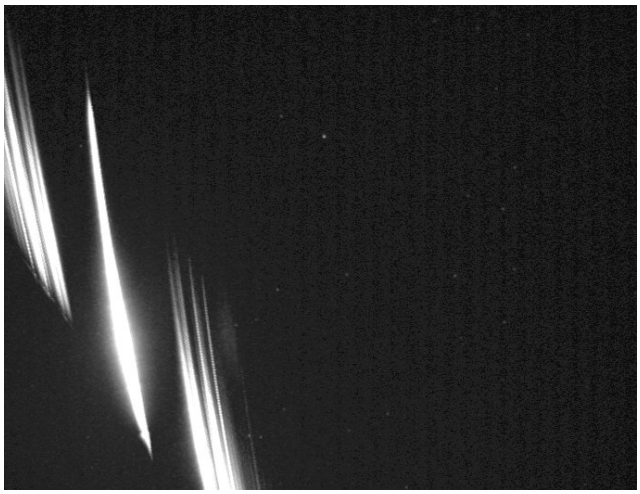

Figure 2 – Fireball of 2020 February 19 at 03^h31^m UT.

3 2020 February 22

On February 22, at around 23^h22^m UT, numerous casual eyewitnesses mainly located at the south and center of Spain[14] saw a bright and slow meteor crossing the night sky. The magnitude –9 sporadic event was generated by a meteoroid following an asteroid-like orbit. This particle hit the atmosphere at about 43000 km/h and generated a fireball that began at an altitude of about 70 km over

[12] https://youtu.be/jxKYtVKNcLg
[13] https://youtu.be/oTwnW9FfXhQ
[14] https://youtu.be/OYPDF3Jl7do

Almería (Andalusia), and ended at a height of around 29 km over the Mediterranean Sea.

The event was recorded in the framework of the SMART project, operated by the Southwestern Europe Meteor Network (SWEMN), from the meteor-observing stations located at Calar Alto (Almería), Sierra Nevada (Granada), La Hita (Toledo), and Sevilla. The fireball has been analyzed by the principal investigator of the SMART project: Dr. Jose M. Madiedo, from the Institute of Astrophysics of Andalusia (IAA-CSIC). According to this analysis, a fragment with a mass of around 25 to 200 grams could have survived, falling into the sea as a meteorite.

Figure 3 – Fireball of 2020 February 22 at $23^{h}22^{m}$ UT.

Stunning fireball 23 February 2020

Gábor Kővágó

fotospentax@gmail.com

On 23 February, 2020 at 19h50m UT a very bright fireball appeared over Hungary. The trajectory and orbit could be calculated by the author.

1 Introduction

On 23 February, 2020 at 19^h50^m UT a very bright fireball lit up the night sky over Hungary. There were a lot of observations around the country which described it as an electric green, sparkling phenomenon rolling down slowly from the sky. As always, I collected the online reachable pictures from meteorological sites including not just Hungarians but Austrians too. Thanks to their persistent work Jónás Károly (Soroksár) and Landy-Gyebnár Mónika (Veszprém) caught the meteor on precise photos.

Figure 1 – Fireball 23 February, 2020 at 19^h50^m UT by Jónás Károly from Soroksár.

Figure 2 – Fireball 23 February, 2020 at 19^h50^m UT by Mónika Landy-Gyebnár from Veszprém.

2 Trajectory and orbit

Unfortunately, it was close but no cigar… It began to emit light at 85 km, the entrance angle was 42 degree, fading and disappearing at about 28 km. The trajectory's end would be low enough for a meteorite dropping but the original 8 kg body was too fast with its 21 km/s and ablated almost totally before the end of the flight. There is a little chance for some 10–100g mass that may have survived, but this is a too small amount to search for, especially in the forested area in Mecsek.

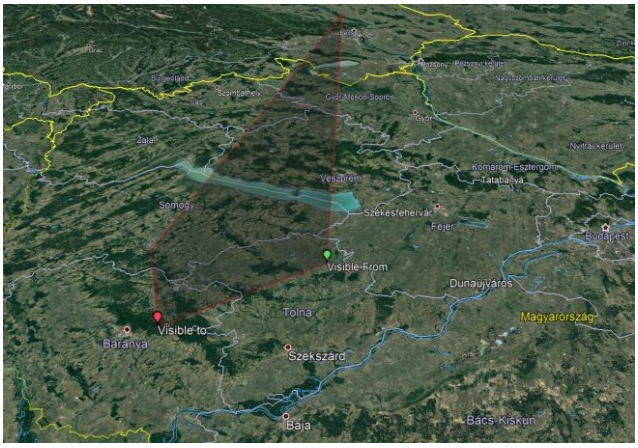

Figure 3 – The trajectory above Hungary.

The orbit in the solar system was an ordinary Apollo type orbit, the meteoroid came from the main belt between Mars and Jupiter.

The resulting orbital elements are:

- $\alpha = 248.6°$
- $\delta = +79.8°$
- $a = 2.4$ A.U.
- $q = 0.984$ A.U.
- $e = 0.589$
- $\omega = 190.2°$
- $\Omega = 334.4°$
- $i = 27.2°$

The mission of MeteorNews is to offer fast meteor news to a global audience, a swift exchange of information in all fields of active amateur meteor work without editorial constraints. MeteorNews is freely available without any fee. To receive a notification: https://www.meteornews.net/newsletter-signup/.

You are welcome to contribute to MeteorNews on a regular or casual basis, if you wish to. Anyone can become an author or editor, send an email to us. For more info read: https://meteornews.net/writing-content-for-emeteornews/

The running costs for website hosting are covered by a team of sponsors. We want to thank Peter Campbell-Burns, Kai Frode Gaarder, Tioga Gulon, J Andreas Howell, Richard Kacerek, Robert Lunsford, Koen Miskotte, Paul Roggemans, Enrico Stomeo and E.J. van Ballegoij for their financial contributions.

Gifts are welcome to share the maintenance costs. To join the team of sponsors send your donation by PayPal: https://www.paypal.com/pools/c/8ks6DnMamJ

Webmaster & account administrator:
Richard Kacerek (United Kingdom): rickzkm@gmail.com

Contributing to this issue:

- ***J. Andreas (Andy) Howell***
- ***Carl Johannink***
- ***Richard Kacerek***
- ***Masahiro Koseki***
- ***Gábor Kővágó***
- ***José María Madiedo***
- ***Pierre Martin***
- ***Paul Roggemans***
- ***Ivan Sergei***
- ***Felix Verbelen***

ISSN 2570-4745 Online publication https://meteornews.net

Listed and archived with ADS Abstract Service: https://ui.adsabs.harvard.edu/search/q=eMetN

MeteorNews Publisher:

Valašské Meziříčí Observatory, Vsetínská 78, 75701 Valašské Meziříčí, Czech Republic